
Pauatahanui inlet: effects of historical catchment landcover changes on inlet sedimentation



**NIWA Client Report: HAM2004-149
April 2005**

NIWA Project: WRC05211



Figure A16: Basin Site Four (BAS4) short-core x-radiograph of 2-cm thick slab. Exposure: 50 kV, 25 mA, 2 minutes. Scale: core width is 10 cm, length is 40 cm.

Pauatahanui inlet: effects of historical catchment landcover changes on inlet sedimentation

A. Swales
S. J. Bentley²
M. S. McGlone¹
R. Ovenden
N. Hermanspahn³
R. Budd
A. Hill
S. Pickmere
R. Haskew
M. J. Okey³

(1) Landcare Research Ltd, Lincoln

(2) Louisiana State University, Department of Oceanography and Coastal Sciences

(3) National Radiation Laboratory, Christchurch

Prepared for

**Greater Wellington Regional Council and
Porirua City Council**

NIWA Client Report: HAM2004-149
April 2005

NIWA Project: WRC05211

National Institute of Water & Atmospheric Research Ltd

Gate 10, Silverdale Road, Hamilton
P O Box 11115, Hamilton, New Zealand
Phone +64-7-856 7026, Fax +64-7-856 0151
www.niwa.co.nz

© All rights reserved. This publication may not be reproduced or copied in any form without the permission of the client. Such permission is to be given only in accordance with the terms of the client's contract with NIWA. This copyright extends to all forms of copying and any storage of material in any kind of information retrieval system.

Contents

1.	Introduction	1
1.1	Study background	1
1.2	Limitations of present knowledge	2
1.3	Study objectives	4
1.4	Potential environmental effects of land development	4
1.5	Catchment and estuary characteristics	6
2.	Methods	14
2.1	Dating of recent estuarine sediments	14
2.1.1	^7Be dating	14
2.1.2	^{137}Cs dating	14
2.1.3	^{210}Pb dating	16
2.1.4	Pollen dating	21
2.1.5	Radiocarbon dating	26
2.2	Sediment accumulation rates (SAR)	26
2.2.1	SAR from ^{210}Pb dating	27
2.2.2	SAR from pollen and ^{137}Cs dating	28
2.3	Field studies	29
2.4	Laboratory analyses	31
2.4.1	Core sub-sampling	31
2.4.2	X-radiography	32
2.4.3	Particle size	32
2.4.4	Heavy metals	32
2.4.5	Pollen	33
2.4.6	Radioisotopes	33
3.	Results	35
3.1	Overview	35
3.2	Browns Bay (BRN)	37
3.2.1	Sedimentary processes	37
3.2.2	Sediment profiles	38
3.2.3	Pollen profiles	40
3.2.4	Sedimentation rates	41
3.3	Duck Creek (DUK)	42
3.3.1	Sedimentary processes	42
3.3.2	Sediment profiles	44
3.3.3	Pollen profiles	45
3.3.4	Sedimentation rates	46
3.4	Pauatahanui (PAT)	47

3.4.1	Sedimentary processes	47
3.4.2	Sediment profiles	48
3.4.3	Pollen profiles	50
3.4.4	Sedimentation rates	51
3.5	Horokiri (HRK)	51
3.5.1	Sedimentary processes	51
3.5.2	Sediment profiles	53
3.5.3	Pollen profiles	54
3.5.4	Sedimentation rates	55
3.6	Kakaho (KAH)	56
3.6.1	Sedimentary processes	56
3.6.2	Sediment profiles	58
3.6.3	Pollen profiles	59
3.6.4	Sedimentation rates	60
3.7	Basin: Site One (BAS1)	61
3.7.1	Sedimentary processes	61
3.7.2	Sediment profiles	62
3.7.3	Pollen profiles	64
3.7.4	Sedimentation rates	65
3.8	Basin: Site Two (BAS2)	66
3.8.1	Sedimentary processes	66
3.8.2	Sediment profiles	67
3.8.3	Pollen profiles	69
3.8.4	Sedimentation rates	70
3.9	Basin: Site Three (BAS3)	70
3.9.1	Sedimentary processes	70
3.9.2	Sediment profiles	72
3.9.3	Pollen profiles	73
3.9.4	Sedimentation rates	74
3.10	Basin: Site Four (BAS4)	75
3.10.1	Sedimentary processes	75
3.10.2	Sediment profiles	77
3.10.3	Pollen profiles	78
3.10.4	Sedimentation rates	79
4.	Recent sedimentation in the Pauatahanui inlet	81
4.1	Historical changes in inlet sedimentation rates	81
4.2	Spatial patterns	84
4.3	Catchment sedimentation loads	88
5.	Sedimentary processes: implications for resource management	91
5.1	Sedimentary processes – summary	91
5.2	Implications for future landcover changes	92

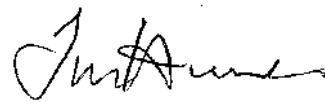
5.2.1	Urbanisation of Duck Creek sub-catchment	92
5.2.2	Exotic forest harvesting	96
5.3	What does the future hold?	98
5.3.1	Inlet evolution – controls and changes	98
5.3.2	Future sedimentation – existing landcover	102
6.	Acknowledgements	104
7.	References	105
8.	Appendix I: ²¹⁰ Pb dating models	113
9.	Appendix II: Solution to general equations for sedimentation and mixing	117
10.	Appendix III: Radiocarbon dating	118
11.	Appendix IV: Sediment core locations	119
12.	Appendix V: Livingston piston core summary	121
13.	Appendix VI: Long-core particle diameter and mud content profiles	122
14.	Appendix VII: Pauatahanui inlet short-core x-radiographs.	126

Reviewed by:



Catherine Chagué-Goff

Approved for release by:



Terry Hume

Formatting checked



Executive Summary

The Pauatahanui inlet is a regionally and nationally significant natural resource and is recognised as an area of significant conservation value. The inlet is small in comparison to its 109 km² steep-land catchment and is therefore sensitive to the effects of human activities on land. The potential for increases in sediment runoff to the inlet associated with earthworks is shown by the adverse effects of urban development in the Browns Bay sub-catchment during the 1970's. At Pauatahanui, there is limited information on the effects of historical landcover changes on inlet sedimentation during the last 150 years. Urban landcover presently accounts for < 4% of the catchment area and future development will be concentrated in the Duck Creek sub-catchment. Some 2000 ha of exotic forest have been planted since the mid-1970's and much of this first-rotation will be harvested over the next 15 years. These activities have the potential to increase sediment delivery to the inlet.

Greater Wellington Regional Council (GWRC) and Porirua City Council (PCC) recognise that the Pauatahanui inlet is a sensitive coastal environment. As part of a GWRC–PCC environmental programme, NIWA was commissioned to reconstruct the sedimentation history of the Pauatahanui inlet and relate this to landcover changes during the last 150 years. The reconstruction was based on radioisotope and pollen dating and analysis of sediment cores. The specific objectives of the study are to: (1) quantify changes in sediment accumulation rates (SAR) due to deforestation and subsequent conversion to pasture and the effects of urban development since the 1960's; (2) spatial variations in SAR, particle size and heavy metal profiles between urban and rural sub-catchment outlets and the central mud basin (CMB); (3) relate observed sediment profiles to landcover history; (4) reconstruct ~annual SAR time series where suitable data are available; and (5) provide an assessment of potential future SAR over the next 50 years based on present-day landcover and land management practices.

We estimate time-averaged SAR for three historical time periods: (1) post ~1850; (2) post ~1950 and (3) post ~1985 based on radioisotope and pollen dating (sections 2.1 & 2.2). The radioisotope and pollen SAR for (1) and (2) are in close agreement so that we can have confidence in these results. The post-1985 estimates are based on the pine-pollen profiles.

Key findings of the study are:

- The Pauatahanui inlet is a dynamic sedimentary environment (sections 2.1.3 & 3.1). Subtidal sediments are rapidly mixed (days–months) by physical–biological processes to ≤ 5-cm depth. Deeper (≤ 14-cm depth) but less intense sediment mixing over years–decades occurs due to the burrowing and feeding activities of infauna. As a result, the temporal resolution of the sediment cores is of the order of decades so that we cannot reconstruct ~annual time-series of sedimentation in the inlet.

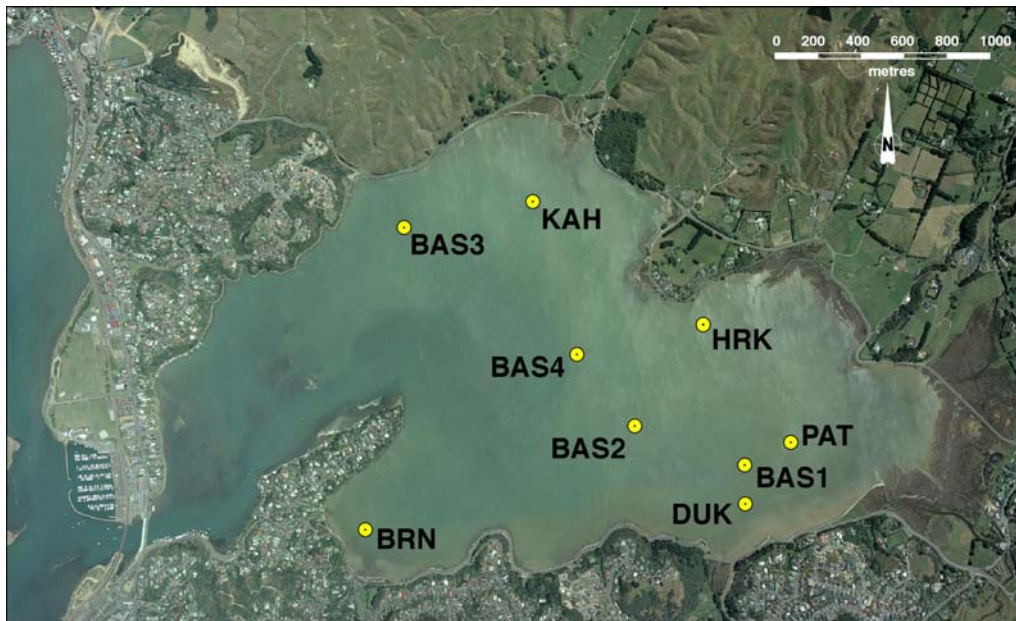


Figure A: Locations of core sites in the Pauatahanui inlet (source: NZAM).

- SAR have increased as a result of catchment deforestation and subsequent landcover changes (section 4.1). During the last several thousand years, sediments accumulated at $\sim 1 \text{ mm yr}^{-1}$ in a subtidal basin. ^{210}Pb SAR have averaged 2.4 mm yr^{-1} over the last ~ 150 years and ^{137}Cs SAR have averaged 3.4 mm yr^{-1} since 1950. The rapid rise in pine pollen abundance indicates that SAR in the inlet have increased since the mid-1980's and averaged 4.6 mm yr^{-1} .
- Average SAR in the central mud basin are $0.1\text{--}0.6 \text{ mm yr}^{-1}$ lower than at sub-catchment outlet sites for each historical time-period (section 4.2). SAR have been consistently high in Browns Bay over the last 150 years. This is notable given the small sub-catchment area and suggests that the bay is a sink for fine-sediments derived from elsewhere in the inlet. Sedimentation near the Horokiri sub-catchment outlet (core HRK) of 10 mm yr^{-1} in the last two decades is double the SAR measured elsewhere in the inlet. This likely reflects the size and steepness of this sub-catchment and coincides with large-scale planting of pine forest since the mid-1970s. Time-averaged SAR at DUK and BAS3 are similar to pre-deforestation values.
- Heavy metal concentrations have doubled in the last ~ 150 years in the upper 0.4 m of the sediment column (section 4.2). Despite this increase, the subtidal sediments remain relatively uncontaminated, with surface concentrations of Cu ($8\text{--}13 \mu\text{g g}^{-1}$) Pb ($15\text{--}26 \mu\text{g g}^{-1}$) and Zn ($55\text{--}90 \mu\text{g g}^{-1}$) being $\leq 50\%$ of ANZECC ISQG-low values.
- Catchment sediment loads have been estimated from the cores based on sediment mass accumulated in the subtidal area (section 4.3). This technique integrates the effects of inter-annual variability associated with climate and landcover changes over years–decades. Background sediment loads of $\sim 50 \text{ t km}^{-2} \text{ yr}^{-1}$ have increased following deforestation, averaging $\sim 90 \text{ t km}^{-2} \text{ yr}^{-1}$ over the last 150 years. Sediment loads have increased to $120 \text{ t km}^{-2} \text{ yr}^{-1}$ during the last 50 years and $160 \text{ t km}^{-2} \text{ yr}^{-1}$ in the last 20 years. This is similar to the

average $210 \text{ t km}^{-2} \text{ yr}^{-1}$ that was estimated using the Hicks and Shanker (2003) empirical model of suspended sediment loads delivered to the NZ coast.

- Future urban development in the Duck Creek sub-catchment will require controls to minimise the potential adverse environmental effects of fine-sediment dispersal and deposition (section 5.2.1). Sediment processes on the subtidal flat near the sub-catchment outlet are extremely dynamic. This is shown by the fact that sediments are rapidly mixed (days–months) to 5-cm depth by physical and biological processes. Also, sediment resuspension occurs episodically due to wave action. Background suspended sediment concentrations (SSC) of $\leq 20 \text{ mg l}^{-1}$ increase by an order of magnitude (e.g., 500 mg l^{-1}) during wave events. Fine sediments and associated contaminants are likely to be widely dispersed from the Duck Creek subtidal flat due to sediment resuspension and the very small fall speeds of these silt particles. These fine sediments and associated contaminants will be deposited elsewhere in the inlet, such as the adjacent bays and in the central mud basin.
- Harvesting of the ~ 800 ha of exotic forest in the Horokiri sub-catchment over the next 10–15 years has the potential to further increase sediment loads delivered to the inlet (section 5.2.2). The ^{210}Pb SAR (3.7 mm yr^{-1}) at site HRK is the maximum value measured in the inlet. This is consistent with the fact that the Horokiri stream formerly had a long and narrow tidal creek, as indicated by an 1852 land survey, which has subsequently infilled with sediment and a delta built at the stream mouth following deforestation (Eiby, 1990). The relatively high sediment loads suggested by these data likely reflects the relative size and steepness of the Horokiri sub-catchment. An apparent increase in SAR to 10 mm yr^{-1} during the last 20 years indicates that sediment loads have further increased.
- The central mud basin is a sink for fine catchment sediments. In the centre of the basin (BAS4) sediment mixing by infauna occurs over years–decades and short-term sediment mixing by physical processes appears to be less important than on its margins (e.g., BAS2).
- The rate of infilling of the Pauatahanui inlet has been offset by: (1) sea level rise, which at Wellington has averaged 1.8 mm yr^{-1} since the late 1800's. At Pauatahanui, an estimated average ^{210}Pb SAR of 2.4 mm yr^{-1} and tectonic uplift rate of $\leq 0.3 \text{ mm yr}^{-1}$ reduces the local rate of sea-level rise to 1.5 mm yr^{-1} ; and (2) flushing of fine sediment due to resuspension and direct discharge of stormwater to Porirua Harbour. Previous studies indicate that suspended sediments are discharged from the inlet during flood events (section 5.3.1). Thus, it is likely that the Pauatahanui inlet is a source of fine sediment deposited in the Porirua Harbour, although this has not been quantified. The fact that SAR have increased in recent decades suggests that the rate of sediment input now exceeds the capacity of the inlet to flush sediment.
- The net estuary-average ^{210}Pb SAR over the last 150 years (2.4 mm yr^{-1}) corrected for local sea-level rise (LSLR) of 1.5 mm yr^{-1} is $2.4 - 1.5 \text{ mm yr}^{-1} = 0.9 \text{ mm yr}^{-1}$ or an average shoaling of the inlet of 0.135 m. The resulting increase in intertidal area from sedimentation of about 12 ha (+15%) has been estimated from the estuary-average ^{210}Pb SAR corrected for LSLR and the average slopes of the intertidal flats (section 5.3). This infilling has reduced the tidal volume by about 600,000 m³ or $\leq 4\%$. These large-scale morphological changes are likely to

have been accompanied by changes in inlet hydrodynamics, sediment transport and benthic ecology, although these are not quantified.

- Future **inlet-average SAR** are predicted from the cores for the **next 50 years** based on **existing landcover**. Note that future large-scale landcover changes have the potential to further increase sediment loads to the inlet. We make **qualitative assessments of likelihood** based on the core data and our expert opinion (section 5.3.2):
 - $\text{SAR} \geq 2.4 \text{ mm yr}^{-1}$ (very high likelihood – certain).
 - $\text{SAR} \geq 3.4 \text{ mm yr}^{-1}$ (high likelihood).
 - $\text{SAR} \geq 4.0 \text{ mm yr}^{-1}$ (likely).

1. Introduction

1.1 Study background

The 4.6 km² Pauatahanui inlet forms the eastern arm of the Porirua Harbour, which is located 20 km north of Wellington City (Fig. 1.1). The inlet is almost entirely enclosed apart from a 100-m wide tidal channel connecting it to the Onepoto arm of Porirua Harbour and receives runoff from a 109 km² catchment (Curry, 1981). The inlet has been identified as a regionally and nationally significant natural resource. The Regional Coastal Plan for the Wellington Region recognises the Pauatahanui inlet as an area of significant conservation value with “natural, conservation, geological and scientific values”. The inlet is also classified by the Department of Conservation (DoC) as a Site of Special Wildlife Interest (SSWI).

Population growth projections for census areas within the inlet’s catchment indicate that growth over the next ~15 years will be largely concentrated in the Duck Creek sub-catchment (Graham Spargo Partnerships Ltd, 2005). Here the projected population increase of 21% (~760 people) by 2021 is approximately double the total growth in all other sub-catchments draining to the Pauatahanui inlet (Table 3: GSP, 2005). These projections indicate: (1) substantial urbanisation of the Duck Creek sub-catchment over the next ~15 years; (2) the Pauatahanui, Ration Point, Horokiri and Kakaho sub-catchments will remain predominantly rural in the foreseeable future, although the GSP (2005) report highlights the potential for lifestyle block development. No data are available on future pasture conversion to pine plantations, while the bulk of the ~2000 ha of pine forest planted since the mid-1970’s (Page et al. 2004) is likely to be harvested in the next 5–10 years. The first of these stands to be harvested, is the Silverwood forest in the Duck sub-catchment, where harvesting began in early 2003 (Mr Tim Porteous, Greater Wellington Regional Council (GWRC) Biodiversity Co-ordinator, pers. com.). Many of these forest plantations occupy steep lands, which are likely to be prone to soil erosion.

Estuaries are naturally depositional environments, however sedimentation rates in many New Zealand estuaries have accelerated in the last ~150 years due to increased soil erosion following large-scale catchment deforestation, conversion to pasture and, in some cases, subsequent urbanisation (Hume and McGlone, 1986; Goff, 1997; Abraham and Parker, 2002; Swales et al. 2002a; Swales et al. 2002b). The Pauatahanui inlet catchment has also been subject to large-scale deforestation (1850–1890) and conversion to pasture. Exotic forest planted since the mid-1970’s now accounts for some 18% of the catchment area. Urban area accounts for <4% of the catchment, (Page et al. 2004) and most of this development has occurred since the late 1960’s in the relatively small Browns Bay (1.23 km²) and Duck (10.5 km²) sub-catchments on

the south side of the inlet. By 1980 the population of the inlet catchment was still less than 8,000 people (Healy, 1980).

In recognition of the inlet's value to the community and the potential adverse environmental effects of future population growth, a comprehensive three-year (1975–1977) study of the Pauatahanui inlet and catchment was undertaken by several government agencies and co-ordinated by the Department of Scientific and Industrial Research (DSIR). The objectives of the Pauatahanui Environmental Programme (PEP) were to: (1) improve understanding of the physical environment and inlet ecology; (2) provide data to resource managers and (3) establish baselines for monitoring future environmental changes. Of particular relevance to the present NIWA study, PEP included investigations of catchment sediment inputs, inlet hydrodynamics and sedimentation processes. Key results of this far-sighted study are summarised by Healy (1980).

1.2 Limitations of present knowledge

The sedimentation processes component of the PEP study was based on the collection of ~15-m long cores from three sites (Fig. 21, Healy, 1980) and monthly monitoring of changes in intertidal flat elevations at 122 sites over a 15 month period (Pickrill, 1979). The coring study was designed to quantify long-term environmental changes in the inlet during the last 15,000 years. This work include particle size analysis, sediment bulk density, time-average sediment accumulation rates (SAR) based on pollen and radiocarbon (^{14}C) dating and changes in diatom assemblages (Mildenhall, 1979).

The PEP sediment cores indicate an average SAR of $\sim 2 \text{ mm yr}^{-1}$ over a 2200 year period 3600–1360 years before present (BP = 1950 AD). Because of the fluid nature of the sediment-water interface, the upper sediment column was not preserved in the cores. Whitehead et al. (1998) analysed ^{210}Pb profiles from sediment cores collected at two sites. One of these, which was taken $\sim 1 \text{ km}$ west of Ration Point (core M354), indicated a post-1968 SAR of about 8 mm yr^{-1} as compared with $\sim 2 \text{ mm yr}^{-1}$ before 1968. Whitehead et al. (1998) data indicate a large increase in SAR from the late-1960's, albeit from only two sites. Consequently, we have limited information about changes in SAR during the last 150 years or so during which time large-scale catchment landcover changes have occurred.

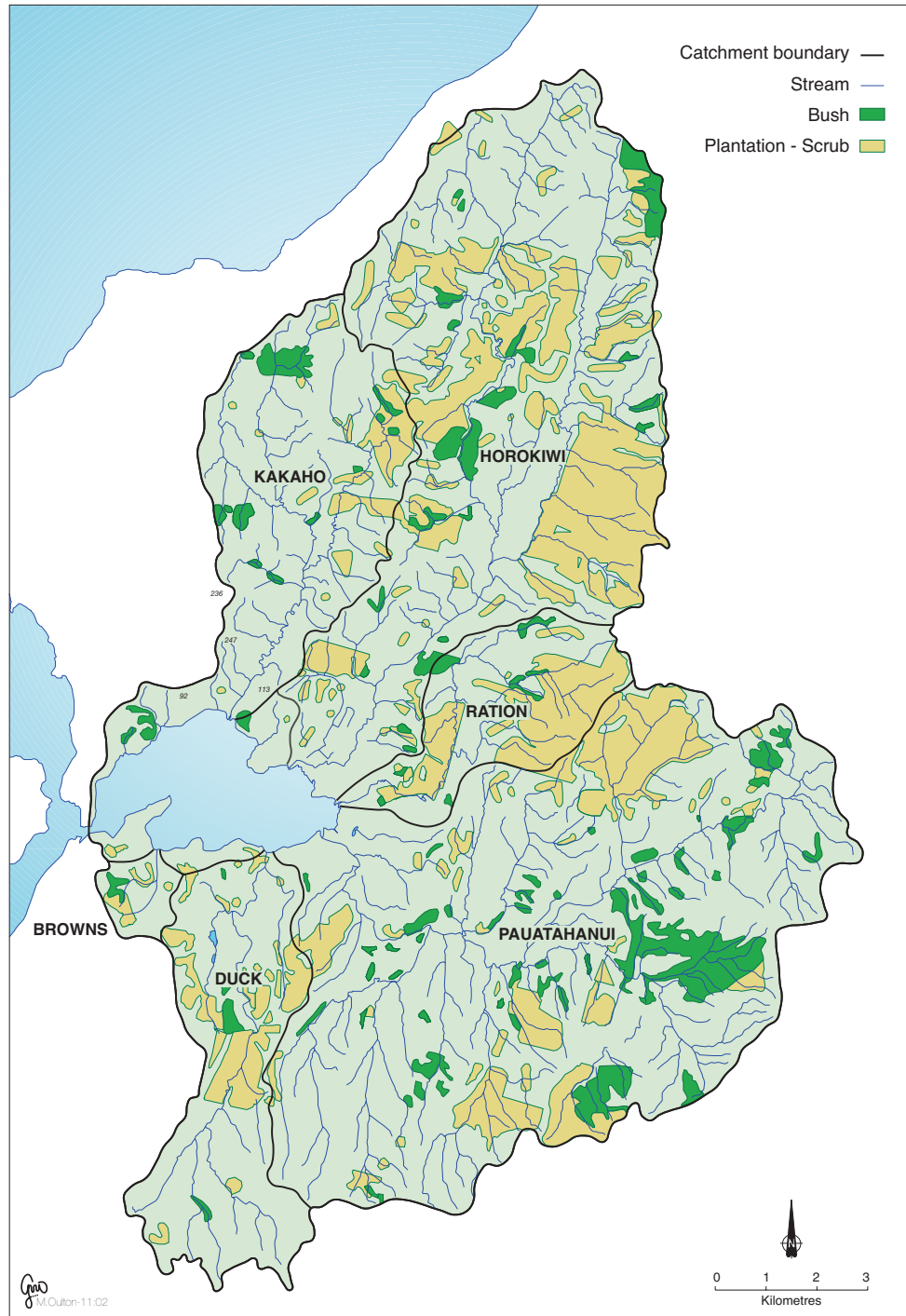


Figure 1.1: Pauatahanui inlet and sub-catchments (sources: Page et al. 2004, LINZ R26 & R27).

Furthermore, because of the small number of core sites in the PEP study, we also have no information about the spatial variability of sedimentation in the inlet. For example, do SAR increase near catchment outlets and do finer sediments accumulate in the

central subtidal basin where wave re-suspension maybe less effective than on intertidal and shallow subtidal flats fringing the shore? The pattern of fine sediment accumulation also influences the fate of contaminants, such as heavy metals, which are preferentially adsorbed by clays and fine silts (e.g., Valette-Silver, 1993).

1.3 Study objectives

GWRC and Porirua City Council (PCC) recognise that the Pauatahanui inlet is a sensitive coastal environment. As part of a wider GWRC–PCC environmental programme, NIWA was commissioned to reconstruct the sedimentation history of the Pauatahanui inlet and relate this to changes in catchment landcover during the last 150 years. The specific objectives of the study are to:

- Quantify changes in average SAR due to large-scale catchment deforestation (from ~1840 AD) and subsequent conversion to pasture and the effects of urban development since the 1960's.
- Quantify spatial variations in SAR, particle size and heavy metal profiles between urban and rural sub-catchment outlets and the central mud basin of the inlet using complementary and independent dating techniques and relate these to landcover history.
- Relate observed sediment particle size and heavy metal concentration profiles in the inlet cores to catchment landcover history, with particular emphasis on changes that have occurred since urban development began.
- At core sites where high quality data are available (i.e., independent dating in agreement and unsupported ^{210}Pb mean supply rates similar between cores), use the unsupported ^{210}Pb profiles to reconstruct annual SAR time series over the last 150 years.
- Provide an assessment of potential future SAR's in the Pauatahanui inlet based on 2003 landcover and land management practices. We adopt a 50 year timeframe in this evaluation.

1.4 Potential environmental effects of land development

The potential for substantial increases in sediment loads delivered to the inlet from even relatively small areas of urban earthworks is shown by the effects of urban

development of the Browns Bay (1.2 km²) sub-catchment in the mid-1970's (Fig. 1.2). During a two year study, Curry (1981) compared sediment loads from the urbanising Browns Bay and rural Ration (6.13 km²) sub-catchments. Suspended sediment concentrations (SSC) in the Browns Bay stream of $\leq 1500 \text{ mg l}^{-1}$, even downstream of a silt pond, were several times higher than the Ration stream ($\leq 250 \text{ mg l}^{-1}$) and the larger and steeper sloping rural Pauatahanui, Horokiri and Kakaho sub-catchments ($\leq 500 \text{ mg l}^{-1}$). During a single flood (5 year return period) in June 1975, the Browns Bay stream discharged $\sim 1600 \text{ t day}^{-1}$ of suspended sediment to the inlet. This sediment load was 35 times the value measured for the Ration sub-catchment and represented 22% of the total flood sediment load to the inlet. Suspended sediment sampled during another flood also showed that more than 90% of the sediment eroded from the urbanising Browns Bay sub-catchment was composed of very fine silts and clay ($< 6 \mu\text{m}$ diameter, Table 7, Curry 1981) whereas this value was 57–77% for the five rural sub-catchments. Much of the clay eroded from the Browns Bay sub-catchment was deposited in the bay itself. Silt eroded from urban earthworks in the adjacent Whitby sub-catchment in 1974 was also deposited, up to 5 cm deep, in Browns Bay and was subsequently removed from the intertidal flats using bulldozers (Kennedy, 1980). This highlights the fact that fine sediments can be widely dispersed in the inlet, although flocculation on contact with seawater causes clays and fine silts to form larger clumps which are then deposited. The cohesive behaviour of fine-sediment deposits substantially increases their resistance to erosion by waves and/or currents (Dyer, 1986), so that they accumulate in bays and inlets.

Recent New Zealand studies of the effects of fine sediment deposition and increased water turbidity on estuarine benthic fauna show that fauna which inhabit sand/muddy-sand substrates (e.g., cockles) are generally more adversely affected than animals which occur in naturally muddy environments, such as tidal creeks (Norkko et al. 2001). The relative ecological toxicity of sediments primarily relates to their mud content because filter-feeding benthic fauna, such as bivalves, some crustacean, and sponges are particularly sensitive to suspended sediments and sedimentation rates (e.g., Moore, 1977; Maurer et al. 1986). Chronic effects of fine sediments include reduced growth and reproductive success due to energy expenditure involved in filtering fine particles. Smothering of benthic fauna also occurs due to burial by flood deposits (McKnight, 1969) and include a variety of effects from mass mortality to changes in community composition (Norkko et al. 2002; Lohrer et al. 2004; Thrush et al. 2004). Furthermore, catchment-derived fine sediments appear to be ecologically more toxic to some shellfish, (e.g., cockles) than similar sized estuarine sediments (Hewitt et al. 2001) that experience cycles of re-suspension and re-deposition.



Figure 1.2: Browns Bay sub-catchment undergoing urban development during the mid-1970's (source: Dr Noel Trustrum, Institute of Geological and Nuclear Sciences).

1.5 Catchment and estuary characteristics

Catchment

The Pauatahanui inlet receives runoff from a 109 km² catchment, with six main sub-catchments (Table 1.1). Hillslopes in the sub-catchments rise gently below 100 m and then rise more steeply to a maximum elevation of 530 m (Fig. 1.2). Catchment geology is dominated by a greywacke basement which is composed of alternating sandstone and mudstone layers. The valley bottoms are mantled by alluvium (gravel, sand and mud) and loess, which is wind-blown silt derived from riverbeds and areas of continental slope, which were exposed during low sea level stands and deposited during the Quaternary. Substantial areas of the Duck and Pauatahanui sub-catchments are mantled by the Kaitoke alluvium and thick layers of weathered loess (Healy, 1980). During earthworks the weathered greywacke and loess are crushed due to the grinding and ripping action of machinery so that additional fines are released (Mr Paul Denton, Policy Advisor-Environment-GWRC, pers. com.). When these earthworks are exposed to rainfall, they are susceptible to erosion. Erodibility is further enhanced by the presence of disperable clays, which are difficult to settle out in sediment retention ponds.

Table 1.1: Sub-catchment characteristics (source: Curry, 1981).

Sub-catchment	Area (km ²)	Max. Elev. (m)	Ave. Channel Slope (degrees)
Browns Bay	1.2	157	3.7
Duck	10.5	490	1.9
Pauatahanui	43.4	431	1.3
Ration	6.1	260	1.5
Horokiri	32.9	530	1.3
Kakaho	11.3	439	2.1

Mean annual rainfall at Judgeford (1979–2004, station E14199, elevation 24 m) in the lower reaches of the Pauatahanui sub-catchment is 1140 mm (standard deviation \pm 173 mm). The estimated long-term specific mean flow to the inlet is \sim 16 litres s⁻¹ km² whereas the maximum specific flow measured during the 1975–1977 PEP study was \sim 600 litres s⁻¹ km² (Curry, 1981, tables 2 and 4).

Catchment landcover history is discussed in detail elsewhere (Mildenhall, 1979; Healy, 1980; Page et al. 2004) and we do so briefly here. Before human habitation, the vegetation was dominated by a mixed podocarp-hardwood forest with totara, matai, rimu, kahikatea, pukatea, rata, maire and hinau. The first Maori arrived in the area some 600 years ago and the descriptions of early European settlers indicate that Maori had a minimal impact on landcover, with settlements concentrated in the coastal fringe. Although Europeans had visited the area from the early 1800's, land clearance for farming did not begin until the early-1840's. Logging of native trees began several years earlier in 1832 (Page et al. 2004). By 1900 relatively small pockets of native forest remained and landcover was dominated by pasture used for sheep, beef and dairying (Healy, 1980).

Page et al. (2004) have mapped landcover changes since 1941 based on analysis of aerial photography. Initially, urban development was restricted to Mana and Golden Gate near the inlet mouth. Browns Bay sub-catchment was urbanised by the late-1970's and development had also occurred in the lower reaches of the Duck sub-catchment. At the same time, exotic forest plantations, composed mainly of pine, began to be established and by 2000 accounted for \sim 18% (\sim 2000 ha) of catchment landcover. A large proportion of this planting has occurred on steepland in the Kakaho (42%), Horokiri (40%) and Pauatahanui (27%) sub-catchments.



Figure 1.2: Kakaho sub-catchment (2 August 1978). Dissected steepland, with a relatively small flood plain. Landcover is dominated by pasture before the establishment of pine forest from the late 1970's. (source: Dr Noel Trustrum, IGNS).

Some idea of the relative increases in catchment sediment loads to the Pauatahanui inlet associated with deforestation and conversion to pasture over the last 150 years can be gained from previous NZ studies. For example, average sediment loads (i.e., suspended and bed load combined) to the Mahurangi estuary (Auckland) were estimated from dated sediment cores and bathymetric data (Swales et al. 1997). This study suggested that specific sediment loads increased by an order of magnitude from $\sim 100 \text{ t km}^{-2} \text{ yr}^{-1}$, under native forest, to $\sim 1200 \text{ t km}^{-2} \text{ yr}^{-1}$ (deforestation phase, 1850–1900) and since 1900 have remained several times higher (than before deforestation) under a largely pasture ($\sim 700 \text{ t km}^{-2} \text{ yr}^{-1}$) catchment. This estimate is similar to the 20-year (1976–1995) average suspended sediment load of $450 \text{ t km}^{-2} \text{ yr}^{-1}$ predicted from catchment modelling (Stroud and Cooper, 1997). The relatively high sediment loads delivered to the Mahurangi estuary reflect the steepland catchment, relatively high rainfall and impermeable clay soils.

Curry (1981) estimated a specific suspended sediment load for the Pauatahanui sub-catchment of $\sim 108 \text{ t km}^{-2} \text{ yr}^{-1}$ (June 1975 – June 1977) as opposed to a long-term

average value of $\sim 31 \text{ t km}^{-2} \text{ yr}^{-1}$. The substantially higher sediment loads during the measurement period were attributed to: (1) the higher than average rainfall intensity and (2) soil erosion in the urbanising Browns Bay sub-catchment, which yielded 10% of the sediment load although accounting for $\sim 1\%$ of the total catchment area. The specific suspended sediment yield from the Brown's Bay sub-catchment of $\sim 1200 \text{ t km}^{-2} \text{ yr}^{-1}$ demonstrates the potential for large increases in soil erosion on exposed ground.

The contribution of bed load to the catchment sediment budget is unknown (Healy, 1980), but is likely to be highest for the steeper and more elevated Pauatahanui, Horokiri and Kakaho sub-catchments. This relates to the fact that bedload transport of sand and gravel depends on flow velocity, which in turn depends on stream discharge, channel dimensions and slope (Richards, 1982). Sediment source characteristics will also be influential. For example, flood-plain alluvium will yield muds–gravel whereas the loess mantling the Duck catchment yields fine silt. Consequently, there are likely to be differences in the type of sediment deposited at sub-catchment outlets.

Inlet

The Pauatahanui inlet forms the eastern arm of Porirua Harbour and is an almost entirely enclosed basin, apart from its $\sim 100\text{-m}$ wide inlet. The inlet was formed by post-glacial flooding of a river-valley system by rising sea level 14,000–10,000 years ago (Irwin, 1976). The inlet is shallow (water depth $< 3\text{m}$) except at the inlet mouth despite infilling with $\sim 13 \text{ m}$ of mud and fine sand overlaying alluvial gravels (Healy, 1980). Averaged over the last 14,000 years, this is equivalent to a $\sim 1 \text{ mm yr}^{-1}$ sedimentation rate. Analysis of long cores collected during the PEP study suggest that sedimentation rates widely varied between $1\text{--}11 \text{ mm yr}^{-1}$ during the one thousand years before the sea reached about its present level $\sim 7,000$ years ago. This is attributed to erosion of river terraces in the upper reaches of the ancestral river basin by rising sea level (Healy, 1980). Time-averaged SAR of $\sim 2 \text{ mm yr}^{-1}$ for native forest landcover (3,600–1,360 years BP) is high in comparison to the long-term average value of 1 mm yr^{-1} over the last 14,000 years and is also higher than the $< 1 \text{ mm yr}^{-1}$ measured in several upper North Island estuaries (Hume et al. 2002, Table 2) or Wellington Harbour (Goff, 1997).

Uplift of intertidal flats in the upper Pauatahanui inlet has been attributed to the magnitude ~ 8.1 Wairarapa earthquake of 23 January 1855 (Grapes and Downes, 1997). Adkin (1921) documents the recollection of a long-time resident, Mr James Jones, of the effects of the 1855 earthquake on the Pauatahanui inlet: “[the tidal flats] were for a time noisome on account of the putrefying shellfish and other marine

matter". The account of Roberts (1855), an engineer, suggests net uplift of the area around Porirua Harbour of about 0.3 m (In: Grapes and Downes, 1997). It is likely that settling of the unconsolidated sediments of then Pauatahanui inlet occurred during the earthquake although this has not been quantified (Dr Gaye Downes, Institute of Geological and Nuclear Sciences, pers. comm. 8 June 2005). Eiby (1990) finds no historical or geological evidence of uplift in the Pauatahanui inlet due to the 1855 earthquake, while there is substantial evidence to the contrary. Furthermore, shoreline changes in the upper inlet first documented in 1902 can be adequately explained by sedimentation resulting from catchment deforestation (Eiby, 1990).

Today the inlet remains largely subtidal, which is not typical of many North Island estuaries. In the Pauatahanui, the intertidal flats that fringe the central mud basin are associated with the deltas formed at sub-catchment outlets (Pickrill, 1979). Thus, the largest intertidal flats occur on the north and eastern shores of the inlet near the Pauatahanui, Horokiri and Kakaho sub-catchment outlets (Fig. 1.3). Intertidal sediments are composed of poorly sorted muddy sand, although they can be well sorted on the upper flats where waves winnow mud from these sediments (Pickrill, 1979). The central basin, in the subtidal compartment, accumulates mud (Healy, 1980).

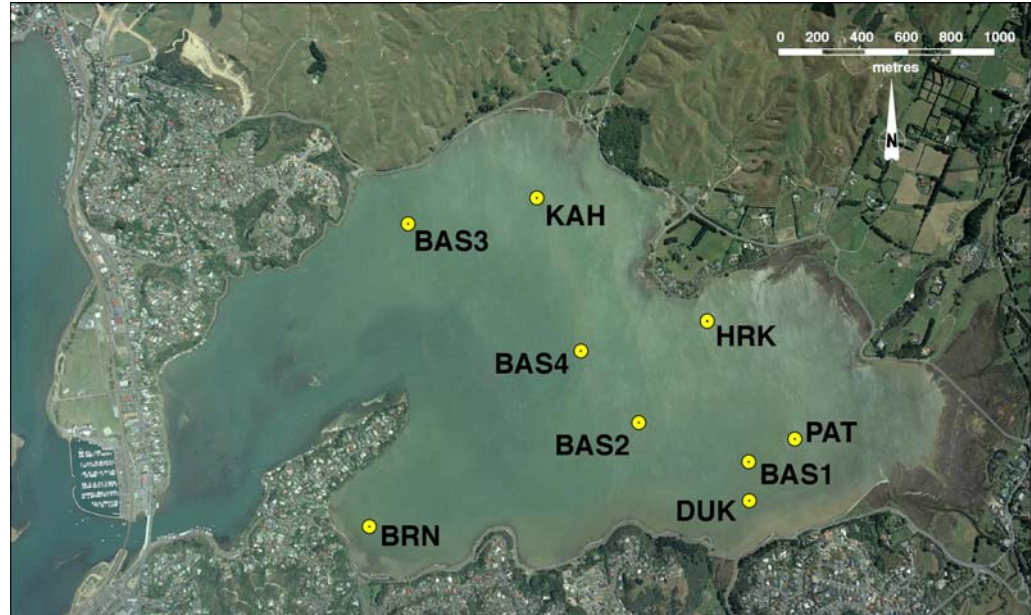


Figure 1.3: Locations of subtidal core sites in the Pauatahanui inlet (source: NZ Aerial Mapping, survey 50363c, 1/15, 1:25000, 10 January 2004).

The fact that the Pauatahanui inlet remains substantially subtidal is notable given the large ratio between catchment and inlet area (~24). Auckland (e.g., Puhoi, Okura) and

Coromandel (e.g., Wharekawa) estuaries with similar catchment-estuary ratios are now largely intertidal. The processes which have maintained the Pauatahanui inlet in its largely subtidal are discussed in section five.

Tides are semi-diurnal with a 12.4 hour period and tidal range varying between 1.4 m (spring) and 0.3 m (neaps). Maximum tidal-current speeds in the inlet channel are $\sim 1 \text{ m s}^{-1}$ (Healy, 1980) although they will be substantially lower (i.e., $\leq 0.2 \text{ m s}^{-1}$) on the flats. The combined mean freshwater inflow of $\sim 1.7 \text{ m}^3 \text{ s}^{-1}$ is small in comparison to the spring (22×10^6) and neap (17×10^6) tidal volumes (Heath, 1977). The ~ 3 day residence time of water in the inlet has been estimated from salinity measurements (Healy, 1980). The 2% density difference between freshwater and seawater results in stratification of the estuarine water column, with a surface, seaward flowing, freshwater layer (Dyer, 1986). In a shallow estuary, such as the Pauatahanui, physical mixing of the water column by tidal currents and waves, is likely to reduce the degree of density stratification, particularly under average freshwater flows. Under these conditions the inlet will be well mixed and salinity is close to that of seawater (Healy, 1980). Stratification will be more likely to occur during catchment floods when freshwater discharge and the vertical density gradient, are sufficient to suppress vertical mixing of the water column. In this case, a salt wedge may develop with the fine catchment sediments transported in the surface freshwater layer. In this way fine sediments are widely dispersed within the inlet and/or discharged to the coast. As these fine cohesive particles sink under gravity into the seawater layer they flocculate to form larger aggregates with fall speeds that can be orders of magnitude greater than their constituent particles. For example, a $5 \text{ }\mu\text{m}$ diameter silt particle has a fall speed of $\sim 0.002 \text{ cm s}^{-1}$, whereas a $500 \text{ }\mu\text{m}$ diameter floc composed of similar sized particles will sink at $\sim 0.4 \text{ cm s}^{-1}$ (McDowell and O'Connor, 1977). Thus, flocculation is likely to be an important process influencing the initial fate of catchment sediments and associated contaminants in the Pauatahanui inlet.

Sediment resuspension and mixing by waves and benthic animals also modify bed sediments after deposition. Wave characteristics and thresholds for bed sediment remobilisation by wave orbital motions can be estimated from empirical formulae and/or measurements. In the Pauatahanui inlet, the available fetch (i.e., distance from shore to shore at high tide) in the direction of the prevailing north-west – south-east winds is $\sim 2.4 \text{ km}$. This indicates that maximum wave heights should be $\leq 0.4 \text{ m}$. Furthermore, wave orbital motions are likely to be capable of mobilising sand and mud in the central mud basin as well as on the fringing intertidal flats (Healy, 1980). The feeding and burrowing activities of benthic animals (bioturbation) also modify the upper part of the sediment column by mixing sediments and contaminants. As a

result, vertical profiles of particle size and contaminant concentrations can be uniform in this Surface Mixed Layer (SML).

Stormwater contamination of sediments has been studied in a number of New Zealand estuaries (e.g., Hume et al. 1989; Glasby et al. 1990; Vant et al. 1993; Williamson and Morrisey, 2000; Morrisey et al. 2000; Swales et al. 2002a). Contaminants commonly associated with urban stormwater include heavy metals and polyaromatic hydrocarbons (PAH). Concentrations of these contaminants in many of New Zealand's urban estuaries are high enough to be of ecological concern (Auckland Regional Council, 1995; Morrisey et al. 1997). Also of potential concern are inputs of organochlorine pesticides, such as dichloro-diphenyltrichloroethane (DDT), from rural catchments. Aerial top-dressing is also another potential source of heavy metals, including Cu and Zn (Glasby et al. 1990).

The Pauatahanui inlet catchment remains largely rural, apart from the Browns Bay and Duck sub-catchments that began to be urbanised from the late 1960's. However, state highways 1 and 58, which run adjacent to the inlet, are major traffic routes and are potential sources of organic and heavy metal contaminants. Glasby et al. (1990) sampled sediments at 72 sites in the Porirua Harbour (inc. Pauatahanui inlet) to assess heavy metal pollution. Their results indicated that the Pauatahanui-inlet sediments are relatively uncontaminated by Pb, Cu and Zn. GWRC have recently established long-term baseline (LTB) monitoring in the Porirua Harbour, including two sites in the Pauatahanui inlet, for state of the environment reporting. The program is designed to detect trends in contaminant concentrations in near-surface (i.e., ≤ 15 -cm) subtidal sediments over time for comparison with sediment quality guidelines. Parameters monitored include mud-fraction and total heavy metals, particle size, PAH and DDT. A discussion of the LTB methodology and results of the first survey are presented in Williamson et al. (2004). These data show that, with the exception of DDT, present contaminant concentrations in Pauatahanui inlet sediments are below thresholds of concern for aquatic ecosystem health (i.e., ANZECC, 2000 sediment quality guidelines).

The biology of the Pauatahanui inlet sediments is described by Healy (1980) and we do so briefly here. The most abundant and widespread fauna of the intertidal sediments is the cockle (*Chione stutchburyi*), a filter-feeding bivalve. Densities of cockle have declined by ~50% since the mid-1970's, from a maximum of 2500 m⁻² to 1200 m⁻² in 2001 (Richardson et al. 1979; Grange and Tovey, 2002). The spatial distribution of cockles is also patchy, with the highest cockle densities occurring along the southern shore of the inlet (Grange and Tovey, 2002). The wedge shell (*Macomona liliana*), nut shell (*Nucula hartvigiana*), mud snails (*Amphibola crenata*),

mud crab (*Helice crassa*) and several species of polychaete worms (*Axiothella* sp.) are also common intertidal fauna. The central mud basin which accounts for a large proportion of the largely subtidal inlet has a characteristic fauna dominated by the nut shell, *Nucula hartvigiana*. This small (length < 10 mm) deposit-feeding bivalve is abundant in the top ~3 cm of the sediment column and moves through the sediment using its plug-like foot (Morton and Miller, 1973). The deposit-feeding bivalve, *Macomona liliana* and the suspension-feeding estuarine trough shell (*Mactra ovata*) are also common. These animals burrow to 20 cm depth and extend long siphon up into the water column to feed on surficial and particulate matter and excrete sediment at depth. *M. ovata* is more tolerant of silt and clay than *M. liliana* (Morton and Miller, 1973). Several species of polychaete worm occur in subtidal sediments. *Nicon aestuariensis*, a predatory polychaete is common in estuarine mud, which moves through the sediment column as well as excavating a y-shaped burrow. These animals are tolerant of wider variations in water salinity. Sedentary polychaete, such as *Axiothella* sp. (bamboo worms) occupy thick-walled fine-sand tubes, which extend ~2 cm above the sediment surface and from which mud casts are ejected. *Boccardia syrtis* is a tube-dwelling deposit-feeding worm which forms long thin (~3mm diameter) sand-lined tubes which extend ~2 cm from the substrate. Surface particles are excreted at depth. These animals also form dense tube mats which also bio-stabilise the substrate (Dr Judi Hewitt, NIWA, pers. comm.). *Phylo novazelandiae* is a large orbinid sub-surface deposit feeding worm. The Maldanid worms are sub-surface deposit feeders which occupy tubes that extend above the sediment surface. They excrete sediments, ingested at depth, at the surface and can also subduct surface particles down their tubes to be ingested at depth.

The burrowing and feeding activities of these subtidal fauna mix the upper 10–20 cm of the sediment column by displacing/intruding and ingesting sediment (e.g., *Nucula*, *Nicon* and *Phylo*). Sedentary and mobile worms may ingest surficial sediments which are excreted at depth or vice-versa. These sediment mixing activities can obliterate sedimentary structures, such as graded beds associated with flood deposits or wave ripples, and depending on the mixing intensity, homogenise the sediment fabric (Bromley, 1996). In the Pauatahanui inlet cores, the intensity and depth of bioturbation will influence the temporal resolution of the sedimentation history that can be reconstructed.

2. Methods

2.1 Dating of recent estuarine sediments

Radioisotopes, such as berillyum-7 (^7Be , $\frac{1}{2}$ -life 53.3 days), caesium-137 (^{137}Cs , $\frac{1}{2}$ -life 30 years) and lead-210 (^{210}Pb , $\frac{1}{2}$ -life 22.3 years), and plant pollen can be used to reconstruct the recent sedimentation history of an estuary. Heavy metal (i.e., Pb, Zn and Cu) profiles in estuarine sediments have also been shown to provide useful additional information to identify the onset of urban development (e.g., Valette-Silver, 1993; Abraham and Parker, 2002; Swales et al. 2002a, 2002b).

Dating of estuarine sediments by several independent methods offsets the limitations of any one approach. This is particularly important given the confounding effects of physical and biological mixing when interpreting sediment profiles from lakes and estuaries (Robbins and Edgington, 1975; Olsen et al. 1981; Alexander et al. 1993; Valette-Silver, 1993; Benoit et al. 1999; Chagué-Goff et al. 2000).

A description of the various methods of dating sediments follows. The S.I. unit of radioactivity used in this study is the Becquerel (Bq), which is equivalent to one disintegration per second.

2.1.1 ^7Be dating

Beryllium-7 (^7Be) is a naturally occurring radioisotope with a half-life of 53.3 days that is formed in the atmosphere by reactions between cosmic rays and nitrogen and oxygen. Because of its short half-life, ^7Be has been widely used to determine short-term (i.e., several months) mixing of marine and lake sediments by biological (bioturbation) and physical processes (Sharma et al. 1987). In the present study, ^7Be is used in conjunction with other information (e.g., x-radiographs) to determine short-term sediment mixing in the Pauatahanui inlet cores.

2.1.2 ^{137}Cs dating

^{137}Cs (half-life 30 yr) was introduced to the environment by atmospheric nuclear-weapons tests in 1953, 1955–1956 and 1963–1964. Peaks in annual ^{137}Cs deposition corresponding to these dates are the usual basis for dating sediments (Wise, 1977; Ritchie and McHenry, 1989). Although direct atmospheric deposition of ^{137}Cs into estuaries is likely to have occurred, ^{137}Cs is also incorporated into catchment soils, which are subsequently eroded and deposited in estuaries (Fig. 2.1). In New Zealand,

^{137}Cs deposition was first detected in 1953 and its annual deposition was been measured at several locations until 1985. Annual ^{137}Cs deposition can be estimated from rainfall using known linear relationships between rainfall and Strontium-90 (^{90}Sr) and measured $^{137}\text{Cs}/^{90}\text{Sr}$ deposition ratios (Matthews, 1989). Experience in Auckland estuaries shows that ^{137}Cs profiles measured in estuarine sediments bear no relation to the record of annual ^{137}Cs deposition (i.e., 1955–1956 and 1963–1964 ^{137}Cs -deposition peaks absent), but rather preserve a record of direct and indirect (i.e., soil erosion) atmospheric deposition since 1953 (Swales et al. 2002b). Similarly in the present study, the maximum depth of ^{137}Cs occurrence in the sediment cores is taken to coincide with the year 1953, when ^{137}Cs deposition was first detected in New Zealand. We assume that there was negligible delay in initial atmospheric deposition of ^{137}Cs in estuarine sediments (e.g., ^{137}Cs scavaging by suspended particles) whereas there is likely to have been a small time-lag (i.e., < 1 yr) in ^{137}Cs inputs to estuaries from topsoil erosion, which would coincide with the occurrence of floods. Sediment mixing after deposition also needs to be taken into account when interpreting ^{137}Cs data.

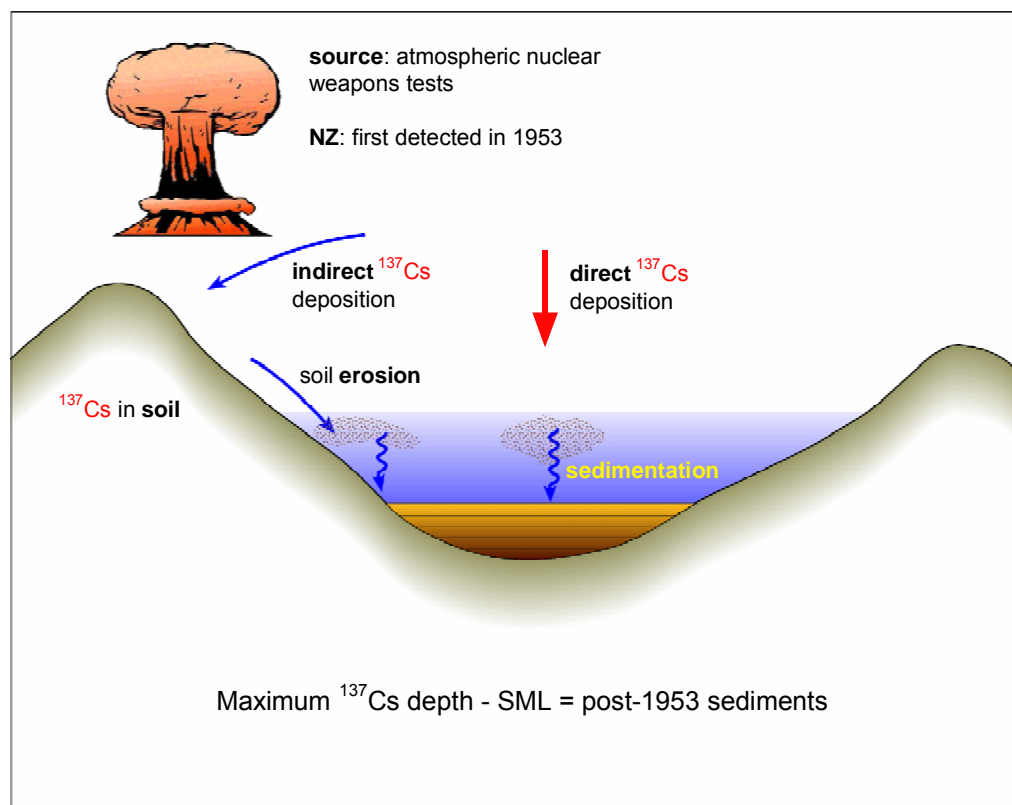


Figure 2.1: ^{137}Cs pathways to estuarine sediments.

If a surface mixed layer (SML) is evident in a core, as shown by an x-ray image and/or a tracer profile (e.g., ^7Be , ^{210}Pb) then ^{137}Cs is likely to have been rapidly mixed through the SML. Therefore to calculate time-averaged sedimentation rates, the maximum depth of ^{137}Cs occurrence is reduced by the maximum depth of the SML.

Uncertainty in the maximum depth of ^{137}Cs ($^{137}\text{Cs}_{\text{max}}$) results from (1) the depth interval between sediment samples and (2) the minimum detectable concentration (MDC) of ^{137}Cs , which is primarily determined by sample size and counting time. The 1963–1964 ^{137}Cs deposition peak was about five-times than deposition plateau that occurred between 1953 and 1972. Thus, depending on the sample size, there is uncertainty in the age of $^{137}\text{Cs}_{\text{max}}$ (i.e., 1953–1963). To address this uncertainty, we have maximised the sample mass that is analysed (section 2.4) and re-sampled to improve the depth resolution of $^{137}\text{Cs}_{\text{max}}$. In the present study, the similarity of the post-1950/1953 SAR estimated from pollen and ^{137}Cs indicates that the assumption that $^{137}\text{Cs}_{\text{max}}$ coincides with the year 1953 is reasonable. In the present study, MDC for ^{137}Cs are typically 0.5–1.0 Bq kg⁻¹ of dry sediment (Bq, Becquerel = one disintegration per second).

2.1.3 ^{210}Pb dating

^{210}Pb (half-life 22.3 yr) is a naturally occurring radioisotope that has been widely applied to dating recent sedimentation (i.e., last 150 yrs) in lakes, estuaries and the sea (Fig. 2.2). ^{210}Pb is an intermediate decay product in the uranium-238 decay series and has a radioactive decay constant (k) of 0.03114 yr⁻¹. The intermediate parent radioisotope radium-226 (^{226}Ra , half-life 1622 years) yields the inert gas radon-222 (^{222}Rn , half-life 3.83 days), which decays through several short-lived radioisotopes to produce ^{210}Pb . ^{226}Ra in estuarine sediments is supplied by catchment sediment inputs and ^{210}Pb derived from the *in situ* decay of ^{226}Ra is termed the supported ^{210}Pb (Oldfield and Appleby, 1984). A proportion of the ^{222}Rn gas diffuses from catchment soils into the atmosphere. Decay of ^{222}Rn in the atmosphere forms ^{210}Pb , which is deposited at the earth surface by dry deposition or with rainfall. Some of this atmospheric ^{210}Pb component is incorporated into catchment soils and is subsequently eroded and deposited in estuaries. Both the direct and indirect (i.e., soil inputs) atmospheric ^{210}Pb input to receiving environments, such as estuaries, is termed the unsupported or excess ^{210}Pb .

The concentration profile of unsupported ^{210}Pb in sediments is the basis for ^{210}Pb dating. It is assumed that supported ^{210}Pb and ^{226}Ra concentrations are in equilibrium, which is reasonable given the substantially longer ^{226}Ra half-life. The unsupported ^{210}Pb concentration is the component of the total ^{210}Pb concentration in excess of the

supported ^{210}Pb value, which in turn is estimated from the ^{226}Ra assay. The validity of the ^{210}Pb dating rests on how accurately the ^{210}Pb delivery processes to the inlet are modelled, and in particular the rates of ^{210}Pb and sediment inputs (i.e., constant versus time variable).

At Pauatahanui, large-scale landcover changes over the last 150 years or so, due to catchment deforestation and conversion to pasture, and the planting of pine forests and urbanisation of the Browns Bay and Whitby sub-catchments during the last 30 years have resulted in substantial increases in catchment sediment loads (Healy, 1980; Curry, 1981). Consequently, sedimentation rates in the inlet are also likely to have increased.

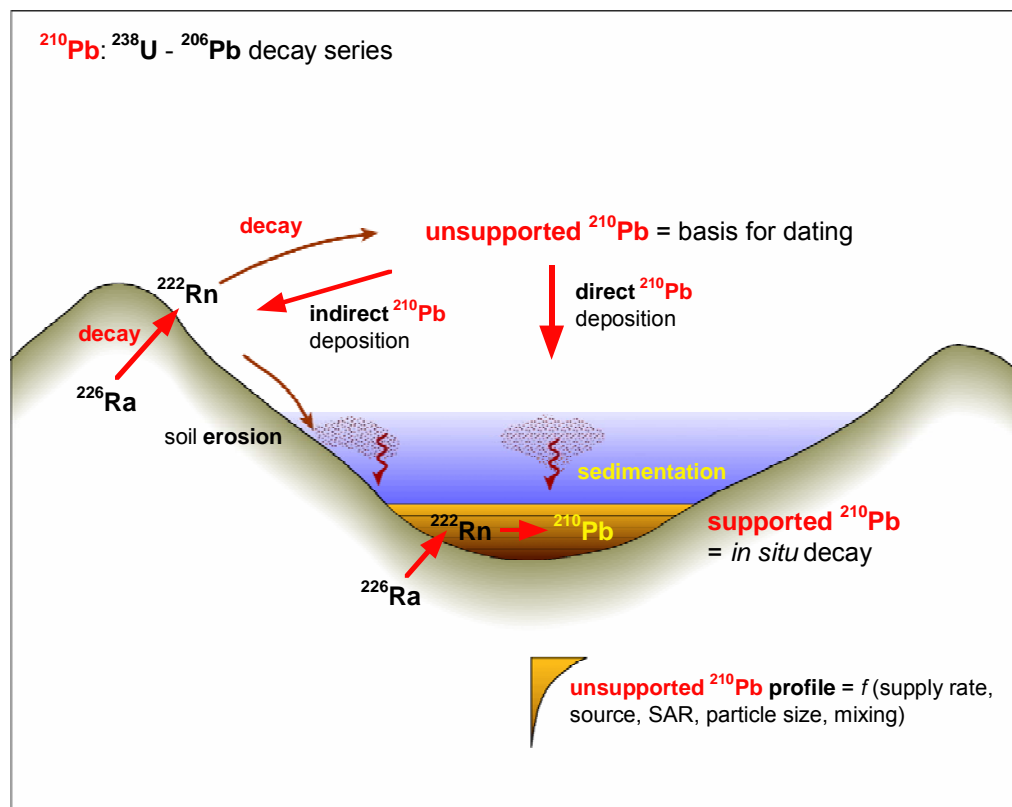


Figure 2.2: ^{210}Pb pathways to estuarine sediments.

There are two possible models that can be applied to date ^{210}Pb profiles under varying sediment accumulation rates (SAR): (1) constant initial concentration (CIC) and (2) constant rate of supply (CRS) models. The usual output from these dating models are ~annual time series of mass deposition fluxes (i.e., $\text{g cm}^{-2} \text{yr}^{-1}$) and sedimentation rates (i.e., mm yr^{-1}). These models have been successfully applied in several Auckland estuaries (Swales et al. 2002b). However, we have not attempted to apply these

models to the Pauatahanui cores because of the depth and intensity of sediment mixing by physical and biological processes. At Pauatahanui, sediment mixing extends to ≤ 14 cm depth. The estimated residence times of sediment in these surface mixed layers are 18–56 years (section 3) so that it is inappropriate to estimate \sim annual sedimentation time-series from these data. Instead, we estimate time-averaged SAR for several historical time periods during the last ~ 150 years. Details of the CIC and CRS models are presented in Appendix I.

^{210}Pb Inventories and Mean Annual Supply Rates

The total unsupported ^{210}Pb inventory in the sediment column, $A(o)$ and mean annual supply rate (P) can be estimated from sediment cores and provide important information about sediment processes in estuaries. P ($\text{Bq cm}^{-2} \text{ yr}^{-1}$) can be estimated from $A(o)$ (Bq cm^{-2}) by:

$$P = kA(o) \quad \text{Eq. 1}$$

$A(o)$ was estimated for each core from log-linear regression fits to the unsupported ^{210}Pb profile and cubic-spline fits to the dry bulk sediment density (ρ_d) data, then integrated at 0.2-cm intervals to 50-cm depth. The $A(o)$ values were checked using equations A4 and A5 based on the theoretical $A(o)$ value constrained by the age of the maximum ^{137}Cs depth corrected for surface mixing (Appendix One). The differences between the constrained and unconstrained $A(o)$ estimates were $\leq 15\%$ (average 7%). These differences are acceptable given the uncertainty in the maximum ^{137}Cs depth due to sediment mixing.

If sedimentation is spatially uniform and occurs at a constant rate then $A(o)$ and P will be similar for each core. Furthermore, P estimated from sediment cores should also be similar to the measured annual atmospheric ^{210}Pb flux if atmospheric deposition is the primary source. This comparison is also a useful test of the validity of the ^{210}Pb chronology determined for a core. Global atmospheric fluxes of ^{210}Pb are typically $0.0074\text{--}0.037 \text{ Bq cm}^{-1} \text{ yr}^{-1}$ (Oldfield and Appleby, 1984). In New Zealand, the mean annual atmospheric ^{210}Pb flux of 0.0117 (range: $0.0086\text{--}0.0136$) $\text{Bq cm}^{-2} \text{ yr}^{-1}$ measured at Hokitika during 1995–2000 is within the range of global values (Tinker and Pilvio, 2000). The mean annual atmospheric ^{210}Pb flux at Pauatahanui is likely to be less than at Hokitika due to the substantially lower annual rainfall. NIWA has measured monthly ^{210}Pb fluxes in rainwater collected at Pakuranga (Auckland) since June 2002. Measured annual ^{210}Pb fluxes to June 2004 averaged $0.0059 \text{ Bq cm}^{-2} \text{ yr}^{-1}$. The mean annual rainfall at Judgeford (station E14199, elevation 24 m), in the lower reaches of the Pauatahanui sub-catchment (1979–2002) of 1140 mm yr^{-1} (standard deviation

± 173 mm) is similar to the mean annual rainfall at Pakuranga (station C64983, elevation 30 m) of 1233 mm yr^{-1} ($s \pm 182$ mm) for the same time period. Thus, it is reasonable to apply the atmospheric ^{210}Pb flux measured at Pakuranga to model and validate the unsupported ^{210}Pb profiles measured in the Pauatahanui sediment cores.

Sediment Mixing

Biological and physical processes, such as the burrowing and feeding activities of animals and/or sediment resuspension by waves mix the upper sediment column. As a result, sediment profiles are modified and limits the temporal resolution of dating. At worst, sediment stratigraphy can be completely erased. Various mathematical models have been proposed to take into account the effects of bioturbation on ^{210}Pb concentration profiles (e.g., Guinasso and Schink, 1975). Biological mixing has been modelled as a one-dimensional particle-diffusion process (Goldberg and Kiode, 1962) and this approach is based on the assumption that the sum effect of ‘random’ biological mixing is integrated over time. In estuarine sediments exposed to bioturbation, the depth profile of unsupported ^{210}Pb typically shows a two-layer form, with a surface layer of relatively constant unsupported ^{210}Pb concentration overlying a zone of exponential decrease (e.g., Fig. 3.6a). In applying these types of models, the assumption is made that the mixing intensity (i.e., Diffusion co-efficient) and mixing depth (i.e., surface-mixed layer, SML) are uniform in time.

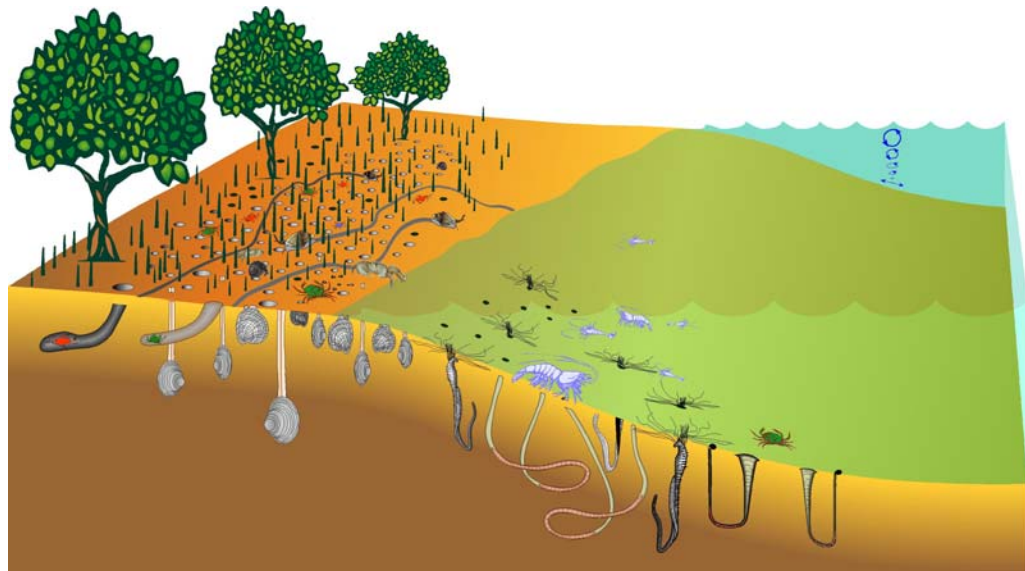


Figure 2.3: Biological and physical processes, such as the burrowing and feeding activities of animals and/or sediment resuspension by waves mix the upper sediment column. As a result, sediment profiles are modified and limits the temporal resolution of dating. The surface mixed layer (SML) is the yellow zone.

The validity of this assumption usually cannot be tested, but changes in bioturbation process could be expected to follow changes in benthic community composition. X-radiography is also useful to identify bioturbation structures in sediment cores (section 2.4.2).

In order to more fully evaluate and support time-averaged SAR and mixing observed in the Pauatahanui inlet cores, the depth profiles of unsupported ^{210}Pb and estimates of sedimentation rate, mixing rate and mixing depth are compared with results from a one-dimensional analytical model for steady-state sedimentation, sediment mixing and radioactive decay (Aller, 1982). The model assumes steady state conditions:

- constant flux of ^{210}Pb to the inlet bed;
- constant mixing depth and rate; and
- constant SAR.

Sedimentary processes in the inlet are extremely dynamic and variable, and the steady state assumptions for this model do not strictly apply. Accordingly, we are using the model as a diagnostic tool, rather than a strict portrayal of actual conditions within the inlet. Nevertheless, model results do provide significant insights into depositional processes within the Pauatahanui inlet and guide our interpretation of the sediment core data.

The general equations above and below the mixing depth, L , (i.e., surface mixed layer) are respectively:

$$\frac{\partial A}{\partial t} = 0 = D \left(\frac{\partial^2 A}{\partial z^2} \right) - \omega \left(\frac{\partial A}{\partial z} \right) - kA \quad \text{Eq. 2}$$

$$\frac{\partial A}{\partial t} = 0 = -\omega \left(\frac{\partial A}{\partial z} \right) - kA \quad \text{Eq. 3}$$

where A is unsupported ^{210}Pb concentration per unit volume of sediment (Bq cm^{-3}), z is depth in the seabed (cm), D is the bio-diffusion coefficient ($\text{cm}^2 \text{ yr}^{-1}$), k is the radioactive decay constant for ^{210}Pb (0.03114 yr^{-1}), and ω is the sediment accumulation rate (cm yr^{-1}). The first term on the right-hand side of equation 2

accounts for changes in unsupported ^{210}Pb concentration due to sediment mixing. The second term accounts for changes due to sedimentation rate and the third term for radioactive decay. The boundary conditions are:

1. $z=0, P = D(\partial A/\partial z) - \omega A$
2. $z = L, A_1 = A_2$
3. $z = L, \partial A/\partial z = 0$
4. $z \rightarrow \infty, A_2(z) = 0$

where P is the excess ^{210}Pb flux to the sediment water interface ($\text{Bq cm}^2 \text{ yr}^{-1}$). The solution to Eq. 2 and 3 is provided in Appendix II.

In order to model the ^{210}Pb profiles, we must specify the flux of ^{210}Pb to the seabed, the mixing depth and rate, and the SAR. Mixing depths were derived from analysis of x-radiographs and unsupported ^{210}Pb profiles and SAR were estimated from regression fits to the unsupported ^{210}Pb profiles observed in cores. The atmospheric ^{210}Pb flux (P) of $\sim 0.006 \text{ Bq cm}^{-2} \text{ yr}^{-1}$ measured by NIWA at Pakuranga (Auckland) is applied here. This is reasonable given the similar long-term average annual rainfalls at Pakuranga and Pauatahanui (section 2.1.1). Because natural depositional processes in the inlet accumulates sediment and particle-associated unsupported ^{210}Pb , so that local inventories exceed that expected from atmospheric deposition alone, a concentration factor (P_x) was introduced (making the modelled ^{210}Pb flux for each core the product of P and P_x), and adjusted as needed to produce a reasonable model fit. As an additional check, measured core inventories of unsupported ^{210}Pb compared favourably with modelled values. The values for D , L , P_x , and SAR were adjusted iteratively until a reasonable fit between model and data was achieved.

2.1.4 Pollen dating

Historical landcover changes, such as catchment deforestation, establishment of pasture, plantation forestry or urbanisation alter the composition of the pollen assemblage. Pollen is delivered to estuaries by direct atmospheric deposition and by eroded catchment soil. Thus, changes in the abundances of plant pollen in estuarine sediments can be used for dating deposits if the history of catchment landcover change is known. The uncertainty in dating sediment cores using pollen largely depends on two factors: (1) the degree of *in situ* sediment mixing, the efficiency of which declines as sedimentation rate increase and (2) the time lag between the initial introduction of new plant species and the production of sufficient pollen to be detectable in the stratigraphic record. The time lag for pollen production varies between plant species. New Zealand native trees take up to 50 years to reach full reproductive maturity

whereas the introduced pine, *Pinus radiata*, develops a substantial pollen rain within 10 years. Grasses, weeds and other short-lived plants flower immediately and enter the stratigraphic record quickly. We assume a pollen dating uncertainty of ~10 yr, based on the time lag for pine pollen production and detection in estuarine sediments.

Pollen grains and spores (palynomorphs) are produced in huge numbers by conifers, flowering plants, ferns, and fern allies. Most palynomorphs are in the size range 5–120 µm, and thus can be easily transported by wind or water. In the presence of oxygen and moisture the cytoplasm decays rapidly, but the tough, decay-resistant outer wall tends to persist although it will eventually breakdown. If sediments are water-saturated, and thus oxygen levels are reduced to very low levels, the outer walls can persist indefinitely. A cubic centimetre of most soils and estuarine sediments will contain thousands of pollen grains and spores. Palynomorphs are most often identified to a familial or generic level, although a substantial number can be attributed to one or several closely related species.

There are three main pathways by which palynomorphs are incorporated into estuarine stratigraphic record (Fig. 2.4):

- airborne palynomorphs may fall directly onto the surface of the inlet or the overlying water mass;
- palynomorphs drop directly onto the surface of catchment soils and waterways and are carried to the inlet;
- palynomorphs in catchment soils, rocks and other sediments are reworked (10^1 – 10^6 yr after initial deposition) and transported down stream networks and into the inlet.

The final palynomorph assemblage will always reflect varying proportions of these three pathways. Airborne palynomorphs suffer no corrosion and little breakage before incorporation in sediments. Palynomorphs reworked along waterways will show some corrosion or breakage if they spend time in sediments along stream-banks and beds where bacteria are active. Soils, however, have a dramatic effect on palynomorphs. Fern spores are highly resistant to corrosion, but flowering plant pollen is highly susceptible and conifers have intermediate resistance to corrosion. The longer a collection of palynomorphs is in the soil, the more fern spores and, in particular, tree fern spores will dominate. A well-drained (aerated) soil will lose nearly all palynomorphs except for extensively corroded tree-fern spores. Thus, an estuarine

sediment dominated by tree-fern spores is nearly always the result of a pollen source dominated by eroded catchment soils.

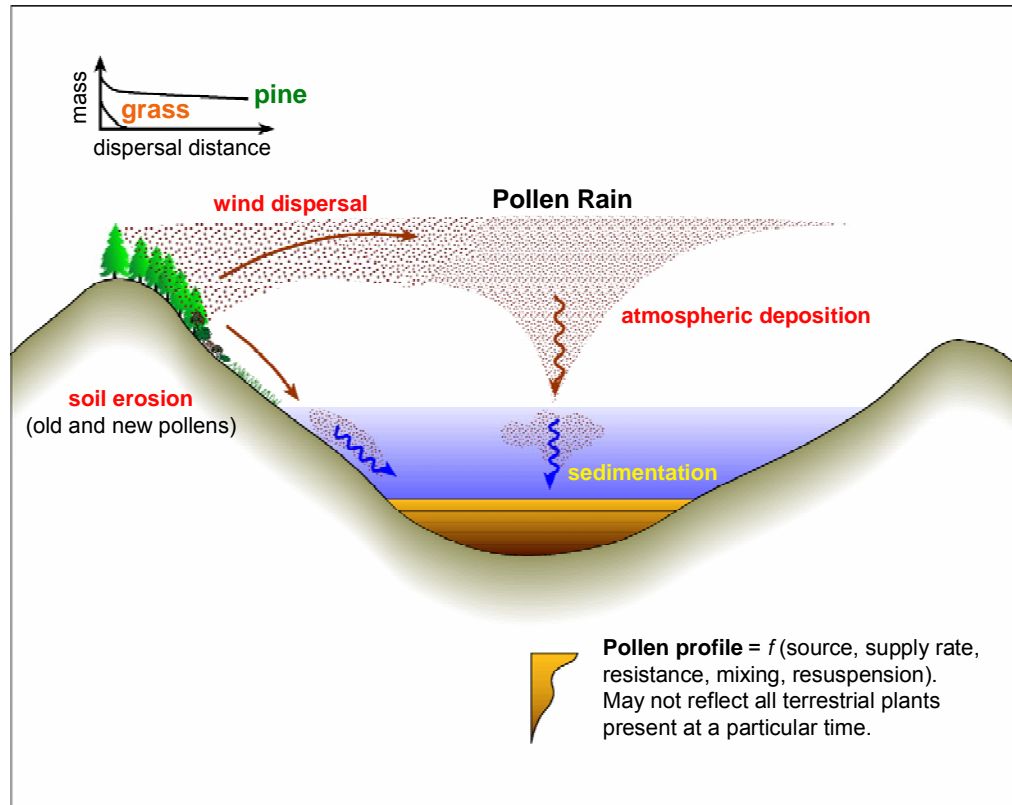


Figure 2.4: Pollen pathways to estuarine sediments.

Major pollen assemblages and their interpretation

At Pauatahanui, catchment landcover was originally dominated by a podocarp-hardwood forest dominated by totara (*Podocarpus totara*), matai (*Prumnopitys taxifolia*), rimu (*Dacrydium cupressinum*), kahikatea (*Dacrydium dacrydioides*), pukatea (*Laurelia novae-zelandiae*); rata (*Metrosideros robusta*); maire (*Nestegis* spp.); and hinau (*Elaeocarpus dentatus*). Associated with these over-storey trees would have been a variety of lower broadleaved trees, shrubs, vines and tree ferns (Mildenhall, 1979; Page et al. 2004). Unlike many areas of New Zealand, Maori had made little impression on the continuous bush cover of the inlet before European settlement began in the 1840's (Healy, 1980). Consequently, the clearance of relatively small areas for cultivation by Maori had a minimal impact on the pollen rain delivered to the inlet.

Bracken (*Pteridium esculentum*) spores are produced in large numbers, and are wind-dispersed and corrosion-resistant. In the Auckland region, bracken and scrub covered large areas after Maori settlement and forest clearance. By comparison at Pauatahanui, the bracken contribution to the pollen rain was negligible before European settlement. In the aftermath of catchment deforestation, bracken was common but was gradually eliminated by improved pasture cultivation and the introduction of improved herbicides in the 1950's. Also, soils rich in bracken spores can continue to provide a steady influx of bracken spores to estuaries even when bracken has been nearly eliminated from the local area (Wilmshurst et al. 1999).

Pine (*Pinus*) pollen is probably the most abundantly produced and widely distributed of all types (exotic and native) in the New Zealand flora. Slicks of yellow pollen that are particularly noticeable after rain on suburban streets are often derived from pine plantations many kilometres distant. At Pauatahanui, pine plantations accounted for less than 1% of the catchment area before the mid-1970's (Page et al. 2004), so that they had a relatively minor impact on the local and regional pollen rain. Large-scale exotic forest plantations (largely pine) were established from the mid-1970's and by 2000 accounted for ~18% of catchment landcover. A large proportion of this planting occurred in the Kakaho (42%), Horokiri (40%) and Pauatahanui (27%) sub-catchments.

Pine trees begin to flower as soon as five years after planting. However, pine pollen production depends on tree size and the distance pollen is dispersed is proportional to the height above the ground at which it is released. Pollen production from a pine plantation therefore gradually increases over time, reflecting the number of saplings coming into flower (as all the trees are not planted at once), tree height and the foliage coverage. Pollen contributions from a plantation should first become apparent after 5 years, but the full effect is delayed until ~10 years after planting. At Pauatahanui, the prevailing north-westerly/north-easterly winds would transport pine pollen from the Kakaho and Horokiri sub-catchments into the inlet. Pine pollen would also be supplied by sediment runoff. Consequently, pine pollen production would have substantially increased from the mid-1980's.

In interpreting the pine pollen signal in our cores, we assume a typical sigmoidal growth curve, in that after an initial period of rapid increase, the rate of pine growth declines and eventually plateaus as maturity is reached. This sigmoidal growth pattern is mirrored in the pollen production, with an initial rapid increase, which eventually stabilises to roughly uniform level of year-to-year pollen production. This pattern has been observed in a regional study of sedimentation in Auckland estuaries (Swales et al. 2002b).

Grass (*Poaceae*) is now the predominant non-urban land cover, although lawns and verges within urban areas are also sources of grass pollen. However, the pollen of grass species are often not well represented in estuarine sediments, which likely reflects relatively low pollen dispersal rates in comparison to other exotic species such as pine.

Historical zone definition

Four pollen assemblages characteristic of discrete historical periods are identified in the Pauatahanui sediment cores, which includes the original native forest and historical landcover changes since Maori settlement:

- *Zone I: Pre-farming* (before 1850 AD), characterised by the native podocarp-hardwood association and the absence of introduced weeds (e.g., *Taraxacum*, (dandelion) and *Rumex* (dock-sorrel)), grasses and pine.
- *Zone II: Early-farming* (1850–1950 AD), characterised by high levels of bracken (*Pteridium esculentum*) following catchment deforestation and its gradual elimination by improved pasture cultivation and herbicides in the 1950's.
- *Zone III: Late-farming* (1950–1985 AD): Reduction of bracken, improved farming techniques and an expansion of pine plantations after the mid-70s characterise this period. The boom in pine planting after 1975 is not reflected immediately in the pollen record because the pines take up to 10 years to begin to produce pollen in any quantity. Comparison of the ¹³⁷Cs limit with pine pollen percentages at the same level, suggests that pine percentages ranged from 1-8% at the beginning of the period. This zone is recognised by increasing grass and pine and falling bracken pollen content.
- *Zone IV: 1985-2004*: Major changes in the catchment included urbanisation and pine plantations coming into flower. Massive pollen production from the plantings in the 1970s is registered after 1985, which is defined by the start of a rapid increase in the pine pollen content of estuarine sediments. Grass levels stabilise. At the sediment surface, pine pollen concentrations vary between 20–70% (average c. 40%), and are unrelated to the pine cover of the adjacent catchment. A more likely explanation is the immediate reworking of pine pollen around the inlet following initial delivery. Pine pollen percentages tend to level off or fluctuate in the upper few cm of most of the profiles which is likely to represent mixing of the upper sediment. Most of

the pollen diagrams show an upsurge in large charcoal particles during this zone which could be a result of increasing urbanisation and household fires, as well as clearance for pine plantations.

2.1.5 Radiocarbon dating

Radiocarbon (^{14}C) dating has been widely applied to sedimentation studies in NZ estuaries and is suitable for dating the remains of plants and animals older than about 500 years. Atmospheric carbon dioxide in the atmosphere is composed of carbon-12 (^{12}C), and a small proportion of radioactive ^{14}C . ^{14}C radioactively decays to nitrogen-14 with a half-life of 5,730 years, so the measured $^{14}\text{C}/^{12}\text{C}$ ratio remaining in a sample is used to estimate the radiocarbon age. Any material that was at one time living can be dated using ^{14}C to a limit of about 70,000 years before present (B.P., 1950 AD).

In estuarine and marine environments, carbonate shells of bivalves and molluscs are particularly suitable for ^{14}C dating. As little as ~5 g of shell can be dated, although larger samples are preferred. Samples smaller than 1 gm can be dated by Acceleration Mass Spectrometry (AMS). Caution is required in selecting samples for dating because 'old' shell can be reworked from old sediments and re-deposited at a higher level in the stratigraphic record. This results in an over-estimation of the age of sediments. Reworking of old shell occurs when channels migrate, and on intertidal flats where waves are energetic. Also shellfish that burrow to substantial depths in the sediment column and subsequently die will result in under-estimation of the age of sediments at that depth. As such, whole, dis-articulated and un-abraded (i.e., no transport) shell valves are most suitable for radiocarbon dating. ^{14}C dating provides a useful tool to estimate long-term average SAR for estuaries based on dating of suitable samples buried at depth in the sediment column. More detailed information on radiocarbon dating is provided in Appendix III.

2.2 Sediment accumulation rates (SAR)

Changes in sedimentation rates in estuaries provide by far the strongest evidence for the effects of catchment sediment runoff on estuarine systems.

Sedimentation rates are measured by calculating the thickness of sediment between dated layers in cores. The layers are dated ideally using complimentary methods as previously discussed in this report. Sedimentation rates calculated from cores are ***net average sediment accumulation rates (SAR), which are usually expressed as mm yr⁻¹***. These SAR are net values because cores integrate the effects of all the processes, which influence sedimentation at a given location usually over years,

decades or centuries. However, at short time-scales (i.e., seconds–months), sediment may be deposited and then subsequently re-suspended by tidal currents and/or waves. Thus, over the long-term, sedimentation rates derived from cores represent net or cumulative effect of potentially many cycles of sediment deposition and re-suspension. However, least disrupted sedimentation histories are found in depositional environments where sediment mixing due to physical processes (e.g., re-suspension) and bioturbation is limited. The effects of bioturbation on sediment profiles and dating resolution reduce as SAR increase (Valette-Silver, 1993).

Net sedimentation rates statistics also mask the fact that inlet sedimentation is an episodic process, which largely occurs during catchment floods, rather than the continuous gradual process that is implied. For example, the June 1975 flood (5-year return period) delivered an estimated ~10,000 tonnes of suspended sediment to the Pauatahanui inlet.

Although sedimentation rates are usually expressed as a sediment thickness deposited per unit time (i.e., mm yr⁻¹) this statistic does not account for changes in dry sediment mass with depth in the sediment column due to compaction. Typically, sediment density ($\rho = \text{g cm}^{-3}$) increases with depth and therefore some workers prefer to calculate dry mass accumulation rates per unit area per unit time (g cm⁻² yr⁻¹). These data can be used to estimate the total mass of sedimentation in an inlet (tonnes yr⁻¹) (e.g., Swales et al. 1997). However, in our experience of estuarine cores (up to 4 m long) the effects of compaction are often offset by changes in bulk sediment density reflecting layering of low-density mud (i.e., dry density <1 g cm⁻³) and higher-density (i.e., dry density, ρ_d , >1 g cm⁻³) sand deposits. Furthermore, the significance of a SAR expressed as mm yr⁻¹ is more readily grasped than a dry-mass sedimentation rate in g cm⁻³ yr⁻¹. For example, the rate of estuary aging due to sedimentation (mm yr⁻¹) can be directly compared with the potential mitigating effect of local sea level rise (mm yr⁻¹).

2.2.1 SAR from ²¹⁰Pb dating

In this study, we calculate an average sediment accumulation rate for the zone of exponential ²¹⁰Pb concentration decrease. In some cases surface mixing is absent but typically a surface mixed layer (SML) ≤ 14 cm thick is apparent from the ²¹⁰Pb profiles. The rate of ²¹⁰Pb concentration decrease with depth can be used to calculate a net sediment accumulation rate. Given an initial unsupported ²¹⁰Pb concentration (C_0), the value of C (Bq kg⁻²) will decline exponentially with age (t):

$$C_t = C_0 e^{-kt} \quad \text{Eq. 4}$$

Assuming that within a finite time period, sedimentation (S) or SAR is constant then $t = z/S$ can be substituted into Eq. 4 and by re-arrangement:

$$\frac{\ln\left[\frac{C_t}{C_0}\right]}{z} = -k/S \quad \text{Eq. 5}$$

For an exponential decay model, a depth profile of $\ln(C)$ should yield a straight line of slope $b = -k/S$. We fitted a linear regression model to natural-log transformed ^{210}Pb concentration data to calculate b . The sedimentation rate over the depth of the fitted data is given by:

$$S = -(k)/b \quad \text{Eq. 6}$$

An advantage of this method is that the sedimentation rate is based on the entire ^{210}Pb profile rather than a single layer, as is the case for ^{137}Cs . Furthermore, if the pollen or ^{137}Cs tracer is present at the bottom of the core then the estimated SAR is a minimum value. The SAR found by the ^{210}Pb method can also be used to estimate the residence time (R) of sediment particles in the SML before they are removed by burial. For example, given an SML (L) depth of 100 mm and S of 2 mm yr⁻¹ then $R = L/S = 50$ years. Although this greatly simplifies the process (i.e., the likelihood of particle mixing reduces with depth in the SML), this approach provides a useful measure of the relative effect of sediment mixing between cores, sub-environments and estuaries.

2.2.2 SAR from pollen and ^{137}Cs dating

Four dated depth horizons were identified using the pollen and ^{137}Cs data:

- **1850 AD:** based on the decline in native forest species, the rise of bracken as catchment deforestation proceeded, the appearance of exotic grasses and only trace quantities of pine.
- **1950 AD:** recognised by increasing pine pollen abundance and declining bracken.
- **1953 AD:** based on the maximum depth of ^{137}Cs occurrence in the sediment column.

- **1985 AD:** recognised by rapidly increasing pine pollen abundance. Pine pollen content exceeding 20% and reaching 70% of the terrestrial pollen sum.

Time-averaged SAR were estimated for four time periods based on the pollen and ^{137}Cs dated horizons and corrected for sediment mixing depths (section 3.2.1):

- 1850–2004 AD (pollen).
- 1950–2004 AD (pollen).
- 1953–2004 AD (^{137}Cs).
- 1985–2004 AD (pollen).

2.3 Field studies

Antecedent Conditions

Sediment cores were collected during late April 2004, some two months after the 15–16 February storm, which caused landslides and flooding in parts of the Greater Wellington Region (Watts and Gordon, 2004). The Pauatahanui area was relatively unaffected by the storm, with twenty-four hour rainfall totals of < 70 mm, in comparison to more than 200 mm in the Orongorongo, Wainuiomata and Lower Hutt catchments. The peak flow in the Porirua River at Town Centre of $50 \text{ m}^3 \text{ s}^{-1}$ (0615 NZST, 16/2/2005) had an estimated return period of six years in comparison to 50 years or more at sites elsewhere in the region (Table 2, Watts and Gordon, 2004). The presence of silt-laden water in the Mana Marina during the storm (Marina manager, pers comm., April 2004) may have been due to stormwater runoff and/or sediment resuspension by waves generated by strong winds that accompanied the storm. The hydrological data suggest that the February 2004 storm was not a large-magnitude event in terms of sediment delivery to Pauatahanui inlet.

Sediment Coring

Sediment core locations were determined in consultation with GWRC and PCC. Sampling was designed to differentiate between sedimentation adjacent to sub-catchment outlets and in the central mud basin. Subtidal cores were favoured because sediments were less likely to be affected by post-depositional physical mixing than intertidal sediments. This is supported by (1) previous analysis of aerial photographs

(Healy, 1980) which show that the intertidal flats adjacent to sub-catchment outlets have experienced substantial morphological changes due to channel migration associated with delta construction. As a result there was a risk that we would sample deeply reworked sediments; (2) intertidal sediments are also likely to be reworked more intensely and more frequently by waves than subtidal sediments (Pickrill, 1979). This is because the orbital motions under short-period waves, which are typical of fetch-limited estuaries, are rapidly attenuated in the water column. As a consequence, wave orbital motions are generally more energetic on intertidal than on subtidal flats; (3) winnowing of silt and clay from intertidal flats by waves will focus fine sediment deposition in subtidal environments. Furthermore, contaminants such as heavy metals, as well as radioisotopes used for sediment dating are largely associated with these fine sediments.

Nine subtidal core sites were selected, with five sites at sub-catchment outlets and four sites located in the central mud basin (Fig. 1.3). The location of each core site was fixed to ± 1 m using differential global positioning (DGPS), which are listed in Appendix IV. The PAT, BAS1 and BAS4 sites were also located in proximity to the original PEP study long cores 1–3 (Healy, 1980, Fig. 21).

A mix of large-diameter (10 cm) short (0.4 m) and smaller diameter (5-cm) long (< 2 m) subtidal sediment cores were collected in PVC tubes at each site to ensure that: (1) we could finely resolve the inlet's sedimentation history during the last 40 years or so, which coincides with initial urban development and the establishment of exotic forestry since the mid 1970's. From experience in other North Island estuaries, this most recent time period of landcover change is preserved in the upper ≤ 0.5 m of the sediment column; (2) the sedimentation history during at least the last 150 years was sampled.

Large diameter short cores are required for radioisotope analysis to minimise the uncertainty in ^{210}Pb and ^{137}Cs concentrations. This relates to the fact that the uncertainty reduces with increasing sample size. From experience, a 10-cm diameter core typically provides 50–80 g per 1-cm depth increment, which substantially reduces analytical uncertainties. An alternative would be to collect smaller diameter cores but sampled at larger depth increments. This reduces the temporal resolution of the dated profiles because the measured radioisotope concentration is averaged over a longer time period.

Sediment coring was undertaken during 27–29 April 2004 from R.V. Rangitahi, a 6 metre catamaran operated by NIWA. Three 10 cm diameter short cores were collected within a 1 m² area of seabed by SCUBA divers. The PVC plastic core barrels were

driven into the substrate using a sledgehammer and specially designed steel end cap to minimise disturbance of surface sediments. Because of the relatively large core diameter and low density subtidal sediment, core compression (the difference between the driven and retained core length) was negligible (i.e., < 2%). One core was selected for detailed sediment dating, particle size and heavy metal analysis and another core was used for x-ray imaging (section 2.4). The third core from each site was frozen immediately on return to NIWA on 30 April 2004.

Long cores were collected using a 50 mm diameter Livingston piston corer, which is particularly suitable for shallow estuarine applications. This is because the piston system creates a partial vacuum at the sediment surface, which minimises sediment compression due to friction as the PVC core barrel penetrates the sediment column. The long cores were collected within ± 25 m of the short core locations. Details of Livingston cores collected are listed in Appendix V.

Wave Gauges

DOBIE wave gauges fitted with Downing Model-3 infra-red optical backscatter sensors (OBS) were also deployed by NIWA at the BAS2 and DUK core sites for seven weeks from 29 April 2004. The OBS response varies linearly with suspended sediment concentrations (SSC) up to concentrations of the order of $\sim 10^3$ mg l⁻¹ and is ten times more sensitive to silt than sand (Bunt et al. 1999). Although these data do not form part of the GWRC–PCC commissioned study, we discuss these data in section 5 to further elucidate sediment processes in the inlet.

2.4 Laboratory analyses

2.4.1 Core sub-sampling

In the laboratory, the dating short cores were split and 1-cm-thick slices sub-sampled at 0–1, 2–3, 4–5, 6–7, 9–10 cm and then at 5-cm depth intervals down to the base of the core at 39–40 cm. Additional samples were collected to: (1) reduce the uncertainty in the maximum ¹³⁷Cs depth (11 samples in total) and thereby better estimate the time-averaged SAR for the time period since 1953; and (2) sample unsupported ²¹⁰Pb and ¹³⁷Cs profiles at sites BRN and BAS2 (2 samples each), from the long cores, where they may have extended below 40 cm depth. The more frequent sampling in the upper part of the core reflects the fact that a large proportion of the unsupported ²¹⁰Pb occurs in the top-most 10 cm of the sediment column. A 39 cm³ half-slice was taken to provide a nominal ~ 60 g of dry sediment for radioisotope analysis, which is the maximum amount that can presently be embedded in epoxy

resin for gamma spectrometry. Samples were weighed, dried at 105°C for 24 hours, re-weighed after 30 minutes cooling and ground to a coarse powder. The wet and dry weights of the samples were used to calculate wet and dry bulk sediment densities (g cm^{-3}) and water contents. The remaining half-slice of each sample was homogenised and 1 cm^3 taken for particle size analysis, with the remaining bulk of the half slice used for heavy metal analysis and pollen dating.

2.4.2 X-radiography

X-radiographs of the upper 0.4 m of the sediment column were prepared from the “B” short core collected at each site. Each 10-cm diameter core was split longitudinally and a 2-cm thick by 0.4 m long slab taken and placed in an open-topped plywood tray. The sediment slabs were imaged by SGS NZ Ltd using a Phillips model 200 Macrotank radiation source and Kodak AA400 film. The slabs were initially exposed at 50 kV and 25 mA for ~ two minutes. Several of the images were under-exposed and re-imaged with 4–5 minute exposures at 50 kV and 25 mA. Variations in sediment density are identified by grey-scale, so that on a negative image relative high density shell and quartz sand (density 2.65 g cm^{-3}) appear white whereas low-density (density $\leq 1 \text{ g cm}^{-3}$) muds are dark grey and wood fragments or voids black. Animal burrows and other biogenic structures are often readily identified because of density differences between the burrow wall or fill and the surrounding substrate. The x-radiographs are used in this study to guide the analysis of the dating cores and ^{210}Pb modelling of sedimentation processes in the inlet. Full-size x-ray images of each core are presented in Appendix VII.

2.4.3 Particle size

Particle size was determined using a Galai CIS-100 ‘time-of-transition’ (TOT) stream-scanning laser particle-sizer operated by NIWA. The sediment sub-samples were wet-sieved through a 2mm sieve to remove leaf and twig fragments and shell hash. Sediment samples were dispersed by ultra-sonic dispersion for four minutes before and during particle size analysis. Typically 10^5 – 10^6 particles were counted per sample. Particle volumes, for spheres, were calculated from the measured particle diameters, which were used to determine the particle-size volume distribution for each sample.

2.4.4 Heavy metals

To enable comparison of heavy metal concentrations in the subtidal sediments with ANZECC (2000) guidelines, total copper, lead and zinc concentrations were

determined on 1 g of dried and ground sediment using a strong acid extraction (10 ml Aqua regia, 1:3 Nitric acid to Hydrochloric acid). Samples were digested at 100–110°C for 3 hours, followed by a further addition and digestion with 5ml Nitric Acid (concentrated) for 1 hour. Digests were decanted, diluted to 50ml and centrifuged to remove any fine particles remaining. Cu, Pb, and Zn concentrations in the supernatant were determined using ICPMS (Inductively-Coupled Plasma Mass Spectrometry). A conservative estimate (i.e., ~twice detection limit) of the accuracy of the Cu and Pb concentrations is $\pm 0.05 \mu\text{g g}^{-1}$ and $\pm 0.1 \mu\text{g g}^{-1}$ for Zn.

2.4.5 Pollen

Sediment samples (2–3 cm³) for pollen analysis were prepared as described by Moore and Webb (1978). Following acid digestion, resistant minerals, pollen and spores were mounted on glass slides. A minimum of 150 pollen grains and spores of terrestrial plants (i.e., all species combined) were counted on regular transects across each slide. The results are presented as percentages of a palynomorph sum including all types. Charcoal shards >50 μm diameter were also counted. Major plant types and charcoal shard counts are presented as depth profiles.

2.4.6 Radioisotopes

Radioisotope concentrations were determined by high resolution, low-level gamma ray spectrometry using a Canberra Model BE5030 50% broad energy range hyper-pure germanium detector. Samples were counted for 23 hours to minimise uncertainties in radioisotope concentrations. The ²²⁶Ra concentrations of the sediment samples were determined from the emissions of the short-lived daughters of the noble gas ²²²Rn gas by embedding samples in epoxy resin. An in-growth period of 30 days allows equilibrium to be reached between ²²⁶Ra and its daughter ²²²Rn. Gamma spectra of ²²⁶Ra, ²¹⁰Pb and ¹³⁷Cs were analysed using Genie2000 software (ver. 3). Radioisotope concentrations are expressed in S.I. units as Becquerel (disintegration s⁻¹) per kilogram (Bq kg⁻¹).

The uncertainty ($U_{2\sigma}$) of the unsupported ²¹⁰Pb concentrations is given by:

$$U_{2\sigma} = \sqrt{({}^{210}\text{Pb}_{2\sigma})^2 + ({}^{226}\text{Ra}_{2\sigma})^2} \quad \text{Eq. 7}$$

where ²¹⁰Pb_{2σ} and ²²⁶Ra_{2σ} are the two standard deviation uncertainties in the total ²¹⁰Pb and ²²⁶Ra concentrations at the 95% confidence level. The primary source of uncertainty in the measurement of radioisotope concentrations relates to the counting

statistics (i.e., variability in the number of detected decay events). This source of uncertainty can be reduced by increasing the sample size. The $U_{2\sigma}$ values of sediment samples in the Pauatahanui cores were in the range 3.2–12.4 Bq kg⁻¹.

In cases where the ²²⁶Ra concentration was higher than the total ²¹⁰Pb concentration (i.e., supported and unsupported ²¹⁰Pb) we assumed that unsupported ²¹⁰Pb was absent in that particular sample and excluded from the regression analysis. The unsupported ²¹⁰Pb profile and time-averaged SAR for each core were calculated, using the fitted regression relation, from the surface to a maximum depth based on Equations 5 and 6. Figure 2.5 shows an example of a linear regression fit to a ²¹⁰Pb profile measured in an estuarine sediment core. It can be seen that the decline in unsupported ²¹⁰Pb concentration with depth in the sediment column is well described by the log-linear regression equation ($r^2=0.96$). Note the absence of a surface mixed layer in this example.

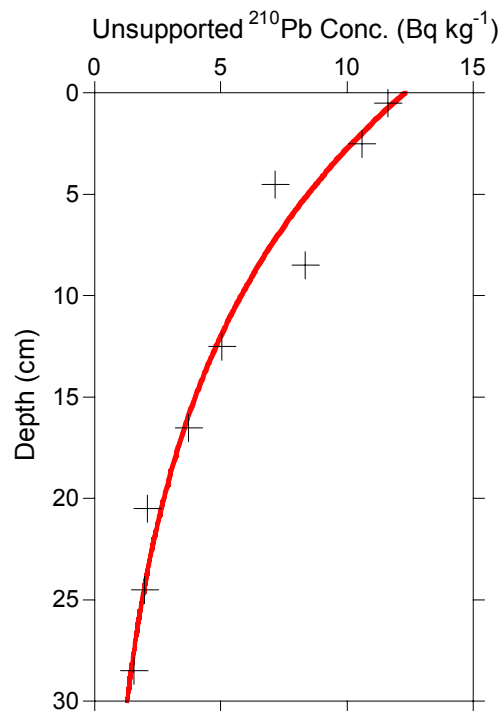


Figure 2.5: Example of log-linear regression fit ($r^2 = 0.96$) to ²¹⁰Pb concentration profile in an estuarine core.

3. Results

3.1 Overview

The Pauatahanui inlet cores show strong evidence of rapid mixing of surficial sediments (≤ 5 cm depth) by physical and biological processes over days–months and deeper (≤ 14 cm depth) but less intense mixing by infauna (i.e., bioturbation) over years–decades. Sediment mixing that occurs in the surface mixed layer (SML) reduces the temporal resolution of the cores as new sediments are mixed with older deposits. The process can be visualised with the SML acting as a filter which smoothes input signals, such as seasonal and annual variations in the pollen rain or sediment and heavy metal loads associated with stormwater runoff. These core mixing characteristics as well as the unsupported ^{210}Pb inventory, $A(o)$, mean annual supply rate (P) and model parameters used to fit the observed unsupported ^{210}Pb profiles are summarised in table 3.1.

The maximum depth of ^7Be occurrence is a useful indicator of short-term (days–months) sediment mixing because of its relatively short half-life (53.3 days). Thus physical processes such as sediment resuspension by waves and the feeding and burrowing activities of benthic infauna (section 1.4) rapidly homogenise the upper 2–5 cm of the sediment column. The x-radiographs and modelling of the unsupported ^{210}Pb profiles shows that the SML extends to 7–14 cm depth and primarily results from the activities of benthic infauna. This bioturbation occurs over time scales of years–decades. The biodiffusion co-efficient (D) also provides a measure of the relative intensity of sediment mixing. Thus, the intensity and depth of sediment mixing is substantially lower in the Browns Bay (BRN) core in comparison to the site-one basin core (BAS1).

The ^{210}Pb inventories, $A(o)$ and mean annual supply rates (P) for each core provide important information about sedimentation processes in the inlet. If direct atmospheric deposition is the dominant ^{210}Pb transport pathway to the inlet sediments then the P derived from cores should be similar to the atmospheric flux (~ 0.006 Bq cm^{-2} yr^{-1}). Table 3.1 shows that the mean annual supply rates derived from the cores are 1.5–2.5 times the atmospheric flux, which indicates unsupported ^{210}Pb is also supplied to the inlet from other sources. The likely indirect sources of unsupported ^{210}Pb are: (1) eroded catchment topsoil and (2) oceanic water delivered by tidal flows, which typically have higher ^{210}Pb concentrations than freshwater. This latter effect is observed in the Hauraki Gulf, where concentrations of unsupported ^{210}Pb in surficial sediments (~ 100 Bq kg^{-1}) are an order of magnitude higher than in Auckland east coast estuaries (Swales et al. 2002b and unpublished NIWA data).

Unsupported ^{210}Pb is largely associated with the clay and fine silt fraction of sediments. The fact that the ^{210}Pb inventories ($0.25\text{--}0.47\text{ Bq cm}^{-2}$) vary between core sites is indicative of winnowing and concentration of these fine sediments due to resuspension and subsequent redeposition in quiescent settling zones, such as the central mud basin. For example, $A(o)$ values for the BAS3, DUK and PAT sites ($0.25\text{--}0.30\text{ Bq cm}^{-2}$) are $\sim 70\%$ of inventories in the central mud basin (BAS1, BAS2, BAS4). This spatial pattern is consistent with the prevailing north-west – south-east winds which generate waves in the inlet. Thus, sedimentary processes in the Pauatahanui inlet are extremely dynamic and variable. The upper decimetre of the sediment column is mixed by physical and biological processes and redistribution of fine sediments by resuspension and subsequent redeposition in sediment sinks, such as the central mud basin.

Table 3.1: Summary of radioisotope results for Pauatahanui inlet short cores and parameters for modelling observed unsupported ^{210}Pb profiles. **Cores:** $^7\text{Be}_{\text{max}}$ and $^{137}\text{Cs}_{\text{max}}$ are the maximum depths of ^7Be and ^{137}Cs , $A(o)$ is the total unsupported ^{210}Pb inventory and P is the mean annual supply rate or flux. M is the ratio P/P_{atmos} , between the mean supply rate estimated from each core, where P_{atmos} is atmospheric flux measured at Pakuranga (Auckland). Nb: < MDC = below minimum detectable concentration. **Model:** L is the mixing depth, D is the bio-diffusion co-efficient and SAR is the time-averaged sedimentation rate for the fitted model profile.

Core	Cores					Model		
	$^7\text{Be}_{\text{max}}$ (cm)	$^{137}\text{Cs}_{\text{max}}$ (cm)	$A(o)$ (Bq cm^{-2})	P ($\text{Bq cm}^{-2}\text{ yr}^{-1}$)	M	L (cm)	D ($\text{cm}^2\text{ yr}^{-1}$)	SAR (mm yr^{-1})
BAS1	3	29.5	0.470	0.0146	2.5	14	20	1.7
BAS2	3	32.5	0.450	0.0140	2.4	14	5	4.0
BAS3	2	19.5	0.245	0.0076	1.3	10	6	0.7
BAS4	< MDC	24.5	0.393	0.0122	2.1	10	10	1.9
BRN	2	39.5	0.416	0.0129	2.2	8	2	3.0
DUK	5	24.5	0.284	0.0088	1.5	11	>20	2.0
PAT	3	26.5	0.304	0.0095	1.6	7	10	3.0
HRK	< MDC	26.5	0.312	0.0097	1.6	10	15	3.5
KAH	2	29.5	0.375	0.0117	2.0	8	15	2.8

In the following sections, the sedimentary characteristics of each short core are discussed in detail. This includes interpretation of the x-ray images, observed and modelled ^{210}Pb profiles, pollen, particle size, bulk density and heavy metal profiles.

3.2 Browns Bay (BRN)

3.2.1 Sedimentary processes

The BRN cores were collected from the centre of Browns Bay (Fig. 1.3) in 2 metres of water (27/4/04, 0908 NZST). The x-radiograph enables the sedimentary fabric of the sediment column to be observed and interpreted. The core contains evidence of sediment re-suspension (≤ 2 cm depth) and the burrowing activities of infauna in subtly bedded sand and mud (Fig. 3.1a). The relatively high density sand and shell material are lighter in hue whereas the lower-density mud is darker. Bioturbation has not been sufficient to homogenise the sediment column, so that stratigraphy is partially preserved.

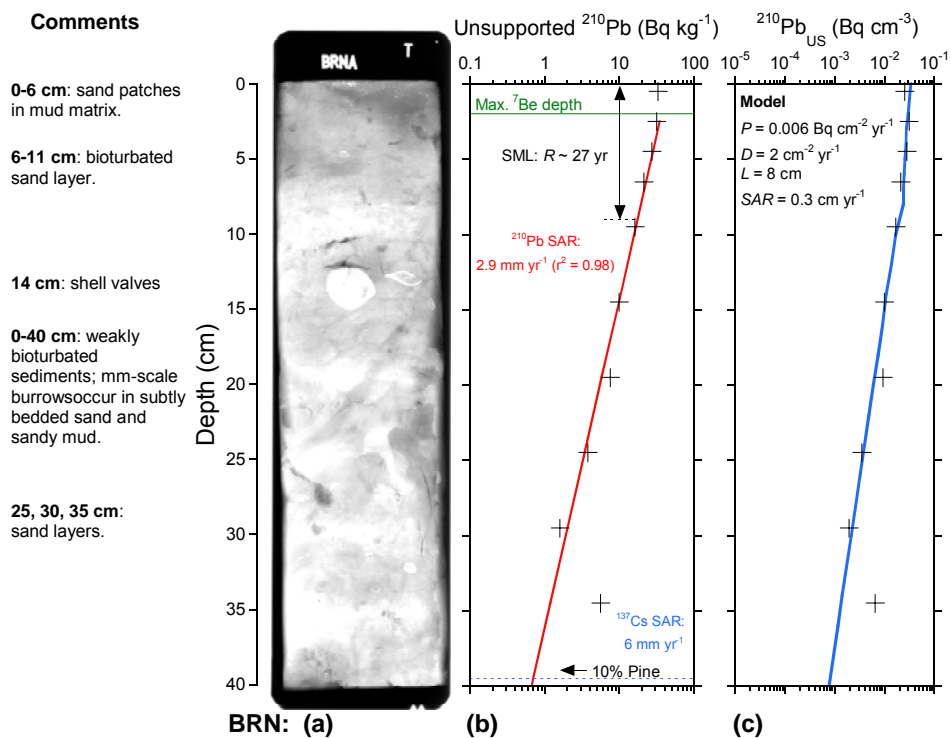


Figure 3.1: Browns Bay core: (a) x-radiograph; (b) unsupported ^{210}Pb profile (Bq kg^{-1}), maximum depths of ^7Be (green) and ^{137}Cs (blue) occurrence and time-averaged SAR; and (c) analytical model fitted to measured unsupported ^{210}Pb profile with fitted model parameter values shown. Note that: (1) the ^{137}Cs SAR are corrected for the mixing depth (L); (2) R is a first-order estimate of sediment residence time in the SML based on the ^{137}Cs SAR and (3) the ^{210}Pb concentration data in (c) are transformed to Bq cm^{-3} to account for down-core variations in dry bulk sediment density.

The presence of ^7Be in the upper 2 cm of the sediment column suggests that freshly deposited sediment is mixed in this layer within days–months (Fig. 3.1b). The ^{210}Pb profile below the ^7Be layer displays a characteristic exponential decay, which plots as a straight line in log-linear space. The time-averaged ^{210}Pb SAR is 2.9 mm yr^{-1} , so that the last 150 years of sedimentation occupies the upper ~44 cm of the sediment column. The good fit of the linear regression model (coefficient of determination, $r^2 = 0.98$) to the natural-log transformed ^{210}Pb data provides confidence in the ^{210}Pb SAR estimate. The presence of ^{137}Cs and pine pollen at the base of the core (39–40 cm) is problematic in that these tracers indicate more recent sediments (i.e., post-1953). In sandy sediments, ^{137}Cs can be remobilised in pore waters and re-deposited at depth. However, this explanation is contradicted by the presence of pine pollen in appreciable quantities (~10% of the terrestrial pollen sum) also at the base of the core. This indicates that the presence of ^{137}Cs at 39–40 cm depth is more likely due to sediment mixing rather than down-core ^{137}Cs migration in pore-water. Analytical modelling (Aller, 1982) of the unsupported ^{210}Pb profile indicates sediment mixing to ~8 cm depth although of low intensity (Fig. 3.1c). If we assume that surface sediments are mixed in the ^{210}Pb SML, then the maximum ^{137}Cs in the absence of surface mixing can be estimated by subtracting the SML depth. In this case, $39.5 \text{ cm} - 8 \text{ cm} = 31.5 \text{ cm}$, so that the time-averaged ^{137}Cs SAR becomes $31.5 \text{ cm}/52 \text{ years} = 6 \text{ mm yr}^{-1}$. A first-order estimate of the residence time (R) of sediment in the SML, before removal by burial, is calculated by $L/^{137}\text{Cs SAR} \sim 27 \text{ years}$.

3.2.2 Sediment profiles

The Browns Bay subtidal sediments are composed of fine-sandy muds (i.e., particle diameter $\leq 63 \mu\text{m}$), with a modal coarse-silt (~55 μm) fraction (Fig. 3.2). Profiles of median and mean particle diameter are similar and show relatively uniform grain size (~50 μm) with depth in the upper 40 cm of the sediment column (Fig. 3.3a). The mud content is ~50% in the top 5 cm and increases to 70% below this depth (Fig. 3.3b). The similarity of the median, mean and modal (Fig 3.2) particle diameters indicate a symmetrical unimodal particle-size distribution in the sediment core. Dry bulk sediment density varies about $\sim 1 \text{ g cm}^{-3}$ and increases from $\sim 0.75 \text{ g cm}^{-3}$ at the surface to $\sim 1.25 \text{ g cm}^{-3}$ at the base of the core (Fig. 3.3c).

The BRN long-core data show that median and mean particle diameters vary about ~50 μm to 125-cm depth and increase to ~100 μm at 150-cm depth at the base of the long core (Appendix VI, Fig. A2). The mud content below 40-cm depth varies about ~75% to 125-cm and then reduces to ~30% at 150-cm depth. The increased variability in the top-40 cm reflects the more frequent sampling in the short core.

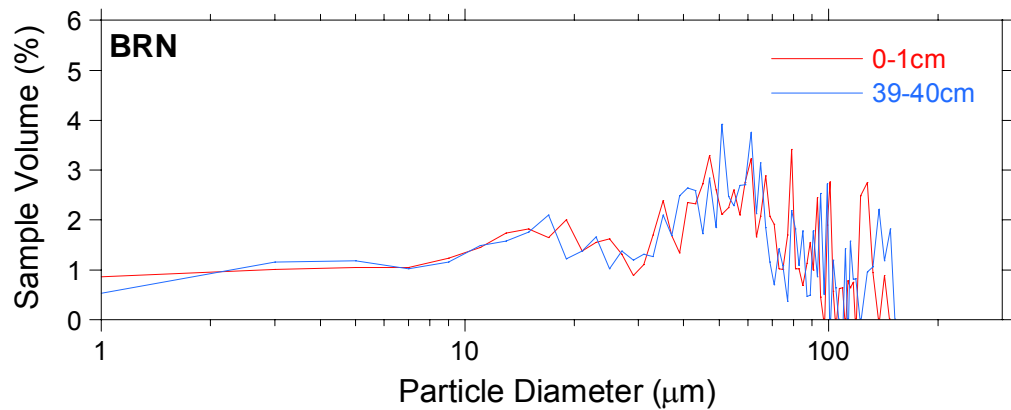


Figure 3.2: Browns Bay short core, particle-size distribution (log-scale) of surface (0-1 cm) and basal (39-40 cm) sediments.

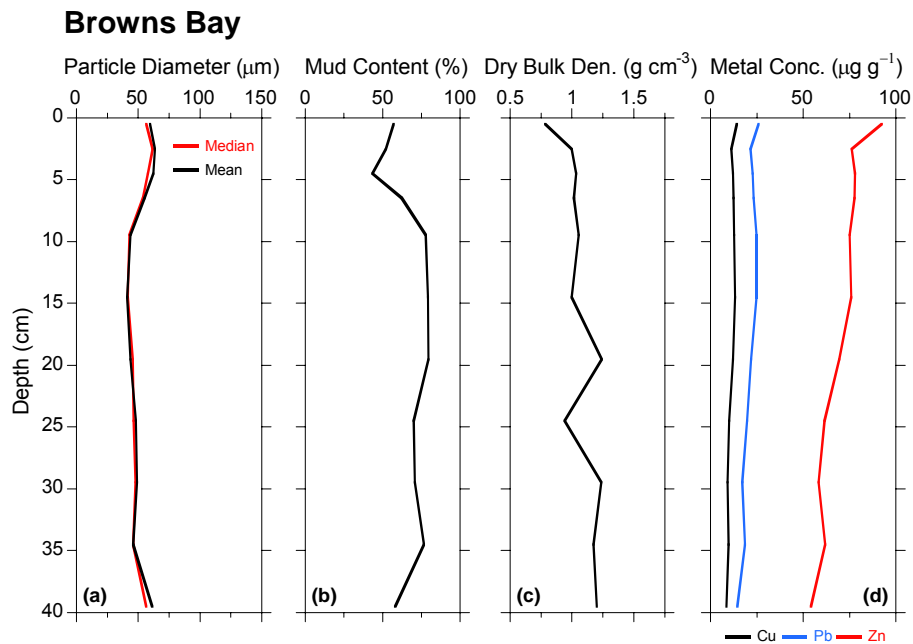


Figure 3.3: Browns Bay subtidal short-core sediment profiles: (a) median and mean particle diameter (μm); (b) mud content (%); (c) dry bulk density (g cm^{-3}); and (d) Total Cu, Pb and Zn concentrations ($\mu\text{g g}^{-1}$).

Heavy metal concentration profiles (total) show a gradual increase towards the sediment surface (Fig. 3.3d). Cu concentrations show a negligible increase whereas Pb concentrations increase from $\sim 12 \mu\text{g g}^{-1}$ (39–40 cm depth) to $25 \mu\text{g g}^{-1}$ at the surface. Zn concentrations are substantially higher than for Cu and Pb and almost double, from $\sim 50 \mu\text{g g}^{-1}$ (39–40 cm depth) to $\sim 90 \mu\text{g g}^{-1}$ at the surface. The more rapid increase in heavy metal concentrations in the top ~ 2 cm of the sediment column

coincides with a similar increase in mud content. Present day (i.e., surface) total Cu Pb and Zn concentrations are $\leq 50\%$ of ANZECC ISQG (Sediment Quality Guidelines)-low values.

3.2.3 Pollen profiles

Figure 3.4 shows the pollen profiles for major native and exotic plant species in core BRN. It can be seen that exotic grass, weed and pine pollens appear in basal sediments and increase in abundance towards the sediment surface. The historical landcover zones have been identified on the basis of the relative abundance of different plant species (section 2.1.5).

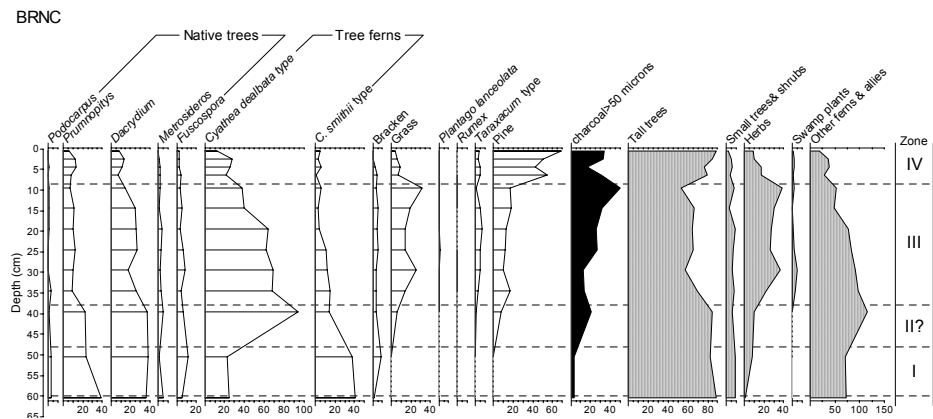


Figure 3.4: Browns Bay subtidal core BRN, pollen and spore profiles for major plant groups expressed as a percentage of the terrestrial pollen and spore sum. Note that these profiles incorporate pollen counts for sediment samples also taken from a long core.

Pine pollen is a particularly useful species for dating recent sedimentation because: (1) it is an exotic species that did not previously occur in the environment and so can be used in a similar way to ^{137}Cs ; (2) it has been planted in large numbers since the mid-1970's and before that time represented $< 1\%$ of catchment landcover; and (3) pine pollen is the most abundantly produced and widely distributed of any NZ plant. A $\geq 10\%$ pine pollen abundance is indicative of the pollen rain that could be expected ~ 10 years (i.e., 1985) after initial planting of local pine forests.

Unfortunately, the depth boundaries between historical landcover zones do not take into account physical–biological sediment mixing effects. We could adjust the depth boundaries by subtracting the SML depth (L) derived from the ^{210}Pb profile as we do for ^{137}Cs . In the case of the Browns Bay core, this is problematic for zone IV (i.e., pine pollen abundance $\geq 10\%$) because the ^{210}Pb SML ($L \sim 8$ cm) exceeds the depth of

the zone IV layer (7.5 cm). This is also the case for several other cores and likely reflects the fact that deep mixing of the sediment column occurs over decadal time-scales. This is supported by the fact that the estimated residence times (R) of sediment in the ^{210}Pb SML are $\sim 20\text{--}60$ years. Thus, the ^{210}Pb mixing time scale is long in comparison to the ≤ 19 years since pine pollen abundance reached the $\geq 10\%$ threshold. The ^7Be mixing depth is more appropriate to apply to the zone IV layer because the mixing time scale (i.e., days–months) is short in comparison to the pine pollen record. We make the steady-state assumption that ^7Be mixing depths have been similar over the last several decades. Thus, the estimated time-averaged SAR for core BRN zone IV pollen (post-1985) is $(75\text{ mm} - 20\text{ mm})/19\text{ years} = 2.9\text{ mm yr}^{-1}$, which is the same as the ^{210}Pb SAR value. For the historical zone II/I (~ 1850 AD) and zone III/II (~ 1950 AD) boundaries, we calculate time-average pollen SAR using the ^{210}Pb SML depth because these time periods are $\geq R$ and full-depth (L) mixing will apply.

3.2.4 Sedimentation rates

Complimentary dating of the Browns Bay core indicates that sedimentation rates have increased by an order of magnitude following catchment deforestation. The ^{14}C age of an articulated cockle shell (sample *Wk-15784*, Uni. Waikato Radiocarbon Lab.) taken from the long core at 141 cm depth (compression corrected) of 2021 ± 31 years BP is used to calculate a time-average SAR of $\sim 0.7\text{ mm yr}^{-1}$ over the last ~ 2000 years. By comparison, pollen and ^{210}Pb SAR have averaged $\sim 2.7\text{ mm yr}^{-1}$ over the last 150 years, which includes catchment deforestation (1840–1900).

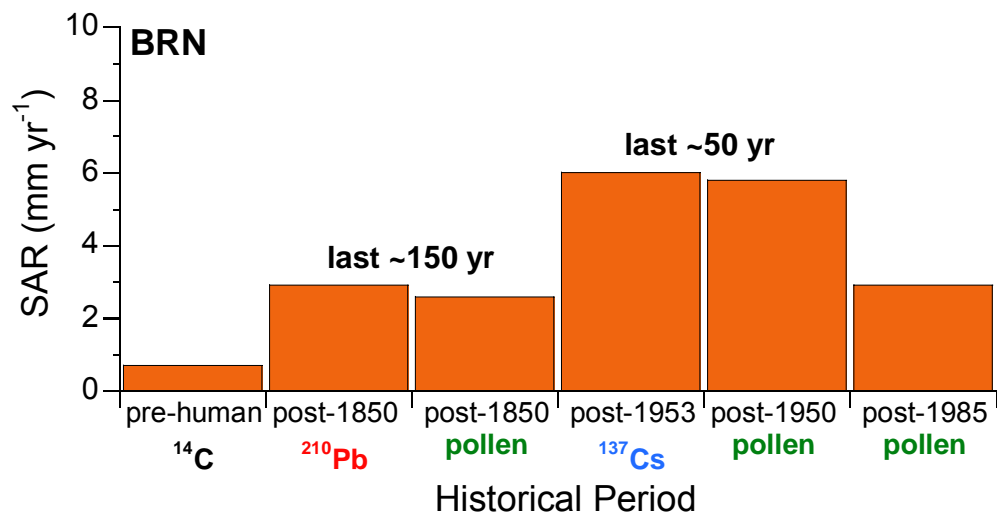


Figure 3.5: Core BRN (Browns Bay) time-averaged sediment accumulation rates (SAR) for historical periods based on radiocarbon, ²¹⁰Pb, ¹³⁷Cs and pollen dating.¹

³⁷Cs and pollen profiles indicate that SAR in Browns Bay have doubled over the last 50 years, averaging ~5.9 mm yr⁻¹. The post-1985 SAR of 2.9 mm yr⁻¹ (zone IV pine-pollen layer) suggests that sedimentation rates have declined to the post-1850 average. This cannot be corroborated by an independent dating method. The intense mixing and winnowing of fine sediment implied by the x-radiograph and ⁷Be profile could account for reduced SAR. Overall, the close agreement between ²¹⁰Pb, ¹³⁷Cs and pollen-derived SAR provides confidence in the recent sedimentation history reconstructed for the Browns Bay core.

3.3 Duck Creek (DUK)

3.3.1 Sedimentary processes

The DUK short cores were collected ~350 m north of the Duck Creek outlet (Fig. 1.3) in 1.8 m water depth (27/4/04, 1010 NZST). The x-radiograph shows abundant mm–cm scale burrows in the upper 25 cm of the sediment column (Fig. 3.6a). The mottling of the core caused by patches of mud (dark) and sand (light) is also indicative of bioturbation, although subtle bedding does persist despite the presence of large bioturbators.

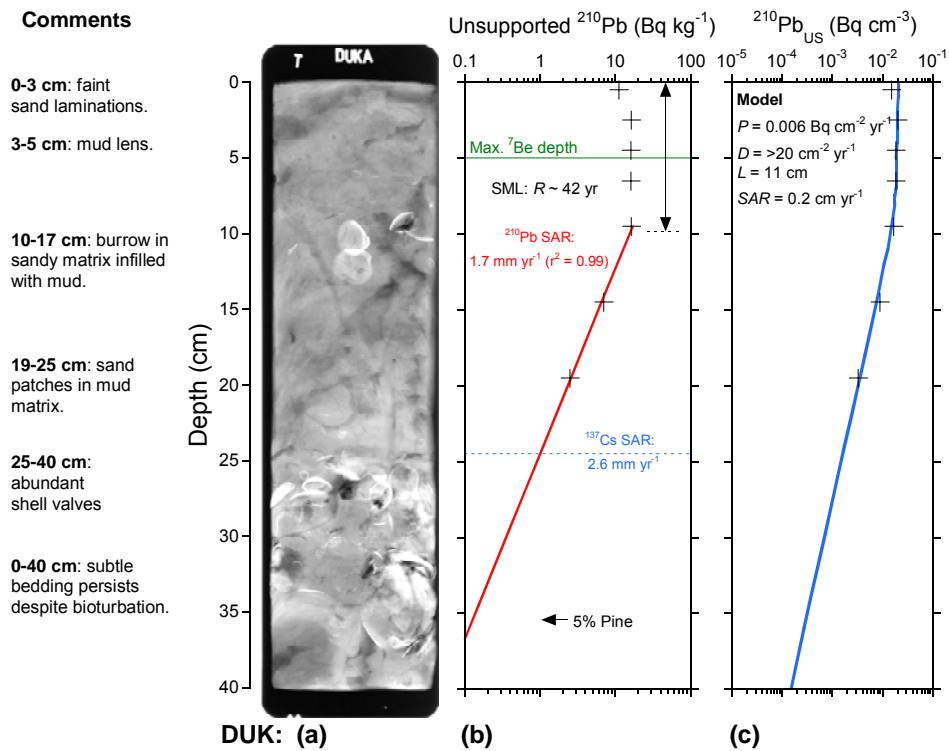


Figure 3.6: Duck Creek core: (a) x-radiograph; (b) unsupported ^{210}Pb profile (Bq kg^{-1}), maximum depths of ^7Be (green) and ^{137}Cs (blue) occurrence and time-averaged SAR; and (c) analytical model fitted to measured unsupported ^{210}Pb profile with fitted model parameter values shown. Note that: (1) the ^{137}Cs SAR are corrected for the mixing depth (L); (2) R is a first-order estimate of sediment residence time in the SML based on the ^{137}Cs SAR and (3) the ^{210}Pb concentration data in (c) are transformed to Bq cm^{-3} to account for down-core variations in dry bulk sediment density.

There are also faint sand laminations in the upper ~ 2 cm, which suggests active resuspension and redeposition of surficial sediments. Below 25 cm depth the core contains abundant shell valves of *Nucula hartvigiana* (nut shell) and *Macomona lilliana*.

^7Be occurs to 5 cm depth, which shows that the upper sediment column is rapidly mixed, within days–months to substantial depth (Fig. 3.6b). It is noteworthy that maximum ^7Be penetration occurs at the Duck Creek site, which has implications for the fate of catchment-derived fine sediments and contaminants. This is discussed in section 4. The unsupported ^{210}Pb profile also shows a deep mixed layer, with uniform ^{210}Pb concentrations, extending to 11 cm depth and is confirmed by the profile modelling (Fig. 3.6c). The estimated residence time (R) of sediments in the SML based on the ^{137}Cs SAR is ~ 42 years. The bio-diffusion coefficient (D) exceeds $20 \text{ cm}^2 \text{ yr}^{-1}$ and indicates relatively intense sediment mixing here. The time-averaged

^{210}Pb SAR below the SML of 1.7 mm yr^{-1} indicates that the last 150 years of sedimentation occupies the top $\sim 25\text{cm}$ of the sediment column. This coincides with the depth boundary between the sandy-muds and the underlying shell unit and suggests a fundamental change in the type of sediments deposited at the site since the mid-1800's.

3.3.2 Sediment profiles

Duck Creek subtidal sediments are composed of fine-sandy muds with a modal coarse silt fraction of $\sim 60 \mu\text{m}$ diameter (Fig. 3.7). The surface sediments contain twice as much clay and fine-medium silt ($< 30 \mu\text{m}$ diameter) as the basal sediments.

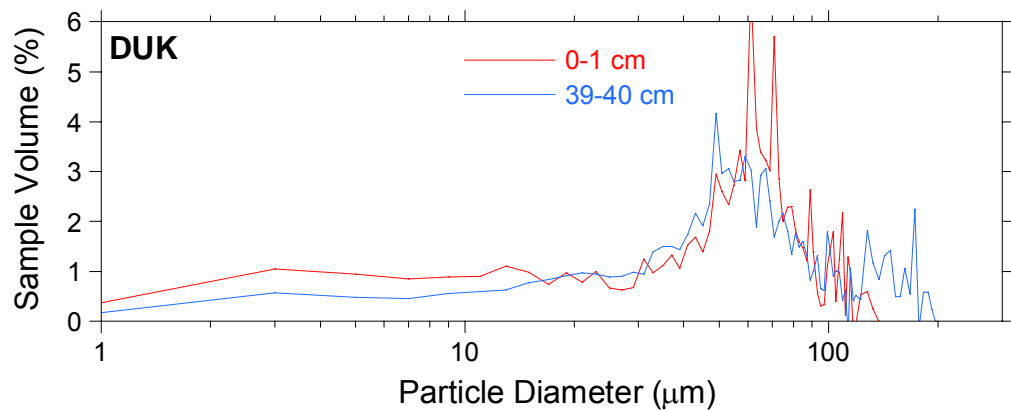


Figure 3.7: Duck Creek short core, particle-size distribution (log-scale) of surface (0-1 cm) and basal (39-40 cm) sediments.

The fine sand fraction ($> 125 \mu\text{m}$ diameter) is also absent in the surficial sediments. The vertical profiles of median and mean particle diameter confirm the increase in particle size (Fig. 3.8a) with depth, although the mud content shows no clear trend (Fig. 3.8b). Dry bulk sediment density varies between $1\text{--}1.4 \text{ g cm}^{-3}$ in the sandy-mud unit and increases ($1.3\text{--}1.5 \text{ g cm}^{-3}$) in the underlying shell layer (Fig. 3.8c).

The DUK long-core data show that median and mean particle diameters are about $\sim 50 \mu\text{m}$ between 40 and 225-cm depth, at the base of the long core (Appendix VI, Fig. A3). The mud content below 40-cm depth ranges between 55–80% and is substantially offset from the short-core data at 40-cm depth. This is most likely due to the fact that the short and long cores were not taken at the same location. The increased variability in the top-40 cm reflects the more frequent sampling in the short core.

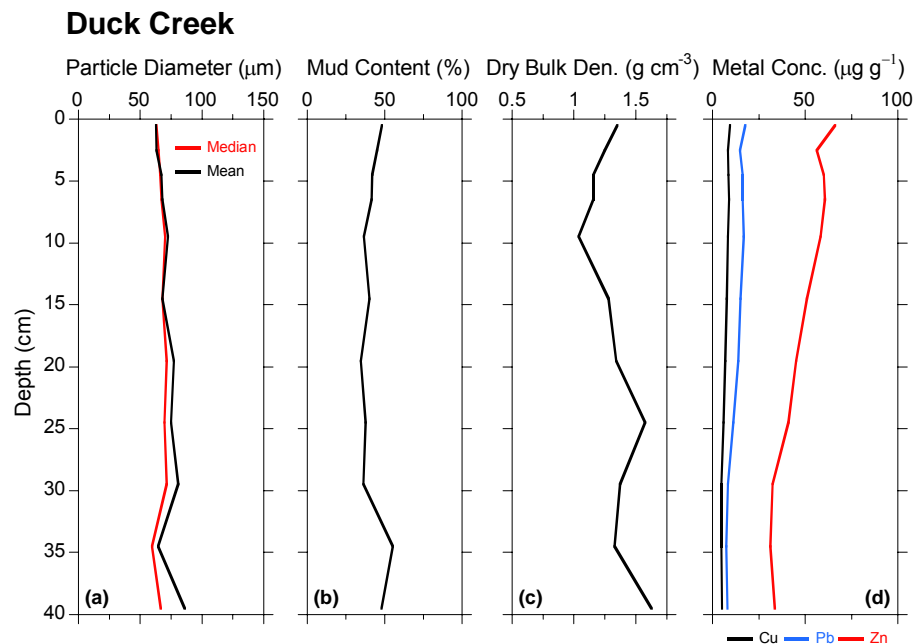


Figure 3.8: Duck Creek subtidal short-core sediment profiles: (a) median and mean particle diameter (μm); (b) mud content (%); (c) dry bulk density (g cm^{-3}); and (d) Total Cu, Pb and Zn concentrations ($\mu\text{g g}^{-1}$).

Heavy metal concentrations increase gradually towards the sediment surface. Cu and Pb concentrations at the surface are $\leq 20 \mu\text{g g}^{-1}$ (Fig. 3.8d). The Zn profile better shows the general trend in the heavy metal profiles because of its higher concentrations in the sediments. Zn concentrations are a uniform $\sim 30 \mu\text{g g}^{-1}$ below 30 cm depth then gradually begin to rise to $\sim 70 \mu\text{g g}^{-1}$ at the surface. The start of the Zn rise at 30 cm depth (in the old shell layer > 150 years old) is likely due to mixing of Zn down from the more recent mud unit. If we take into account the present day SML thickness of 11 cm, then this increase coincides with the mid-1890's (i.e., 300 - 110 mm = $190 \text{ mm} / ^{210}\text{Pb SAR} = 110$ years) as pasture was established in the catchment. Surface concentrations of Zn are also substantially lower than in the Browns Bay core ($\sim 90 \mu\text{g g}^{-1}$). This likely represents the more urbanised state of the Browns Bay sub-catchment as the mud content of surface sediments (i.e., 50%) are the same at both sites. Present day (i.e., surface) total Cu Pb and Zn concentrations are $\leq 40\%$ of ANZECC ISQG-low values.

3.3.3 Pollen profiles

Figure 3.9 shows the pollen profiles for the Duck Creek short core and record the decline in native plant species and rise of exotic grass, weed and tree species. Historical landcover zones have been identified on the basis of the relative abundance

of different plant species (section 2.1.5). The pollen profiles of recently introduced species, such as pine, show the results of substantial downward mixing of sediments into older sediments. We correct the time-averaged pollen SAR for each historical zone as discussed in section 3.2.3 above.

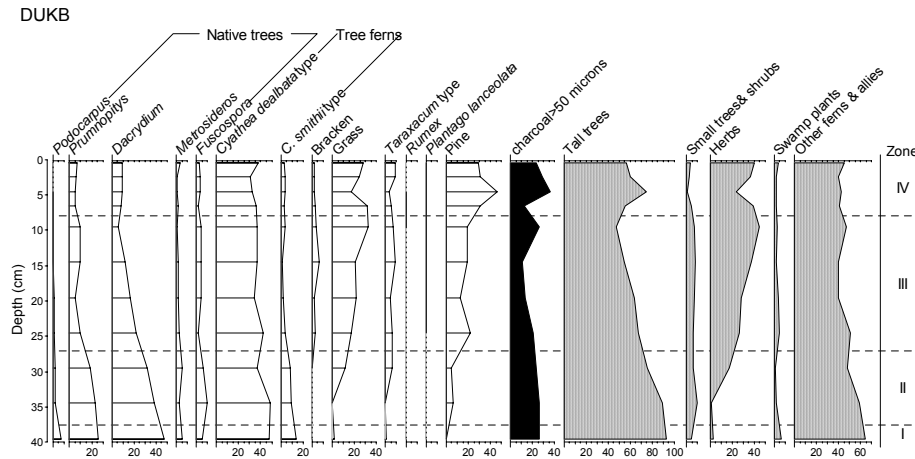


Figure 3.9: Duck Creek subtidal core DUK, pollen and spore profiles for major plant groups expressed as a percentage of the terrestrial pollen and spore sum.

3.3.4 Sedimentation rates

Complimentary dating of the Duck Creek core indicates that sedimentation rates have increased following European settlement (Fig. 3.10). Time-averaged pollen and ^{210}Pb SAR of $\sim 1.7 \text{ mm yr}^{-1}$ for the last 150 years are in close agreement as are the pollen and ^{137}Cs SAR for the post-1950 period, which have averaged $2.6\text{--}3.0 \text{ mm yr}^{-1}$. Thus, post-1950 SAR have increased by some $\sim 50\%$ over the post-1850 SAR. As also observed at Browns Bay, there is an apparent reduction in post-1985 SAR (zone IV pine-pollen layer) to 1.6 mm yr^{-1} , which is similar to the long-term ^{210}Pb SAR value. This suggests that sedimentation rates have declined to the post-1850 average. Again, this cannot be corroborated by an independent dating method. The close agreement between ^{210}Pb , ^{137}Cs and pollen-derived SAR provides confidence in the recent sedimentation history reconstructed for the Duck Creek core.

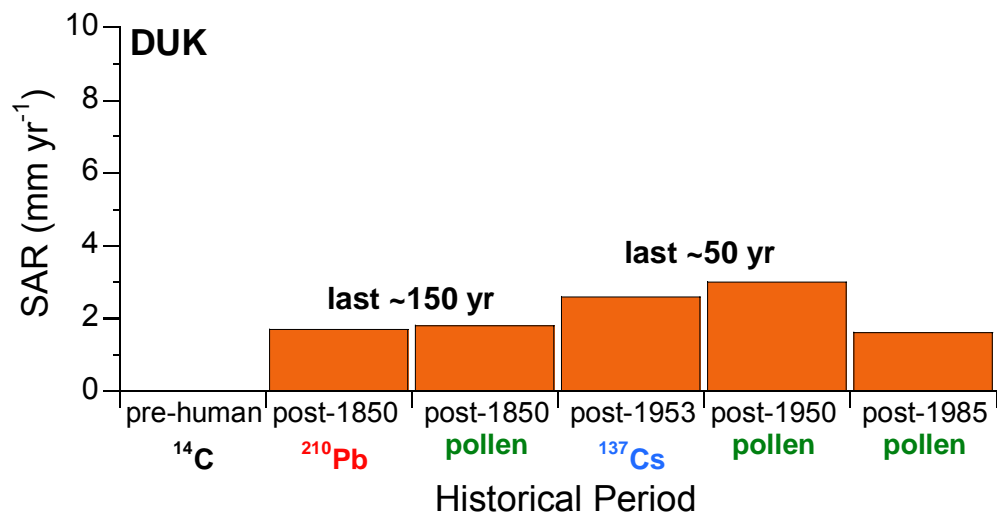


Figure 3.10: Core DUK (Duck Creek) time-averaged sediment accumulation rates (SAR) for historical periods based on ²¹⁰Pb, ¹³⁷Cs and pollen dating.

3.4 Pauatahanui (PAT)

3.4.1 Sedimentary processes

The PAT short cores were collected ~600 m west of the stream outlet (Fig. 1.3) in 1.8 m water depth (27/4/04, 1121 NZST). The x-radiograph shows substantial mottling in the upper 25 cm of the sediment column, with sand patches (light) in a mud matrix (dark) (Fig. 3.11a). This is indicative of sand layers subsequently disrupted by bioturbators. The presence of shell layers at 5–9 cm and 15–20 cm depth have likely been produced by physical and/or biological processes, such as winnowing of fine sediments by waves that produces a shell lag. The dark voids below 25-cm depth are wood fragments, which have substantially lower densities than either mud or sand.

⁷Be occurs to 3 cm depth, which shows that the upper sediment column is rapidly mixed, within days–months to substantial depth (Fig. 3.11b). The unsupported ²¹⁰Pb profile also shows a deep mixed layer, with uniform ²¹⁰Pb concentrations, extending to 7-cm depth and is confirmed by the profile modelling (Fig. 3.11c). The estimated residence time (*R*) of sediments in the SML based on the ¹³⁷Cs SAR is ~18 years. The bio-diffusion coefficient (*D*) of 10 cm² yr⁻¹ is a relatively moderate sediment mixing rate for the inlet. The time-averaged ²¹⁰Pb SAR below the SML of 2.8 mm yr⁻¹ indicates that the last 150 years of sedimentation occupies the top ~42cm of the sediment column.

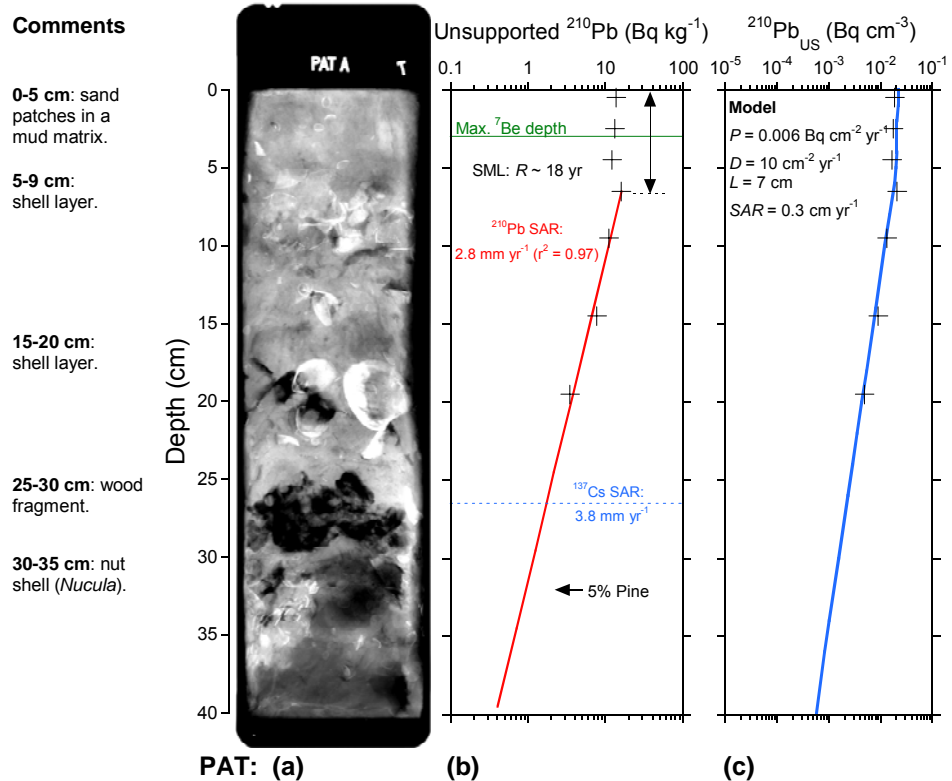


Figure 3.11: Pauatahanui core: (a) x-radiograph; (b) unsupported ^{210}Pb profile (Bq kg^{-1}), maximum depths of ^7Be (green) and ^{137}Cs (blue) occurrence and time-averaged SAR; and (c) analytical model fitted to measured unsupported ^{210}Pb profile with fitted model parameter values shown. Note that: (1) the ^{137}Cs SAR are corrected for the mixing depth (L); (2) R is a first-order estimate of sediment residence time in the SML based on the ^{137}Cs SAR and (3) the ^{210}Pb concentration data in (c) are transformed to Bq cm^{-3} to account for down-core variations in dry bulk sediment density.

3.4.2 Sediment profiles

The Pauatahanui sediment data show a substantial shift in particle size over the last 150 years (i.e., from the bottom to the top of the core). The basal sediments at 39–40 cm have a modal coarse silt fraction of $\sim 60 \mu\text{m}$ diameter and a minor fine sand content (Fig. 3.12). By comparison, surficial sediments are largely composed of fine sand with a minor clay–fine silt content.

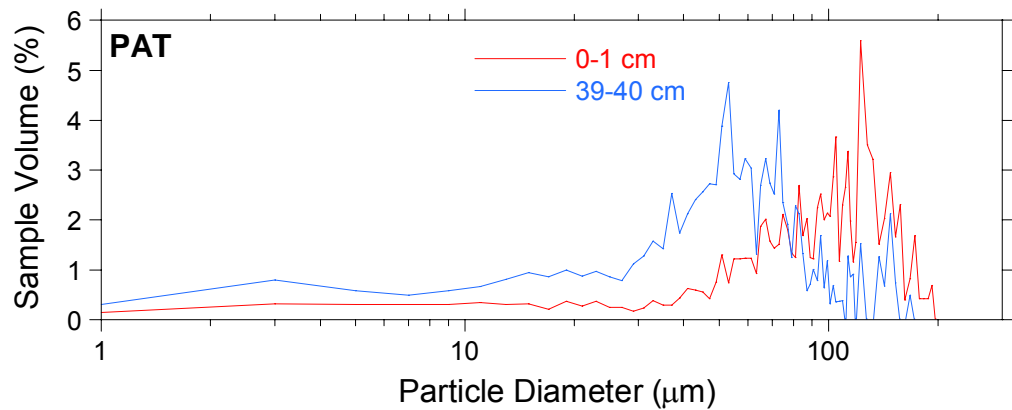


Figure 3.12: Pauatahanui Stream short core, particle-size distribution (log-scale) of surface (0-1 cm) and basal (39-40 cm) sediments.

This shift from silt to sand over the last 150 years is captured by the vertical profiles of median and mean particle diameter (Fig. 3.13a), and mud content, which reduces from 50% at 39–40 cm to 20% at 0–1 cm depth (Fig. 3.13b). Dry bulk sediment density ranges from 1 to 1.5 g cm⁻³ and displays a weak trend of increasing bulk density towards the surface (Fig. 3.13c).

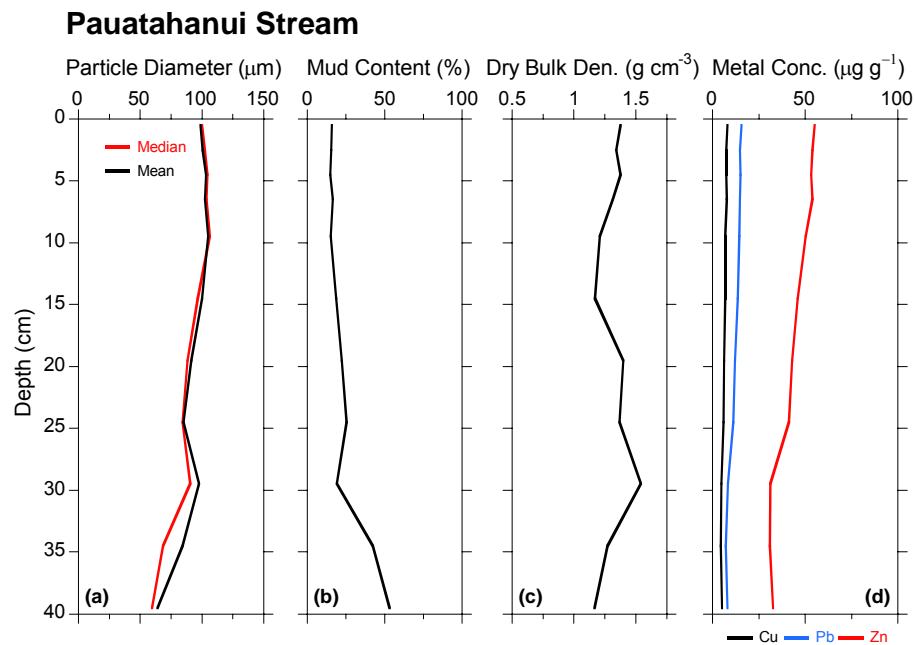


Figure 3.13: Pauatahanui Stream subtidal short-core sediment profiles: (a) median and mean particle diameter (µm); (b) mud content (%); (c) dry bulk density (g cm⁻³); and (d) Total Cu, Pb and Zn concentrations (µg g⁻¹).

Heavy metal concentration increase gradually towards the sediment surface. Cu and Pb concentrations at the surface are $\leq 20 \mu\text{g g}^{-1}$ (Fig. 3.13d). As observed at Duck Creek, the Zn profile better shows the general trend in the heavy metal profiles. Again, Zn concentrations are a uniform $\sim 30 \mu\text{g g}^{-1}$ below 30 cm depth then gradually begin to rise to $\sim 55 \mu\text{g g}^{-1}$ at the surface. The start of the Zn rise at 30 cm depth and corrected for the present day SML thickness of 7 cm coincides with the early-1920's (i.e., $300 - 70 \text{ mm} = 230 \text{ mm}/^{210}\text{Pb SAR} \sim 82 \text{ years}$). Surface concentrations of Zn are lower than at Duck Creek ($\sim 70 \mu\text{g g}^{-1}$), which in turn are lower than at Browns Bay ($\sim 90 \mu\text{g g}^{-1}$). This trend of declining Zn concentration alongshore likely represents: (1) the effect of distance from source (i.e., urban Browns Bay sub-catchment); and/or (2) reduced mud content of the PAT core. Present day (i.e., surface) total Cu Pb and Zn concentrations are $\leq 40\%$ of ANZECC ISQG-low values.

3.4.3 Pollen profiles

Figure 3.14 shows the pollen profiles for the Pauatahanui Stream short core and record the decline in native plant species and rise of exotic grass, weed and tree species. Historical landcover zones have been identified on the basis of the relative abundance of different plant species (section 2.1.4). The pollen profiles of recently introduced species, such as pine, show the results of substantial downward mixing of sediments into older sediments. We correct the time-averaged pollen SAR for each historical zone as discussed in section 3.2.3 above.

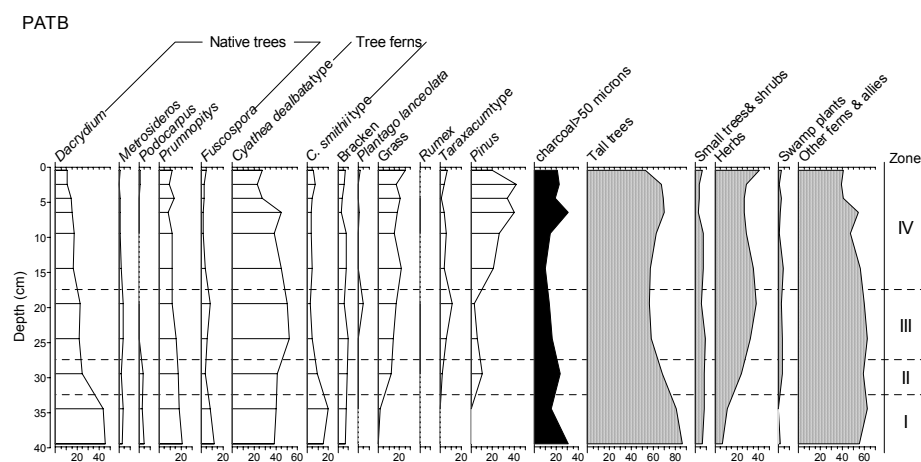


Figure 3.14: Pauatahanui subtidal core PAT, pollen and spore profiles for major plant groups expressed as a percentage of the terrestrial pollen and spore sum.

3.4.4 Sedimentation rates

Complimentary dating of the Pauatahanui Stream subtidal core documents the increase in sedimentation rates that have occurred following European settlement (Fig. 3.15). The time-averaged ^{210}Pb SAR (2.8 mm yr^{-1}) is higher than the pollen SAR of 1.7 mm yr^{-1} during the last 150 years. We favour the ^{210}Pb SAR value because the dating method is less subjective than for pollen and is also supported by modelling. Sedimentation rates have increased by $\sim 35\%$ in the post-1950 period and ^{137}Cs and pollen derived SAR of 3.8 mm yr^{-1} are in close agreement. Unlike the BRN or DUK sites, an apparent **increase** in post-1985 SAR (zone IV pine-pollen layer) to 5.5 mm yr^{-1} is observed in PAT core. This cannot be corroborated by an independent dating method. The good agreement between ^{210}Pb , ^{137}Cs and pollen-derived SAR provides confidence in the recent sedimentation history reconstructed for the Duck Creek core.

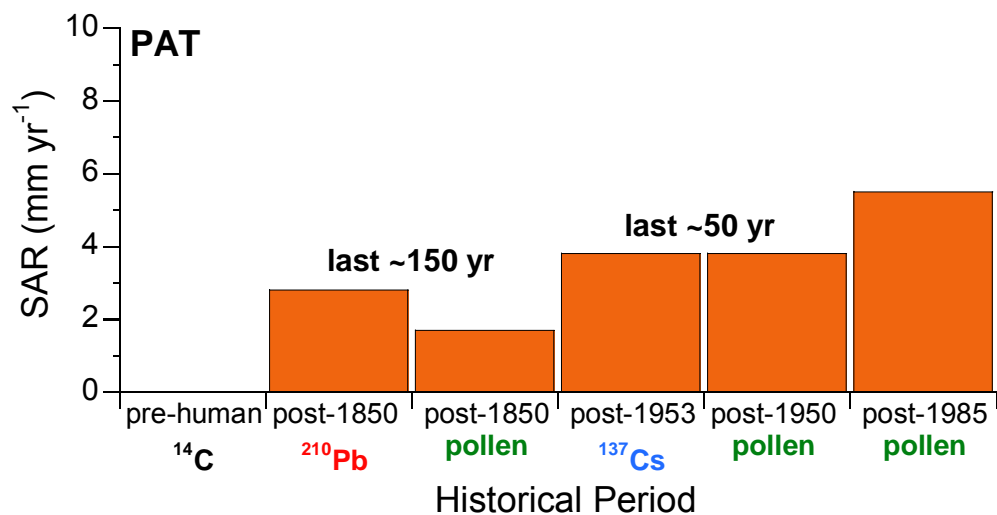


Figure 3.15: Core PAT (Pauatahanui Stream) time-averaged sediment accumulation rates (SAR) for historical periods based on ^{210}Pb , ^{137}Cs and pollen dating.

3.5 Horokiri (HRK)

3.5.1 Sedimentary processes

The HRK short cores were collected $\sim 500 \text{ m}$ south-west of the Horokiri Stream outlet (Fig. 1.3) in 1.5 m water depth (27/4/04, 1500 NZST). The x-radiograph clearly shows a 3-cm thick homogenous sand layer (light) with no apparent laminations and a sharp contact with the underlying mud (dark) (Fig. 3.16a). There are abundant mm-scale borrows in the underlying mud unit between $3\text{--}13 \text{ cm}$ depth and there is mm-cm

scale mottling which is likely due to the disruption of sediment layers by bioturbators. Between 13–19-cm depth there is a distinct shell-rich sand layer that contains mud-filled burrows in places (19–23 cm). Below 23-cm depth there are numerous thin (~1–2 mm thick) inter-layered sand and mud units that are convex in shape, which are likely an artefact of sediment coring.

The absence of ^7Be in the HRK core reflects the low mud content of the surface homogenous sand unit. It is reasonable to assume that the sediment column at this site is well mixed to ~3-cm depth within days–months. The unsupported ^{210}Pb profile displays a deep mixed layer, with relatively uniform ^{210}Pb concentrations, extending to 10-cm depth (Fig. 3.16b) and is confirmed by the profile modelling (Fig. 3.16c). The estimated residence time (R) of sediments in the SML based on the ^{137}Cs SAR is ~31 years. The time-averaged ^{210}Pb SAR below the SML of 3.7 mm yr^{-1} indicates that the last 150 years of sedimentation occupies the top ~56cm of the sediment column.

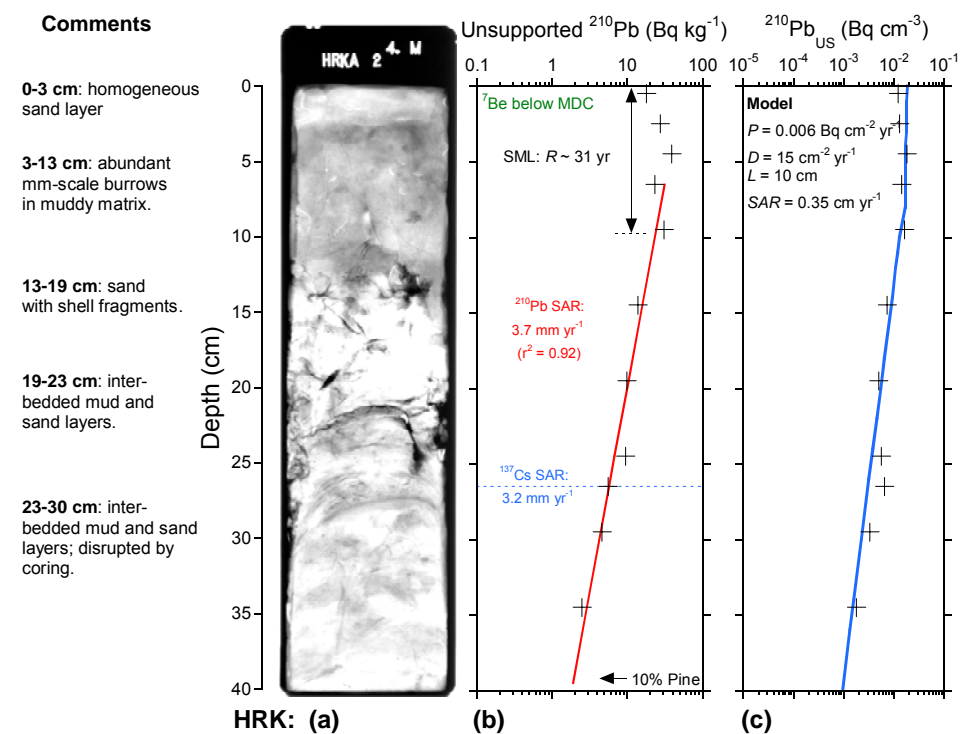


Figure 3.16: Horokiri core: (a) x-radiograph; (b) unsupported ^{210}Pb profile (Bq kg^{-1}), maximum depths of ^7Be (green) and ^{137}Cs (blue) occurrence and time-averaged SAR; and (c) analytical model fitted to measured unsupported ^{210}Pb profile with fitted model parameter values shown. Note that: (1) the ^{137}Cs SAR are corrected for the mixing depth (L); (2) R is a first-order estimate of sediment residence time in the SML based on the ^{137}Cs SAR and (3) the ^{210}Pb concentration data in (c) are transformed to Bq cm^{-3} to account for down-core variations in dry bulk sediment density.

3.5.2 Sediment profiles

The Horokiri subtidal sediments are composed of muddy fine-sand, with a modal fine sand ($\sim 140 \mu\text{m}$) fraction (Fig. 3.17). The particle size distributions at base and the top of the core are generally similar, although there is less fine sand and almost twice as much clay and fine silt in the 0–1 cm sample (20% by volume) than at 39–40 cm depth (13% by volume). Profiles of median and mean particle diameter show that median and mean particle diameters have reduced over time, from $\sim 150 \mu\text{m}$ below 30-cm depth to $\sim 110 \mu\text{m}$ at the surface (Fig. 3.18a). At the same time, mud content increases from $\sim 10\%$ at 30-cm depth to 20–25% in the upper 15 cm of the sediment column (Fig. 3.18b). The relatively low dry bulk densities measured in the HRK core of $\leq 0.75 \text{ g cm}^{-3}$ (Fig. 3.18c) are due to the high water content of these sediments ($\sim 50\%$).

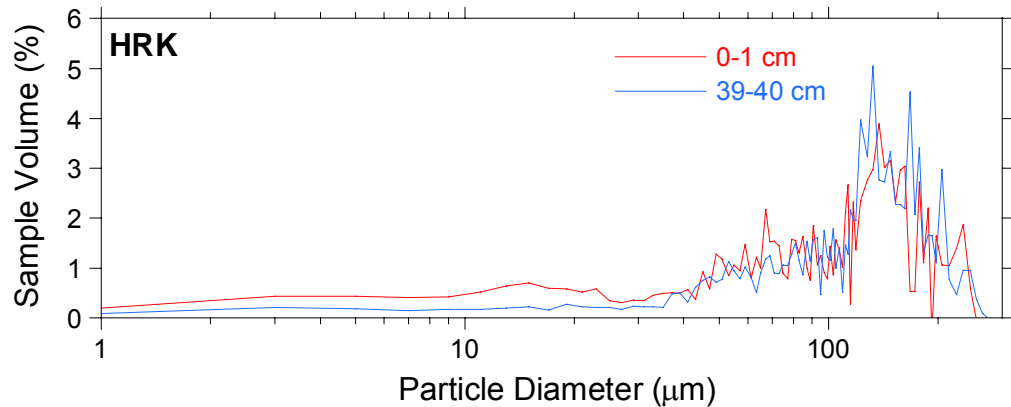


Figure 3.17: Horokiri short core, particle-size distribution (log-scale) of surface (0-1 cm) and basal (39-40 cm) sediments.

Changes in heavy metal concentration profiles also reflect the increase in mud content above 25-cm depth. Cu and Pb concentrations below 25-cm depth of $\sim 5\text{--}7 \mu\text{g g}^{-1}$ double to $10\text{--}16 \mu\text{g g}^{-1}$ at the surface (Fig. 3.18d). Again, Zn concentrations are $\sim 30 \mu\text{g g}^{-1}$ below 30 cm depth and then rapidly increase to $\sim 60 \mu\text{g g}^{-1}$ at 20-cm depth. Zn concentrations are uniform in the upper 20 cm of the sediment column.

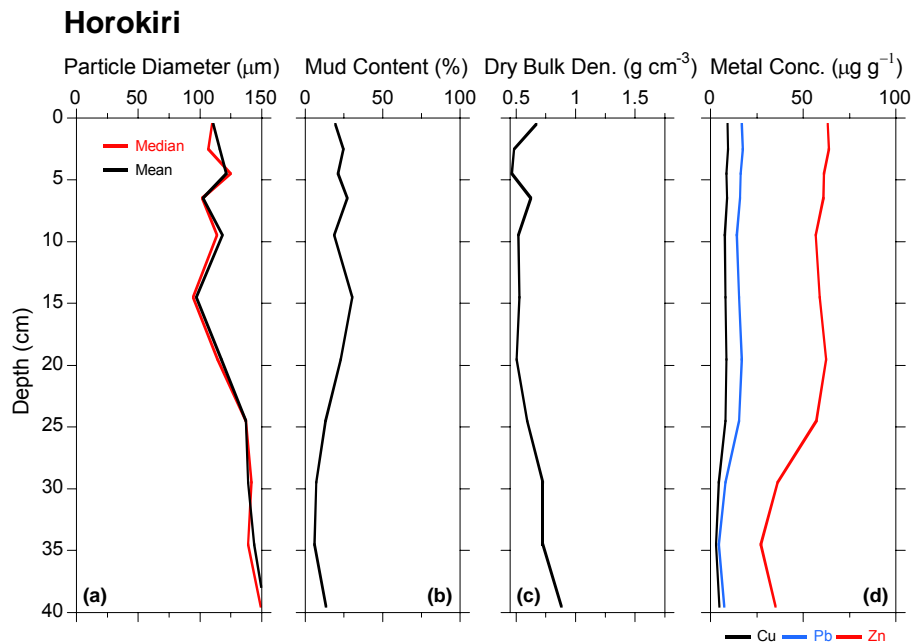


Figure 3.18: Horokiri subtidal short-core sediment profiles: (a) median and mean particle diameter (μm); (b) mud content (%); (c) dry bulk density (g cm^{-3}); and (d) Total Cu, Pb and Zn concentrations ($\mu\text{g g}^{-1}$).

The start of the Zn rise at 30 cm depth and corrected for the present day SML thickness of 10 cm coincides with ~ 1950 AD (i.e., $300 - 100 \text{ mm} = 200 \text{ mm}^{210}\text{Pb}$ SAR ~ 54 years). Surface concentrations of Zn are similar to the Pauatahanui core and lower than at Duck Creek ($\sim 70 \mu\text{g g}^{-1}$) and Browns Bay ($\sim 90 \mu\text{g g}^{-1}$). Present day (i.e., surface) total Cu Pb and Zn concentrations are $\leq 40\%$ of ANZECC ISQG-low values.

3.5.3 Pollen profiles

Figure 3.19 shows the pollen profiles for the Horokiri short core, which record the decline in native plant species and rise of exotic grass, weed and tree species. Historical landcover zones have been identified on the basis of the relative abundance of different plant species (section 2.1.4). The pollen profiles of recently introduced species, such as pine, show the results of deep mixing and relatively rapid sedimentation. For example, the increase in pine pollen from ~ 30 cm to uniform levels above 20-cm depth matches the Zn profile (Fig. 3.18d). We correct the time-averaged pollen SAR for each historical zone as discussed in section 3.2.3.

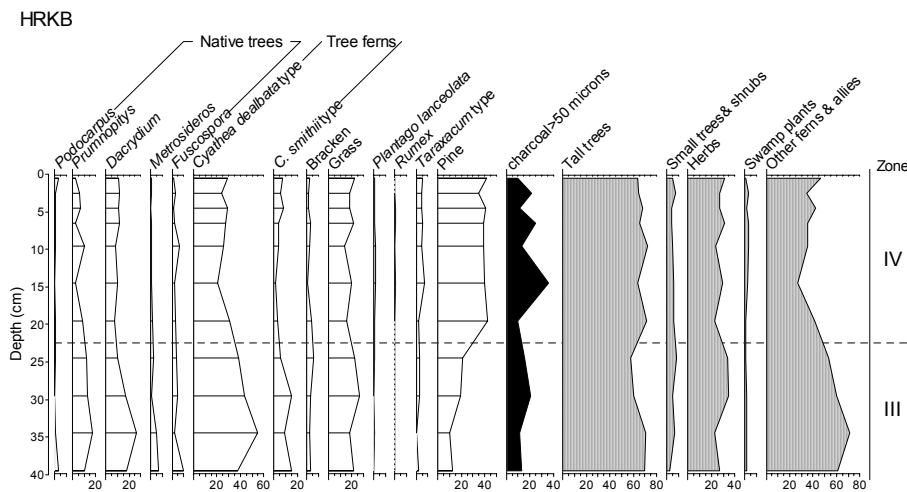


Figure 3.19: Horokiri subtidal core HRKB, pollen and spore profiles for major plant groups expressed as a percentage of the terrestrial pollen and spore sum.

3.5.4 Sedimentation rates

Time-averaged ^{210}Pb (3.7 mm yr^{-1}) and ^{137}Cs (3.2 mm yr^{-1}) SAR are similar and indicate that sedimentation rates have been relatively constant over the last 150 years following catchment deforestation. The ^{210}Pb SAR is substantially higher than for the BRN, DUK and PAT cores at sub-catchment outlets ($1.7\text{--}2.9 \text{ mm yr}^{-1}$). This likely reflects the relative size and steep terrain of the Horokiri catchment such that soil erosion and delivery rates at the sub-catchment outlet are higher. As also observed in the PAT core, there is an apparent **increase** in the post-1985 SAR (zone IV pine-pollen layer) to $\sim 10 \text{ mm yr}^{-1}$. This post-1985 SAR takes into account rapid (days–months) mixing of the top $\sim 3 \text{ cm}$ of the sediment column.

The large apparent increase in SAR since 1985 for core HRK suggested by the pine-pollen profile coincides with an increase in mud content (Fig 3.18b) and heavy metal concentrations (Fig 3.18d). The increases in heavy metal concentrations are most likely due to the increased mud content. Furthermore, the HRK site is relatively sheltered from the prevailing northerly winds, so that the observed changes in the sediment profiles more likely reflect changes in the quantity and size distributions of sediments delivered by the Horokiri sub-catchment rather than post-depositional processes. For example, wave resuspension would winnow silt from the sediment rather than increase the silt content. Furthermore, $\geq 70\%$ of the sediment is composed of sand, which is much less easily remobilised by waves than silt, so that the Horokiri sub-catchment is the most likely source of sediments in core HRK. These lines of

evidence, taken together, suggest changes in the Horokiri sub-catchment sediment inputs.

Although the three-fold increase in SAR during the last 20 years cannot be corroborated by another dating method it is consistent with: (1) sub-catchment characteristics; and (2) the fact that 40% of the 2000 ha of exotic forest planted in the inlet's catchment since the mid-1970's has occurred in the Horokiri catchment (Page et al. 2004). This also represents 24% of the sub-catchment area. Most of the exotic forest has been planted on class VI and VII land on west facing slopes, which have moderate to high erosion potential (Healy, 1980). The establishment of exotic forest plantations, which typically require land clearance and construction of access roads, can substantially increase soil erosion in steep-land catchments (e.g., Fahey and Coker, 1992).

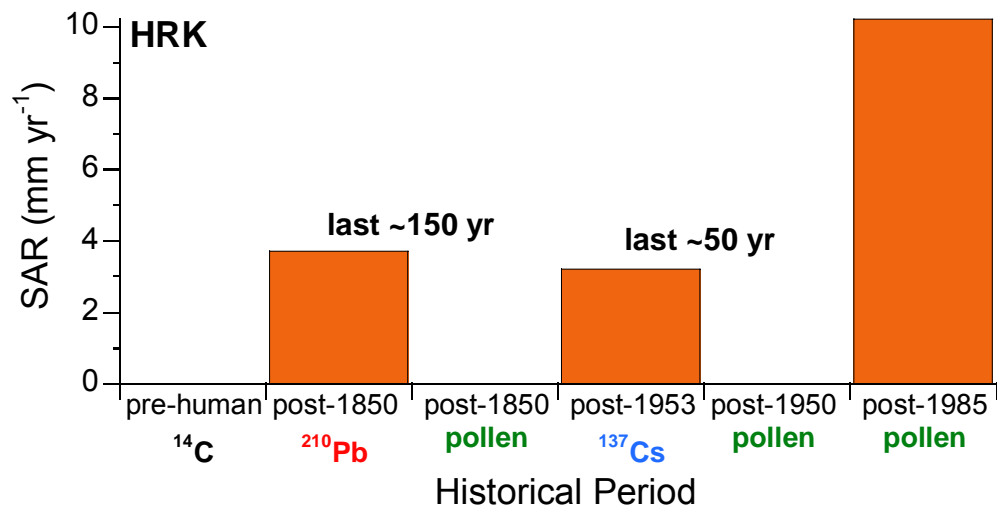


Figure 3.20: Core HRK (Horokiri) time-averaged sediment accumulation rates (SAR) for historical periods based on ²¹⁰Pb, ¹³⁷Cs and pollen dating.

3.6 Kakaho (KAH)

3.6.1 Sedimentary processes

The KAH short cores were collected ~375 m south-west of the Kakaho Stream mouth (Fig. 1.3) in 1.5 m water depth (27/4/04, 1700 NZST). The x-radiograph shows a 3-cm thick surface layer of finely inter-bedded sand (light) and mud (dark) that is indicative of recent sediment resuspension (Fig. 3.21a). Cross-bedding in this surface layer is indicative of wave reworking of sediments. There are abundant mm-scale

borrows throughout the core and faint sand layers at 8 cm and 14 cm depth. Shell valves and fragments are common below 20-cm depth. A large shell-filled and funnel-shaped burrow is also apparent between 20–30 cm depth. The presence of bedding preserved in the KAH core shows that sediment mixing by bioturbators is intense enough to erase these physical structures.

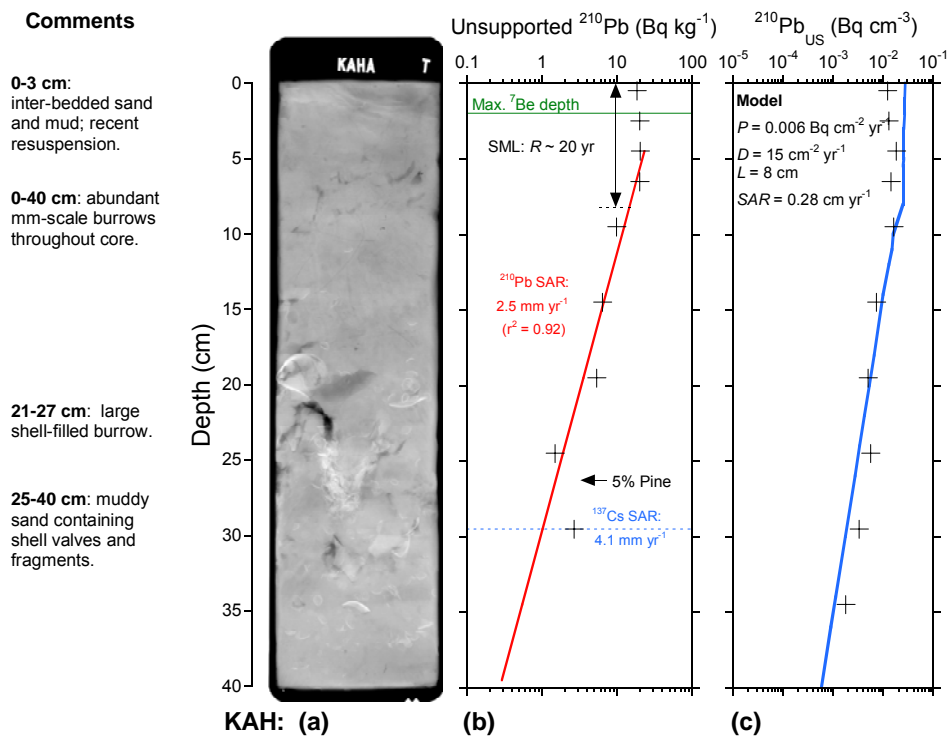


Figure 3.21: Kakaho core: (a) x-radiograph; (b) unsupported ^{210}Pb profile (Bq kg^{-1}), maximum depths of ^7Be (green) and ^{137}Cs (blue) occurrence and time-averaged SAR; and (c) analytical model fitted to measured unsupported ^{210}Pb profile with fitted model parameter values shown. Note that: (1) the ^{137}Cs SAR are corrected for the mixing depth (L); (2) R is a first-order estimate of sediment residence time in the SML based on the ^{137}Cs SAR and (3) the ^{210}Pb concentration data in (c) are transformed to Bq cm^{-3} to account for down-core variations in dry bulk sediment density.

^7Be occurs to 2-cm depth, which indicates sediment mixing over days–months to this depth (Fig. 3.21b), which is consistent with the x-radiograph. The unsupported ^{210}Pb profile also shows a deep mixed layer, with uniform ^{210}Pb concentrations, extending to 8-cm depth and is confirmed by the profile modelling (Fig. 3.21c). The estimated residence time (R) of sediments in the SML based on the ^{137}Cs SAR is ~ 20 years. The bio-diffusion coefficient (D) of $15 \text{ cm}^2 \text{ yr}^{-1}$ is an intermediate value for the inlet cores. The time-averaged ^{210}Pb SAR below the SML of 2.5 mm yr^{-1} indicates that the last 150 years of sedimentation occupies the top ~ 38 cm of the sediment column.

3.6.2 Sediment profiles

The Kakaho subtidal sediments are composed of very-fine sandy mud, with a modal coarse-silt ($\sim 50 \mu\text{m}$) fraction (Fig. 3.22). The particle size distributions at the base and the top of the core are similar.

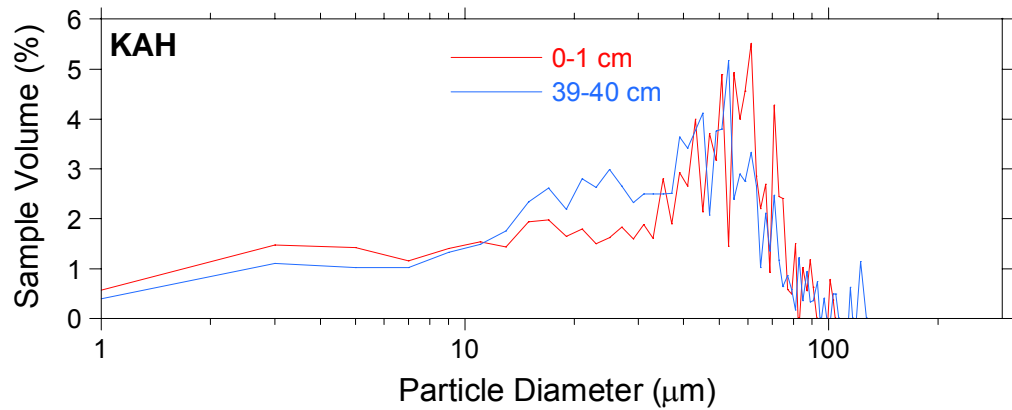


Figure 3.22: Kakaho short core, particle-size distribution (log-scale) of surface (0-1 cm) and basal (39-40 cm) sediments.

Profiles of median and mean particle diameter show that median and mean particle diameters of $\sim 50 \mu\text{m}$ (Fig. 3.23a) and mud content of $\sim 75\%$ (Fig. 3.23b) have not varied measurably over the last 150 years. Dry bulk sediment density are in the range $1.25\text{--}1.5 \text{ g cm}^{-3}$ and show no clear trend with depth in the sediment column (Fig. 3.23c). These particle size data, in conjunction with the radioisotope profiles show that the Kakaho subtidal flat is a long-term sink for fine sediments.

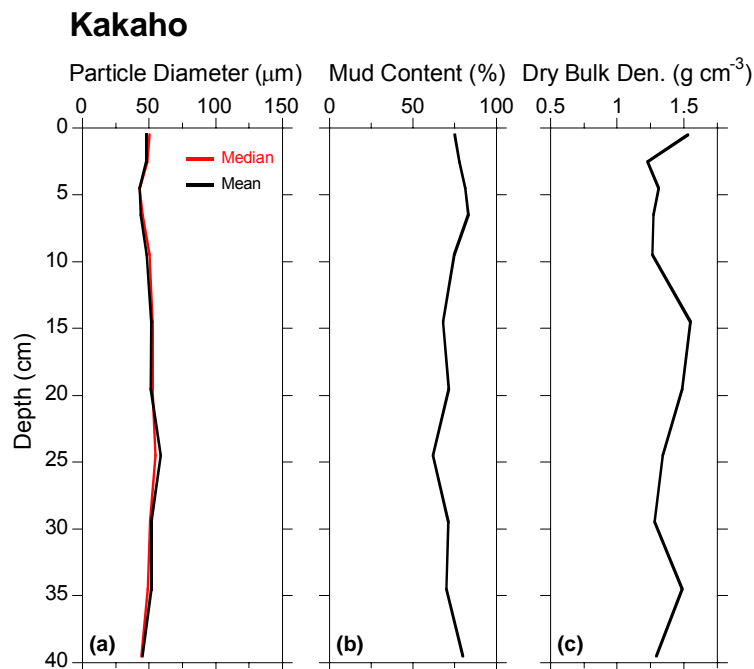


Figure 3.23: Kakaho subtidal short-core sediment profiles: (a) median and mean particle diameter (μm); (b) mud content (%); and (c) dry bulk density (g cm^{-3}). No heavy metal analysis of sediments undertaken at this site.

3.6.3 Pollen profiles

Figure 3.24 shows the pollen profiles for the Kakaho short core, and record the decline in native plant species and rise of exotic grass, weed and tree species. Historical landcover zones have been identified on the basis of the relative abundance of different plant species (section 2.1.4). The pollen profiles of recently introduced species, such as pine, show the results of deep sediment mixing, with pine pollen present to 30 cm depth. However, pine pollen abundance only substantially increases towards the surface from ~15 cm depth. Time-averaged pollen SAR for each historical zone are corrected for sediment mixing as discussed in section 3.2.3.

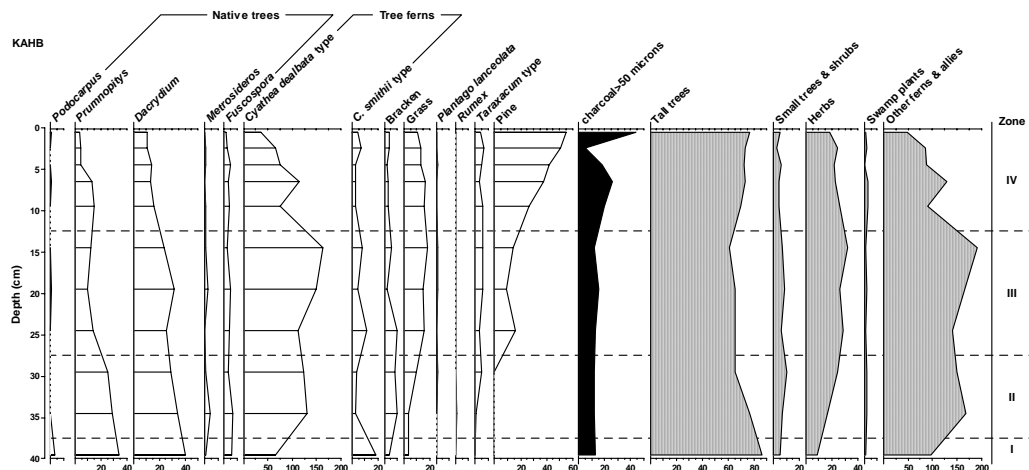


Figure 3.24: Kakaho subtidal core KAH, pollen and spore profiles for major plant groups expressed as a percentage of the terrestrial pollen and spore sum.

3.6.4 Sedimentation rates

Complimentary dating of the Kakaho subtidal core documents increases in sedimentation rates that have occurred following European settlement (Fig. 3.25). The time-averaged ^{210}Pb SAR (2.5 mm yr^{-1}) is similar to the pollen SAR of 2.0 mm yr^{-1} during the last 150 years. Sedimentation rates have increased by $\sim 60\%$ in the post-1950 period and ^{137}Cs SAR (4.1 mm yr^{-1}) and pollen (3.6 mm yr^{-1}) derived SAR are similar. As observed in the PAT and HRK cores, there is an apparent **increase** in the post-1985 SAR (zone IV pine-pollen layer) for core KAH to $\sim 5 \text{ mm yr}^{-1}$. This cannot be corroborated by an independent dating method. The good agreement between ^{210}Pb , ^{137}Cs and pollen-derived SAR provides confidence in the recent sedimentation history reconstructed for the Kakaho subtidal core.

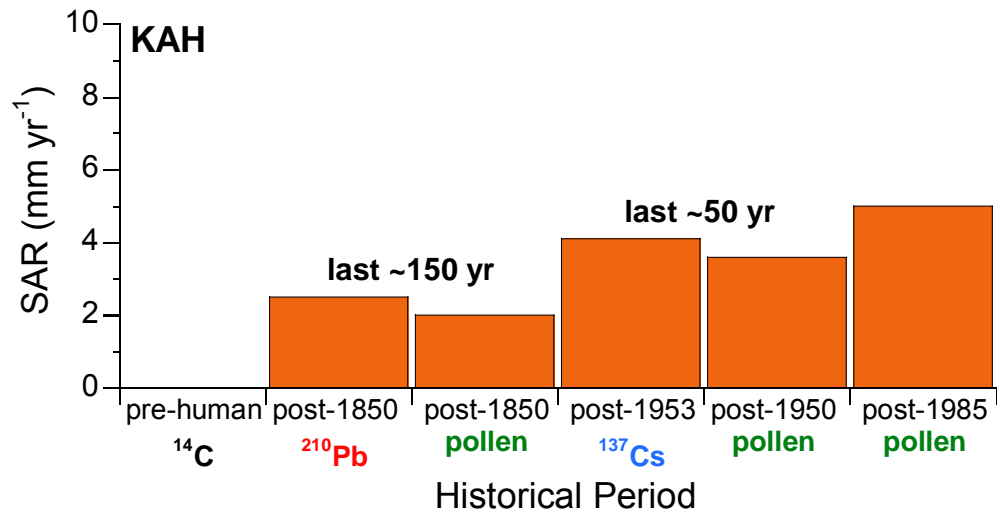


Figure 3.25: Core KAH (Kakaho) time-averaged sediment accumulation rates (SAR) for historical periods based on ²¹⁰Pb, ¹³⁷Cs and pollen dating.

3.7 Basin: Site One (BAS1)

The four basin core sites were selected to quantify sedimentary processes and reconstruct the recent sedimentation history (i.e., last 150 years) of the central mud basin. Previous work (e.g., Healy, 1980) suggests that the central mud basin is a long-term sink for catchment derived fine-sediments. The central mud basin is remote from the sub-catchment outlets, where “local” effects maybe observed and this is where the overall effects of catchment landcover changes on the inlet should be preserved. The BAS1 and BAS4 sites are also located in proximity to the original PEP study long-core sites (Healy, 1980, Fig. 21).

3.7.1 Sedimentary processes

The BAS1 short cores were collected ~500 m north of the Duck Creek mouth (Fig. 1.3) in 2.2 m water depth (27/4/04, 1202 NZST). The x-radiograph shows a 4-cm thick bedded-fining upward surface layer, as shown by the reduction in sediment density towards the surface (light to dark) (Fig. 3.26a). A light-coloured thin sand layer can be clearly identified at ~4-cm depth. This unit is indicative of recent sediment resuspension. There is an overall reduction in sediment density, which indicates a shift to muddier sediments towards the sediment surface. Abundant shell valves and fragments occur below 30-cm depth. The effects of infauna are also clearly seen, for example the large shell-filled burrow between 15–27-cm depth. The mottling of the x-radiograph is indicative of sediment mixing by abundant bioturbators. No obvious sediment layers are preserved below ~5cm depth.

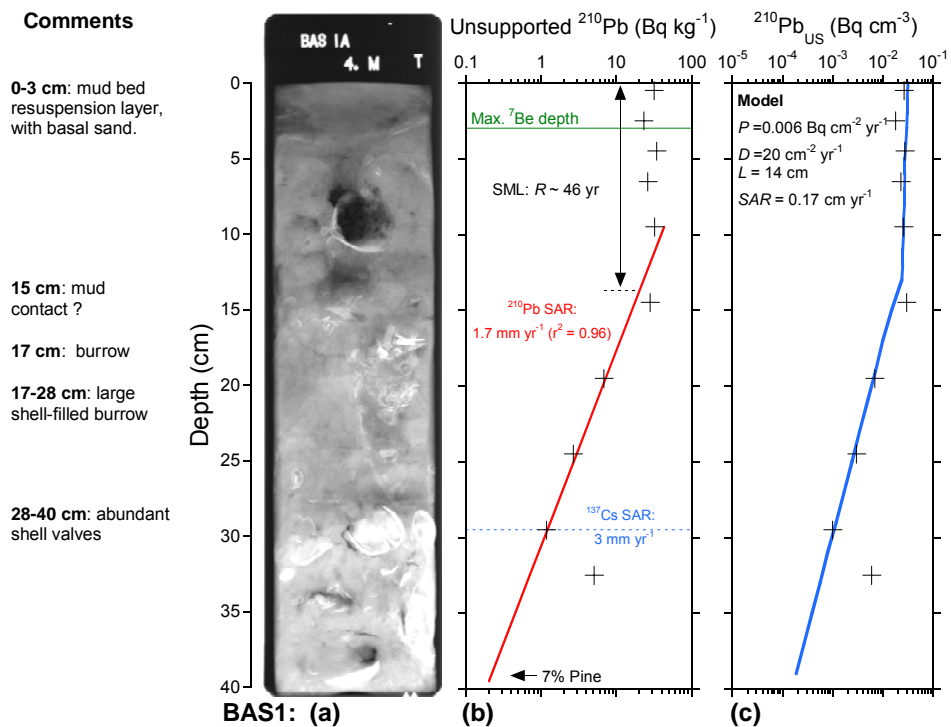


Figure 3.26: Basin Site One (BAS1) core: (a) x-radiograph; (b) unsupported ^{210}Pb profile (Bq kg^{-1}), maximum depths of ^7Be (green) and ^{137}Cs (blue) occurrence and time-averaged SAR; and (c) analytical model fitted to measured unsupported ^{210}Pb profile with fitted model parameter values shown. Note that: (1) the ^{137}Cs SAR are corrected for the mixing depth (L); (2) R is a first-order estimate of sediment residence time in the SML based on the ^{137}Cs SAR and (3) the ^{210}Pb concentration data in (c) are transformed to Bq cm^{-3} to account for down-core variations in dry bulk sediment density.

^7Be occurs to 3-cm depth, which indicates sediment mixing over days–months to this depth (Fig. 3.26b), as indicated by the x-radiograph. The unsupported ^{210}Pb profile also displays deep sediment mixing, with uniform ^{210}Pb concentrations, extending to 14-cm depth. The unsupported ^{210}Pb profile modelling (Fig. 3.26c) indicates deep and intense ($D = 20 \text{ cm}^2 \text{ yr}^{-1}$) sediment mixing. Consequently, the estimated residence time (R) of sediments in the SML (based on ^{137}Cs SAR) of ~ 46 years is long in comparison to most of the sub-catchment outlet cores. The time-averaged ^{210}Pb SAR below the SML of 1.7 mm yr^{-1} indicates that the last 150 years of sedimentation occupies the top $\sim 26\text{cm}$ of the sediment column. This is immediately above the shell-rich sand layer below 28-cm depth.

3.7.2 Sediment profiles

The BAS1 subtidal sediments preserve evidence of a shift towards increasingly fine-sediment deposition during the last 150 years. Sediments in the sand-shell layer below

28-cm depth are composed of muddy very-fine sand, with a modal coarse-silt ($\sim 60 \mu\text{m}$) fraction and substantial quantities of fine-medium sand (Fig. 3.27). By comparison, surface sediments are almost entirely composed of mud with 30% of this material being fine silt and clay (i.e., particle diameter $\leq 20 \mu\text{m}$).

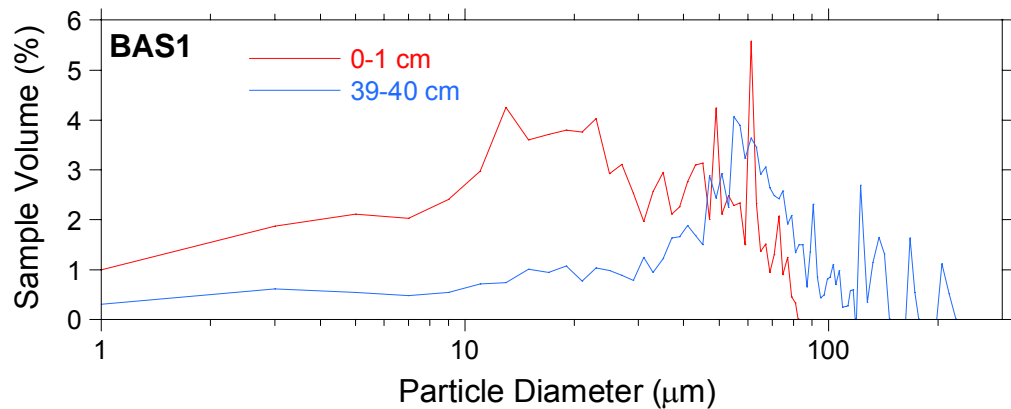


Figure 3.27: Basin Site One (BAS1) short core, particle-size distribution (log-scale) of surface (0-1 cm) and basal (39-40 cm) sediments.

Profiles of median and mean particle diameters are similar and confirm the shift to fine-sediment deposition with values decreasing from $\sim 70 \mu\text{m}$ (39–40 cm depth) to $\sim 30 \mu\text{m}$ at the surface (Fig. 3.28a). The mud content of the sand-shell layer below 28-cm depth averages 45% and this increases to $\sim 85\%$ at the sediment surface (Fig. 3.28b) have not varied measurably over the last 150 years. Dry bulk sediment density decreases from 1.7 g cm^{-3} at the base of the core to 0.7 g cm^{-3} at the surface (Fig. 3.28c).

Changes in heavy metal concentration profiles also reflect the increase in mud content above 30-cm depth. Cu and Pb concentrations below 30-cm depth (in the sand-shell layer) of $\sim 5\text{--}10 \mu\text{g g}^{-1}$ double to $12\text{--}19 \mu\text{g g}^{-1}$ at the surface (Fig. 3.28d). Likewise, Zn concentrations almost double from $\sim 40 \mu\text{g g}^{-1}$ in the sand-shell layer and then gradually increase to $\sim 75 \mu\text{g g}^{-1}$ at the surface. The effects of the rapid homogenisation of the top-most 4-cm of the sediment column can be seen in the Zn profile. The start of the Zn rise at 28-cm depth and corrected for the present day SML thickness of 14 cm coincides with the early-1920's (i.e., $280 - 140 \text{ mm} = 140 \text{ mm} / ^{210}\text{Pb SAR} \sim 82 \text{ years}$). Present day (i.e., surface) total Cu Pb and Zn concentrations are $\leq 40\%$ of ANZECC ISQG-low values.

These sediment profile data, in conjunction with the x-radiographs and radioisotope profiles show: (1) a shift to fine-sediment accumulation during the last 150 years; and

(2) that these fine sediment deposits are frequently resuspended and deeply and intensely mixed by physical and biological processes.

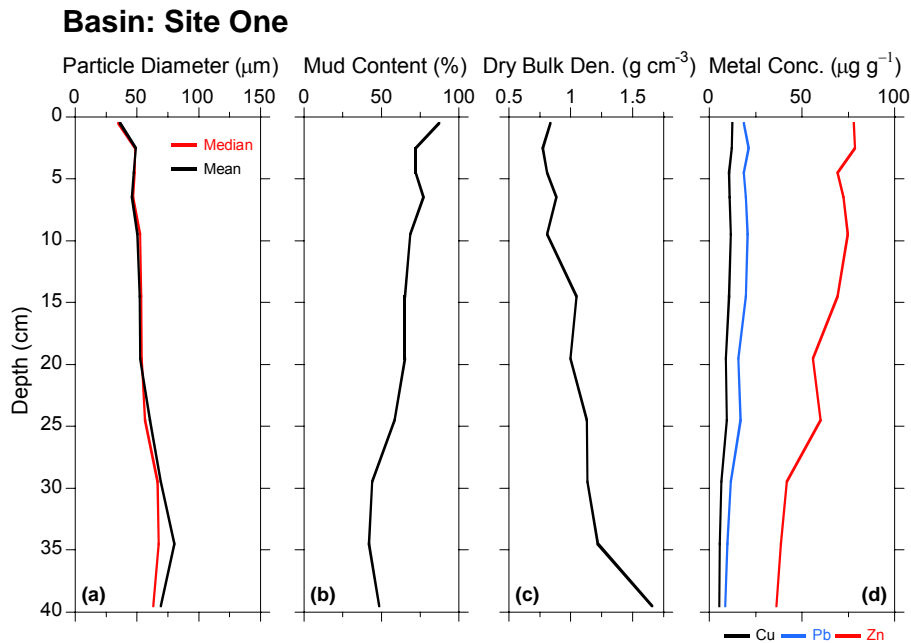


Figure 3.28: Basin Site One (BAS1) subtidal short-core sediment profiles: (a) median and mean particle diameter (μm); (b) mud content (%); (c) dry bulk density (g cm^{-3}); and (d) Total Cu, Pb and Zn concentrations ($\mu\text{g g}^{-1}$).

3.7.3 Pollen profiles

Figure 3.29 shows the pollen profiles for the BAS1 short core, and record the decline in native plant species and rise of exotic grass, weed and tree species. Historical landcover zones have been identified on the basis of the relative abundance of different plant species (section 2.1.4). As in several of the other cores, the pollen profiles of recently introduced species, such as pine, show the results of deep sediment mixing, with pine pollen present in trace amounts to 40 cm depth. Pine pollen abundance substantially increases from $\leq 15\%$ to $\sim 40\%$ above 15-cm depth. Time-averaged pollen SAR for each historical zone are corrected for sediment mixing as discussed in section 3.2.3.

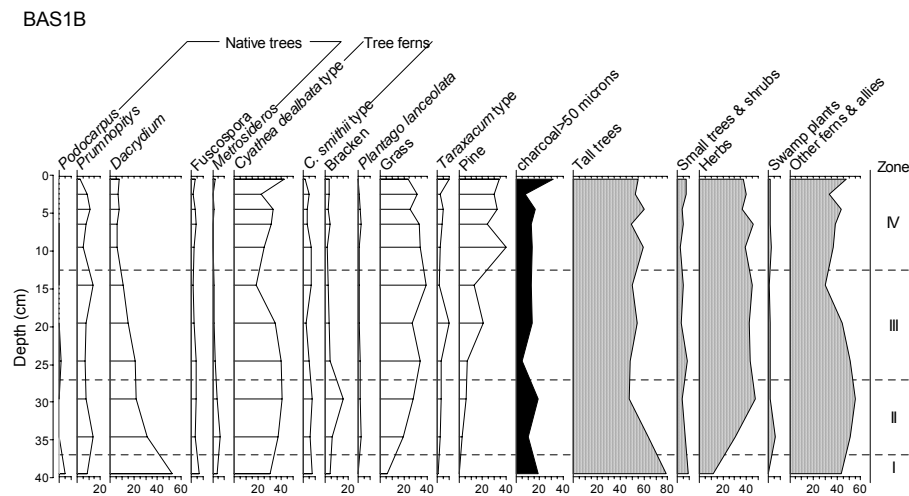


Figure 3.29: Basin Site One (BAS1), pollen and spore profiles for major plant groups expressed as a percentage of the terrestrial pollen and spore sum.

3.7.4 Sedimentation rates

Complimentary dating of the BAS1 subtidal core enables us to quantify changes in sedimentation rates following European settlement (Fig. 3.30). The time-averaged ^{210}Pb SAR (1.7 mm yr^{-1}) is similar to the pollen SAR of 1.5 mm yr^{-1} during the last 150 years. Sedimentation rates have almost doubled in the post-1950 period, as indicated by ^{137}Cs SAR (3 mm yr^{-1}) and pollen (2.4 mm yr^{-1}) SAR. As observed in the PAT, HRK and KAH cores, there is an apparent **increase** in the post-1985 SAR (zone IV pine-pollen layer) for the BAS1 core to $\sim 5 \text{ mm yr}^{-1}$. This cannot be corroborated by an independent dating method. The good agreement between ^{210}Pb , ^{137}Cs and pollen-derived SAR provides confidence in the recent sedimentation history reconstructed for the BAS1 core.

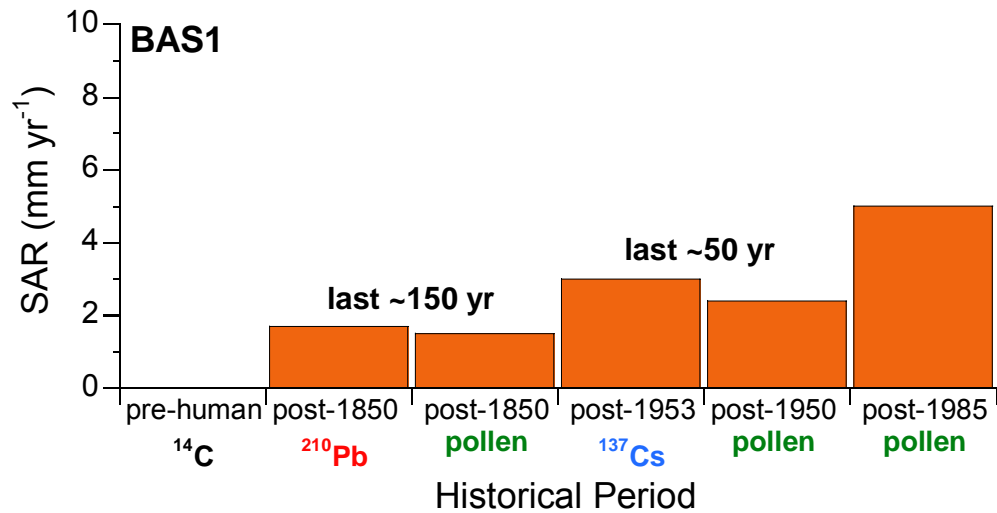


Figure 3.30: Core BAS1 time-averaged sediment accumulation rates (SAR) for historical periods based on ²¹⁰Pb, ¹³⁷Cs and pollen dating.

3.8 Basin: Site Two (BAS2)

3.8.1 Sedimentary processes

The BAS2 short cores were collected ~750 m north-west of the Duck Creek mouth (Fig. 1.3) in 2.5 m water depth (27/4/04, 1400 NZST). The x-radiograph shows a faintly bioturbated ~4-cm thick surface layer. There is a general trend of decreasing particle size towards the surface, which is indicated by a change in grey-scale colour (i.e., light to dark). Abundant valves of *Nucula hartvigiana* (nut shell) occur between 5–20-cm. It is notable that they are absent in the upper ~3cm of the sediment column where they are usually found when living. The core contains abundant mm-scale burrows and the mottled appearance of the x-radiograph is due to the mixing of sand and mud. There are also faint contacts between mud and underlying ~1-cm thick sand layers at 30-cm and 35-cm depth.

⁷Be occurs to 3-cm depth, which indicates sediment mixing over days–months to this depth (Fig. 3.31b). Like BAS1, the unsupported ²¹⁰Pb profile in BAS2 displays deep sediment mixing, with uniform ²¹⁰Pb concentrations, extending to 14-cm depth. The unsupported ²¹⁰Pb profile modelling (Fig. 3.31c) indicates deep but less intense ($D = 5 \text{ cm}^2 \text{ yr}^{-1}$) sediment mixing than at BAS1. Consequently, the estimated residence time (R) of sediments in the SML (based on ¹³⁷Cs SAR) of ~39 years of a similar order to BAS1. The time-averaged ²¹⁰Pb SAR below the SML of 3.4 mm yr^{-1} is double that at BAS1 and indicates that the last 150 years of sedimentation occupies the top ~51cm of the sediment column.

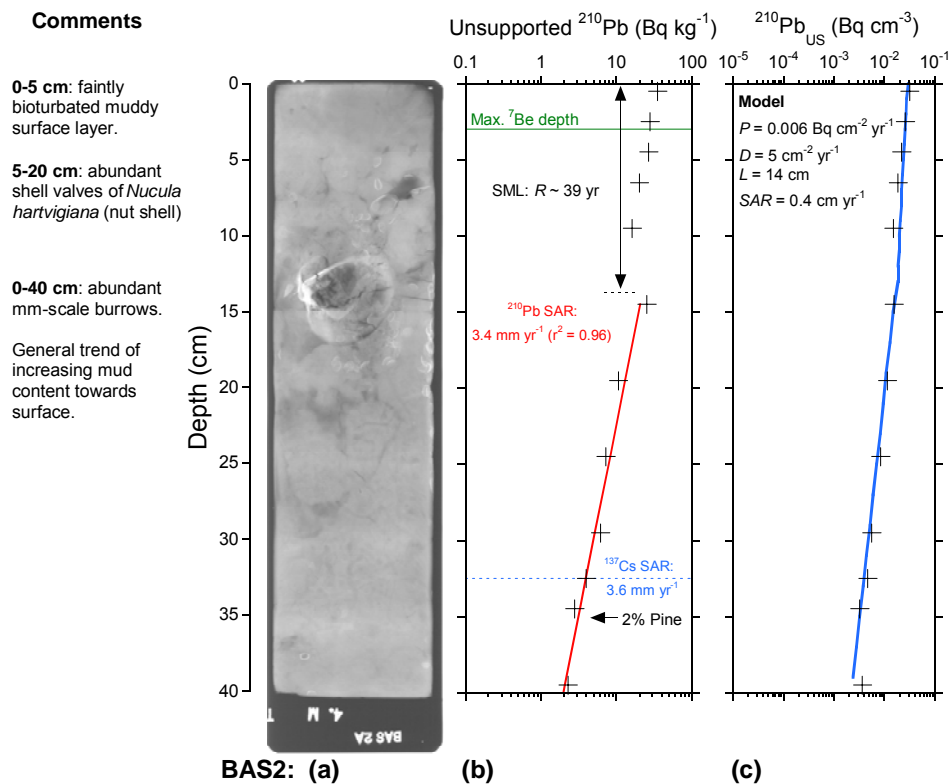


Figure 3.31: Basin Site Two (BAS2) core: (a) x-radiograph; (b) unsupported ^{210}Pb profile (Bq kg^{-1}), maximum depths of ^7Be (green) and ^{137}Cs (blue) occurrence and time-averaged SAR; and (c) analytical model fitted to measured unsupported ^{210}Pb profile with fitted model parameter values shown. Note that: (1) the ^{137}Cs SAR are corrected for the mixing depth (L); (2) R is a first-order estimate of sediment residence time in the SML based on the ^{137}Cs SAR and (3) the ^{210}Pb concentration data in (c) are transformed to Bq cm^{-3} to account for down-core variations in dry bulk sediment density.

3.8.2 Sediment profiles

Like BAS1, the BAS2 core preserves evidence of a shift towards increasingly fine-sediment deposition during the last 150 years. Basal sediments are composed of muddy very-fine sand, with a modal coarse-silt ($\sim 60 \mu\text{m}$) fraction and substantial quantities of fine-medium sand (Fig. 3.32). By comparison, surface sediments are almost entirely composed of mud (87%) with 27% of this material being fine silt and clay (i.e., particle diameter $\leq 20 \mu\text{m}$).

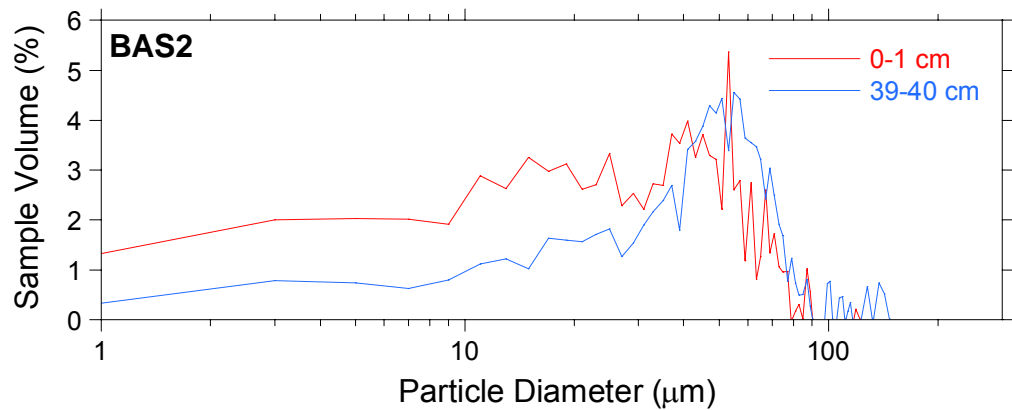


Figure 3.32: Basin Site Two (BAS2) short core, particle-size distribution (log-scale) of surface (0-1 cm) and basal (39-40 cm) sediments.

Sediment profiles of median and mean particle diameters are identical, with values reducing from ~51 µm (39–40 cm depth) to ~38 µm at the surface (Fig. 3.33a). The mud content gradually increases from 74% at the base of the core to ~87% at the sediment surface (Fig. 3.33b)

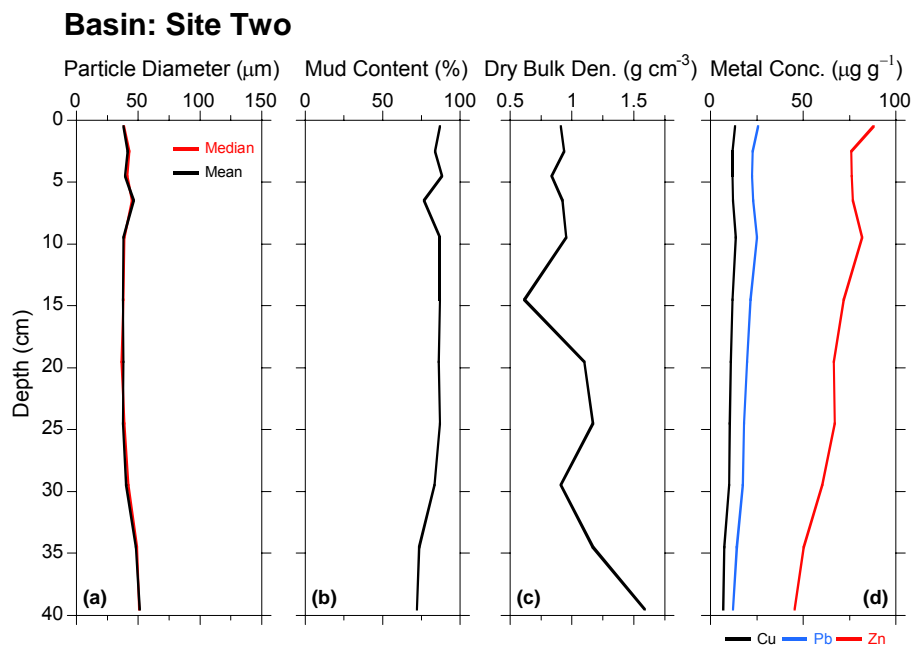


Figure 3.33: Basin Site Two (BAS2) subtidal short-core sediment profiles: (a) median and mean particle diameter (µm); (b) mud content (%); (c) dry bulk density (g cm⁻³); and (d) Total Cu, Pb and Zn concentrations (µg g⁻¹).

Dry bulk sediment density show some variability with depth, although the overall trend is a reduction from 1.6 g cm^{-3} at the base of the core to 0.9 g cm^{-3} at the surface (Fig. 3.33c). Changes in heavy metal concentration profiles also reflect the increase in mud content towards the sediment surface. Cu and Pb concentrations at 39–40-cm depth of ~ 6 and $12 \mu\text{g g}^{-1}$ (respectively) double to $13\text{--}26 \mu\text{g g}^{-1}$ at the surface (Fig. 3.33d). Zn concentrations also double, from $\sim 45 \mu\text{g g}^{-1}$ at the base then gradually rising to $\sim 87 \mu\text{g g}^{-1}$ at the surface. Present day (i.e., surface) total Cu Pb and Zn concentrations are $\leq 50\%$ of ANZECC ISQG-low values.

The BAS2 long-core data show a gradual trend of increasing particle size from 240-cm depth to the surface. Median and mean particle diameters at 240-cm depth are $\sim 30 \mu\text{m}$ and increase to $\sim 40 \mu\text{m}$ at the surface (Appendix VI, Fig. A4). Mud content decreases from 90% at 240-cm depth to $\sim 75\%$ at 50-cm depth before increasing again to $\sim 87\%$ at the surface. The increased variability in the top-40 cm reflects the more frequent sampling in the short core.

3.8.3 Pollen profiles

Figure 3.34 shows the pollen profiles for the BAS2 short core, and records the rise of exotic grass, weed and tree species. Historical landcover zones have been identified on the basis of the relative abundance of different plant species (section 2.1.5). As elsewhere in the inlet, the pine pollen profile shows the effects of deep sediment mixing, with pine pollen present in trace amounts to 40-cm depth. Pine pollen abundance increases from $\leq 5\%$ to $\sim 20\%$ above 10-cm depth. Time-averaged pollen SAR for each historical zone are corrected for sediment mixing as discussed in section 3.2.3.

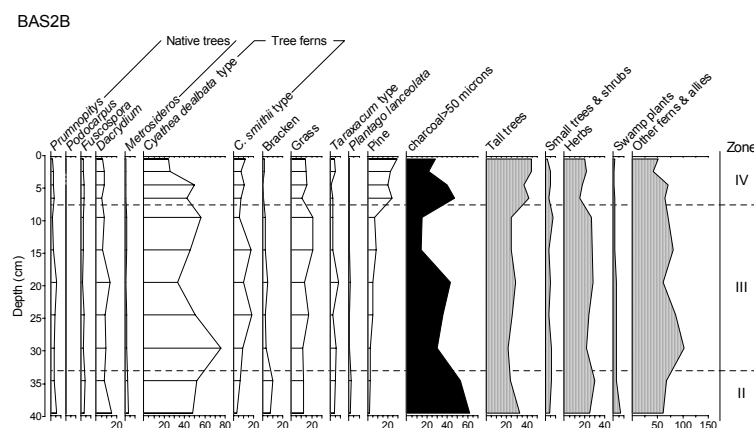


Figure 3.34: Basin Site Two (BAS2), pollen and spore profiles for major plant groups expressed as a percentage of the terrestrial pollen and spore sum.

3.8.4 Sedimentation rates

Complimentary dating of the BAS2 core enables us to quantify changes in sedimentation rates following European settlement (Fig. 3.35). The time-averaged ^{210}Pb SAR (3.4 mm yr^{-1}) for the last 150 years is very similar to ^{137}Cs SAR (3.6 mm yr^{-1}) and pollen (3.5 mm yr^{-1}) SAR for the last 50 years. These data indicate that annual sedimentation has occurred at a relatively constant rate. The post-1985 SAR (zone IV pine-pollen layer) of $\sim 2.4 \text{ mm yr}^{-1}$ suggests a $\sim 30\%$ reduction in sedimentation rates during the last 20 years, although we have no independent dating to confirm this change.

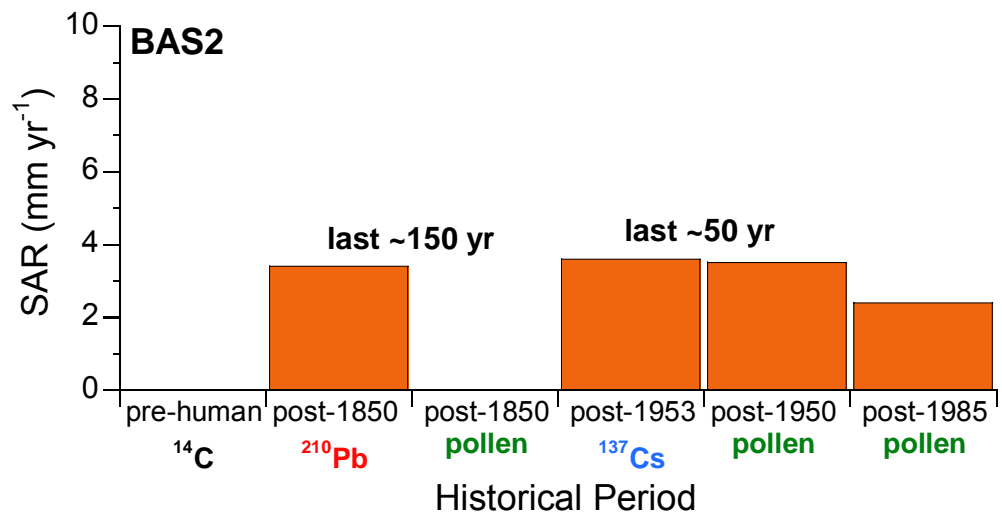


Figure 3.35: Core BAS2 time-averaged sediment accumulation rates (SAR) for historical periods based on ^{210}Pb , ^{137}Cs and pollen dating.

3.9 Basin: Site Three (BAS3)

3.9.1 Sedimentary processes

The BAS3 short cores were collected $\sim 750 \text{ m}$ north of Moorhouse Point (Fig. 1.3) in 1.9 m water depth (27/4/04, 1620 NZST). This core was collected in a secondary mud basin closer to the inlet mouth and as such the sedimentary environment maybe subtly different to that in the central mud basin. The x-radiograph shows evidence that sand layers have been disrupted by bioturbation (Fig. 3.36). The upper 10-cm of the sediment column contains interbedded sand and mud layers. A layer of shell valves

and fragments in a sand matrix occurs at 8–16-cm depth, which contains abundant valves of *Nucula hartvigiana* (nut shell). The BAS3 core also contains abundant mm–cm-scale burrows below the shell layer. There are also 1–2-cm thick sand layers at 25 cm, 30 cm and 35-cm depth, through which mud-filled burrows have been excavated.

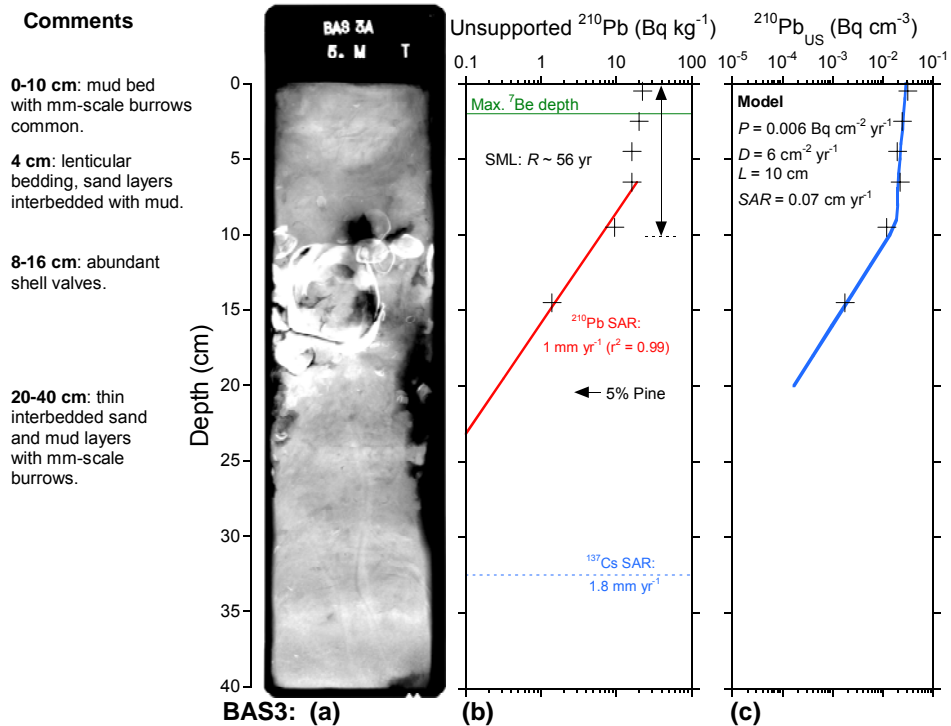


Figure 3.36: Basin Site Three (BAS3) core: (a) x-radiograph; (b) unsupported ^{210}Pb profile (Bq kg $^{-1}$), maximum depths of ^7Be (green) and ^{137}Cs (blue) occurrence and time-averaged SAR; and (c) analytical model fitted to measured unsupported ^{210}Pb profile with fitted model parameter values shown. Note that: (1) the ^{137}Cs SAR are corrected for the mixing depth (L); (2) R is a first-order estimate of sediment residence time in the SML based on the ^{137}Cs SAR and (3) the ^{210}Pb concentration data in (c) are transformed to Bq cm $^{-3}$ to account for down-core variations in dry bulk sediment density.

^7Be occurs to 2-cm depth, which indicates sediment mixing over days–months to this depth (Fig. 3.36b). Like BAS1 and BAS2, the unsupported ^{210}Pb profile in BAS3 displays deep sediment mixing, with uniform ^{210}Pb concentrations, extending to 10-cm depth. Modelling of the unsupported ^{210}Pb profile (Fig. 3.36c) indicates deep but relatively low intensity ($D = 6 \text{ cm}^2 \text{ yr}^{-1}$) sediment mixing. This may explain the fact that sediment layers are preserved in this core. The estimated residence time (R) of sediments in the SML (based on ^{137}Cs SAR) of ~56 years is of a similar order to BAS1 and BAS2. The time-averaged ^{210}Pb SAR below the SML of 1 mm yr^{-1} is substantially less than at BAS1 and BAS2, so that the last 150 years of sedimentation

occupies only the top ~15cm of the sediment column. This is consistent with the maximum depth of unsupported ^{210}Pb observed in the core.

There is some uncertainty about the maximum ^{137}Cs depth (i.e., last 150 years), given that it occurs below the depth of the unsupported ^{210}Pb profile (i.e., last 150 years). This is the case even when the ~10cm SML is taken into account. Down-core migration of ^{137}Cs in pore water can occur in sandy sediments

3.9.2 Sediment profiles

Unlike the BAS1 and BAS2 cores, BAS3 shows a shift towards increasingly coarse-grained sediments during the last 150 years. Basal sediments are composed of very-fine sandy mud, with a modal fine-silt (~20 μm) fraction and a negligible fine sand component (Fig. 3.37). By comparison, the modal particle diameter of surface sediments is ~60 μm and are composed of 55% fine sand as opposed to 25% fine sand at 39–40-cm depth.

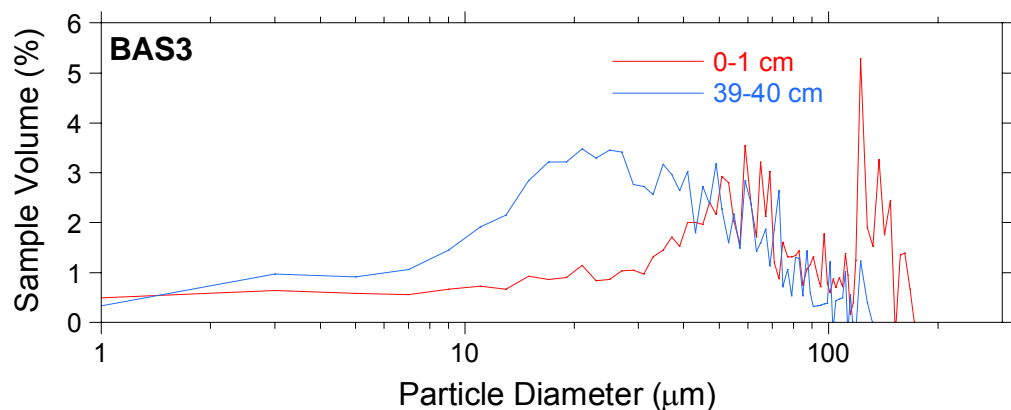


Figure 3.37: Basin Site Three (BAS3) short core, particle-size distribution (log-scale) of surface (0-1 cm) and basal (39-40 cm) sediments.

Sediment profiles of median and mean particle diameters are similar, and show an increase in particle diameter towards the sediment surface from ~45 μm (39–40 cm depth) to ~70 μm at the surface (Fig. 3.38a), with most of this increase occurring below 35-cm depth. The mud content at the base of the core is ~75% in comparison to 45% at the sediment surface (Fig. 3.38b). Dry bulk sediment density varies between 1.25–1.5 g cm^{-3} (Fig. 3.38c). No heavy metal analyses were undertaken for the BAS3 core.

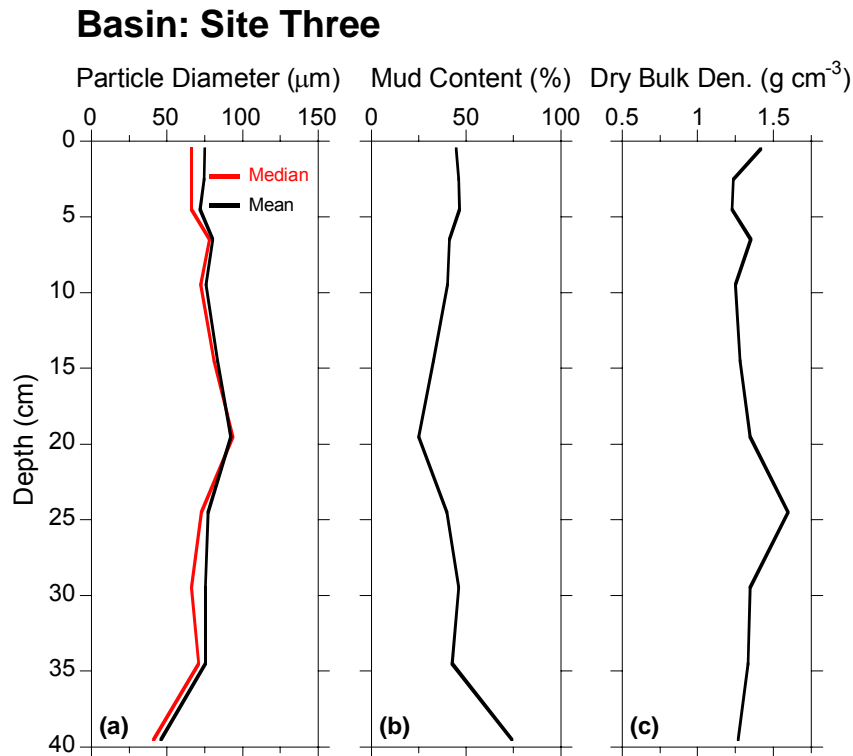


Figure 3.38: Basin Site Three (BAS3) subtidal short-core sediment profiles: (a) median and mean particle diameter (μm); (b) mud content (%); and (c) dry bulk density (g cm^{-3}). No heavy metal analysis of sediments undertaken at this site.

3.9.3 Pollen profiles

Figure 3.39 shows the pollen profiles for the BAS3 short core, and record rise of exotic grass, weed and tree species. Historical landcover zones have been identified on the basis of the relative abundance of different plant species (section 2.1.4). As elsewhere in the inlet, the pine pollen profile shows the effects of deep sediment mixing, with pine pollen present in trace amounts below 20-cm depth. Pine pollen abundance substantially increases from $\leq 1\%$ to $\sim 50\%$ above this depth. Time-averaged pollen SAR for each historical zone are corrected for sediment mixing as discussed in section 3.2.3.

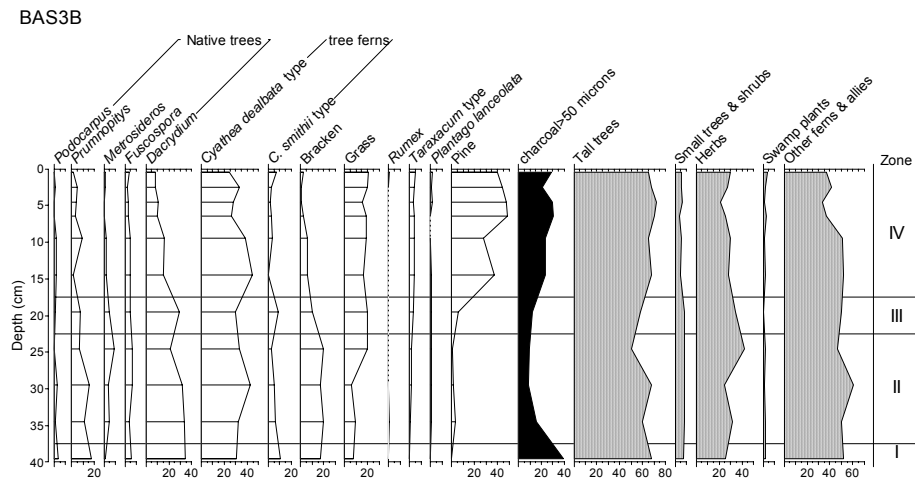


Figure 3.39: Basin Site Three (BAS3), pollen and spore profiles for major plant groups expressed as a percentage of the terrestrial pollen and spore sum.

3.9.4 Sedimentation rates

Time-averaged ^{210}Pb SAR (1 mm yr^{-1}) is substantially lower than the 1.8 mm yr^{-1} estimated from the pollen profile for the last 150 years (Fig. 3.39). We favour the ^{210}Pb SAR value because the dating method is less subjective than for pollen and is also supported by profile modelling. Time-averaged ^{137}Cs SAR (1.8 mm yr^{-1}) and pollen (2.3 mm yr^{-1}) SAR are similar over the last 50 years, although there is some uncertainty regarding the ^{137}Cs data (section 3.9.1). The post-1985 SAR (zone IV pine-pollen layer) of $\sim 3.9 \text{ mm yr}^{-1}$ suggests that sedimentation rates have doubled in the last 20 years, although we have no independent dating to confirm this result.

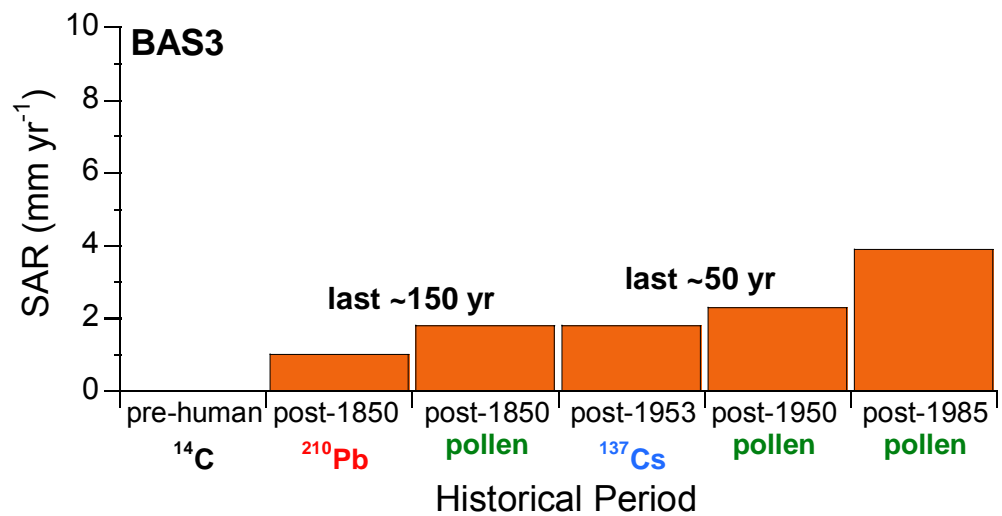


Figure 3.40: Core BAS3 time-averaged sediment accumulation rates (SAR) for historical periods based on ²¹⁰Pb, ¹³⁷Cs and pollen dating.

3.10 Basin: Site Four (BAS4)

3.10.1 Sedimentary processes

The BAS4 short cores were collected ~550 m south-west of Ration Point (Fig. 1.3) in 2.5 m water depth (27/4/04, 1600 NZST). The x-radiograph, despite re-imaging, is under-exposed below 8-cm depth (Fig. 3.41). The muddy surface layer contains numerous mm-scale burrows, which suggests that sediment resuspension by waves does not occur as frequently and/or as intensely at BAS4 as elsewhere. For example, at BAS1 where the x-radiograph and ⁷Be shows a rapidly-mixed surface mud layer with no evidence of animal burrows. Dark voids (i.e., low density) on the BAS4 x-radiograph are wood fragments.

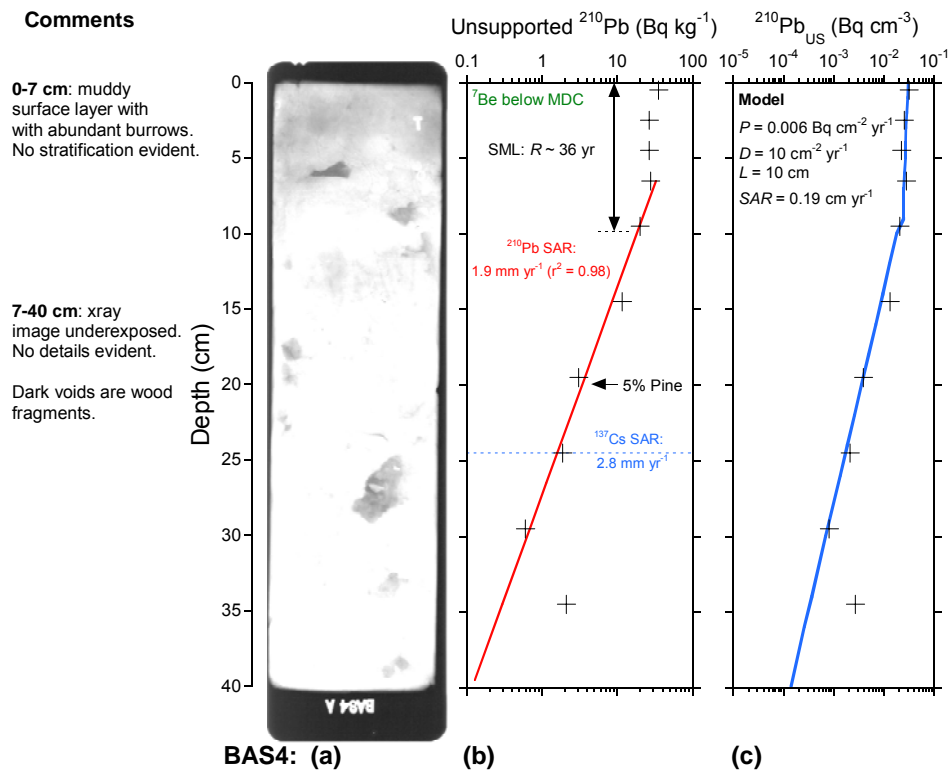


Figure 3.41: Basin Site Four (BAS4) core: (a) x-radiograph; (b) unsupported ^{210}Pb profile (Bq kg^{-1}), maximum depths of ^7Be (green) and ^{137}Cs (blue) occurrence and time-averaged SAR; and (c) analytical model fitted to measured unsupported ^{210}Pb profile with fitted model parameter values shown. Note that: (1) the ^{137}Cs SAR are corrected for the mixing depth (L); (2) R is a first-order estimate of sediment residence time in the SML based on the ^{137}Cs SAR and (3) the ^{210}Pb concentration data in (c) are transformed to Bq cm^{-3} to account for down-core variations in dry bulk sediment density.

^7Be is absent from the surface mud layer (Fig. 3.41b). This is consistent with the lack of recent surface sediment mixing implied by the x-radiograph. Like the other BAS sites, the unsupported ^{210}Pb profile in BAS4 indicates deep sediment mixing, with uniform ^{210}Pb concentrations, extending to 10-cm depth. Modelling of the unsupported ^{210}Pb profile (Fig. 3.41c) indicates deep but relatively moderate intensity ($D = 10 \text{ cm}^2 \text{ yr}^{-1}$) sediment mixing. The estimated residence time (R) of sediments in the SML (based on ^{137}Cs SAR) of ~ 36 years is also of a similar order to the other BAS sites (i.e., 39–56 years). The time-averaged ^{210}Pb SAR below the SML of 1.9 mm yr^{-1} indicates that the last 150 years of sedimentation occupies only the top ~ 29 cm of the sediment column.

3.10.2 Sediment profiles

The BAS4 subtidal sediments are composed of silty-mud, with a modal coarse-silt (~50 μm) fraction and small quantities of very-fine sand (Fig. 3.42). The similarity of the particle-size distributions for the 0–1 cm and 39–40-cm depth samples suggests a supply of uniformly fine sediments over the last 150 years or so.

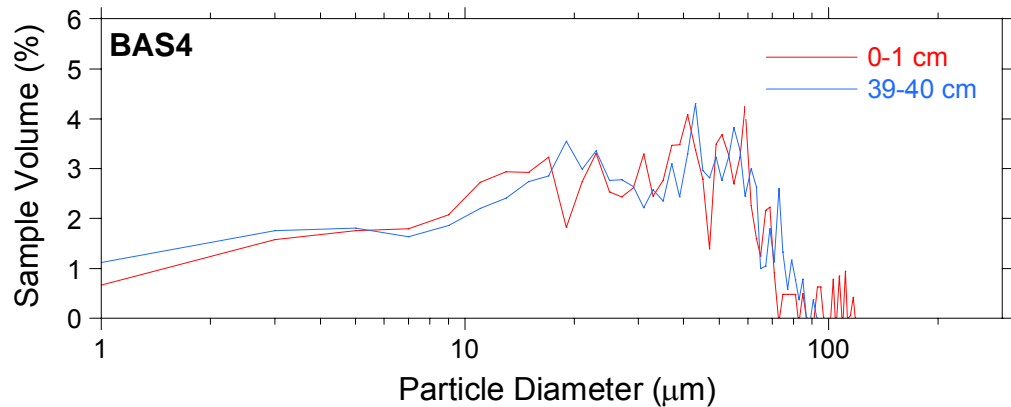


Figure 3.42: Basin Site Four (BAS4) short core, particle-size distribution (log-scale) of surface (0-1 cm) and basal (39-40 cm) sediments.

Sediment profiles of median and mean particle diameters are identical and uniform at ~40 μm from the surface to the base of the core (Fig. 3.43a), as is the mud content at 84% (Fig. 3.43b). In this uniform sediment, dry bulk sediment density increases with depth due to compaction/de-watering from 0.8 g cm^{-3} at the surface and 1.5 g cm^{-3} at the base (Fig. 3.43c). Changes in heavy metal concentration profiles reflect historical inputs to the inlet. Cu concentrations do not substantially change (9–12 $\mu\text{g g}^{-1}$) whereas Pb concentrations almost double from 13 $\mu\text{g g}^{-1}$ at 39–40-cm depth to ~22 $\mu\text{g g}^{-1}$ at the surface (Fig. 3.43d). Zn concentrations increase by 45%, from ~53 $\mu\text{g g}^{-1}$ at the base and gradually rising to ~77 $\mu\text{g g}^{-1}$ at the surface. Present day (i.e., surface) total Cu Pb and Zn concentrations are $\leq 44\%$ of ANZECC ISQG-low values.

The BAS4 long-core data show that sediment characteristics have been relatively uniform over the last ~2000 years (Appendix VI, Fig. A5). The data show that median and mean particle diameters have varied about ~30 μm from 250-cm depth to the surface. Mud content decreases from 90% at 250-cm depth to ~80% at 45-cm depth before increasing again towards the surface. The increased variability in the top-40 cm reflects the more frequent sampling in the short core.

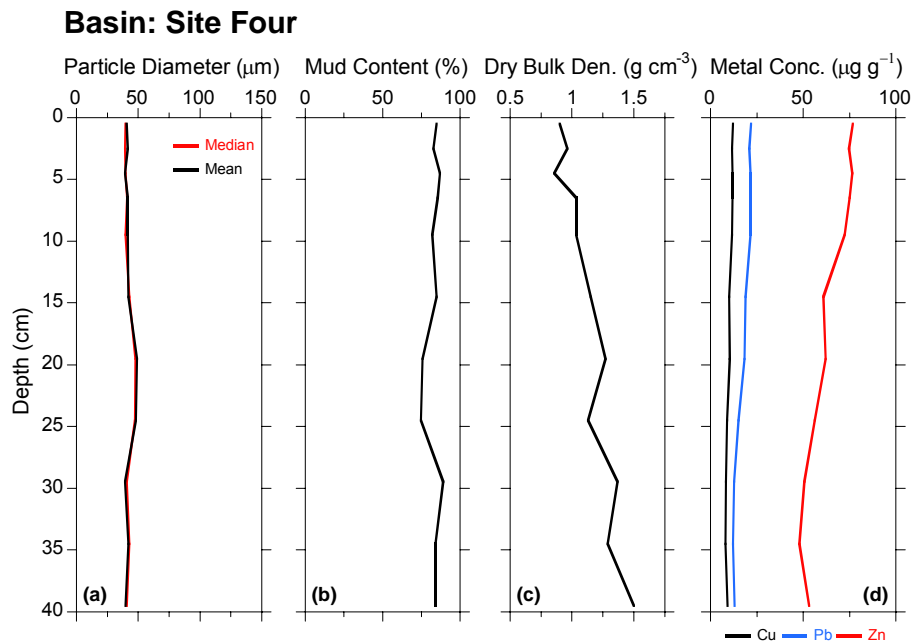


Figure 3.43: Basin Site Four (BAS4) subtidal short-core sediment profiles: (a) median and mean particle diameter (μm); (b) mud content (%); (c) dry bulk density (g cm^{-3}); and (d) Total Cu, Pb and Zn concentrations ($\mu\text{g g}^{-1}$).

3.10.3 Pollen profiles

Figure 3.44 shows the pollen profiles for the BAS4 short core, and records the rise of exotic grass, weed and tree species. Historical landcover zones have been identified on the basis of the relative abundance of different plant species (section 2.1.5). As elsewhere in the inlet, the pine pollen profile shows the effects of deep sediment mixing, with pine pollen present in trace amounts below 20-cm depth. Pine pollen abundance increases from $\leq 5\%$ to $\sim 50\%$ above this depth. Time-averaged pollen SAR for each historical zone are corrected for sediment mixing as discussed in section 3.2.3.

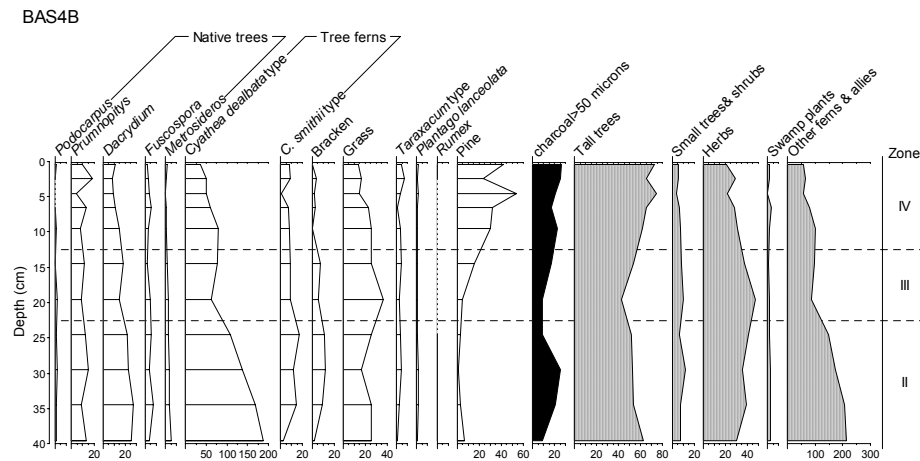


Figure 3.44: Basin Site Four (BAS4), pollen and spore profiles for major plant groups expressed as a percentage of the terrestrial pollen and spore sum.

3.10.4 Sedimentation rates

Complimentary dating of the BAS4 core indicates that sedimentation rates have increased following catchment deforestation. The ^{14}C age of *Macomona lilliana* shell valves (sample *Wk-15783*, Uni. Waikato Radiocarbon Lab.) taken from the long core at 232 cm depth (compression corrected) of 1934 ± 31 years BP is used to calculate a time-average SAR of $\sim 1.2 \text{ mm yr}^{-1}$ for the last ~ 2000 years. Time-averaged sedimentation rates increased following catchment deforestation to $\sim 1.9 \text{ mm yr}^{-1}$ (^{210}Pb SAR) and to 2.8 mm yr^{-1} (^{137}Cs SAR) – 2.3 mm yr^{-1} (pollen) during the last ~ 50 years. The post-1985 SAR (zone IV pine-pollen layer) of $\sim 5.3 \text{ mm yr}^{-1}$ is within the range estimated for other core sites. The pollen data suggest that SAR have almost doubled in the last 20 years, although we have no independent dating to confirm this result.

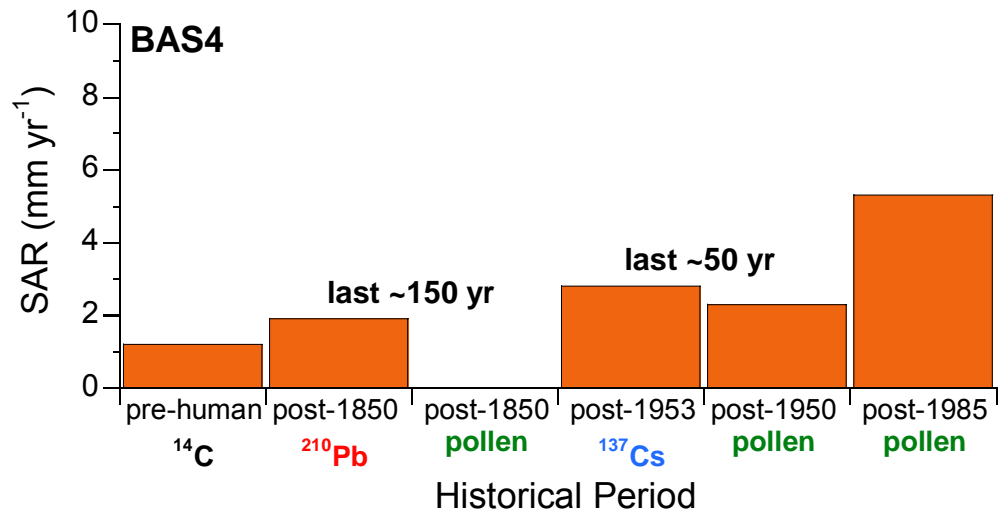


Figure 3.45: Core BAS4 time-averaged sediment accumulation rates (SAR) for historical periods based on ¹⁴C, ²¹⁰Pb, ¹³⁷Cs and pollen dating.

4. Recent sedimentation in the Pauatahanui inlet

4.1 Historical changes in inlet sedimentation rates

Complimentary and independent dating of the Pauatahanui sediment cores enable us to reconstruct the changes in inlet sedimentation rates that have occurred as a consequence of catchment deforestation (1840–1900 AD), conversion to pasture and in the last 30 years exotic forest planting (~2000 ha) and urbanisation in the Browns Bay and Duck sub-catchments. Figure 4.1 summarises the results by averaging the SAR (time-average) data for: (1) all cores sites; (2) central mud basin (CMB) sites (BAS1, BAS2, BAS4); and (3) sub-catchment outlet sites for each historical time period. We have classified BAS3 as a sub-catchment outlet site because it is remote from the primary CMB and the sediment profile data (section 3.9.2) are characteristic of type (3) sites. The variability in these average SAR values, as indicated by the standard deviations largely reflect the small sample size. It should also be borne in mind that these time-averaged sedimentation rates integrate the effects of changes in landcover over different time-scales. For example, annual sedimentation rates during and for several decades immediately after initial catchment deforestation were likely to be higher than the time-averaged value over the last 150 years. Furthermore, these sedimentation rates are *net* values, in that they integrate cycles of sediment resuspension and deposition at a particular location.

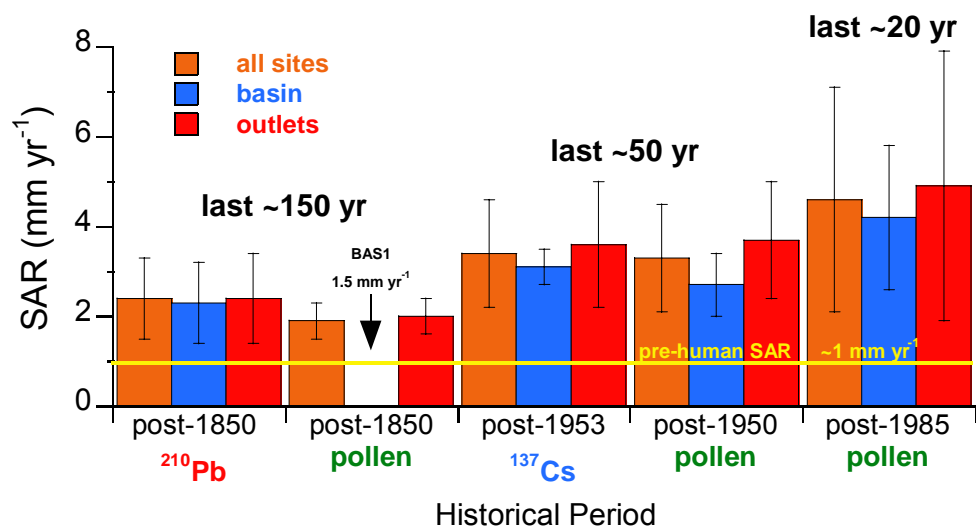


Figure 4.1: Average SAR (mm yr⁻¹) for each historical time period classified by sedimentary environment: (1) all core sites; (2) central mud basin sites; and (3) sub-catchment outlet sites. One standard deviation values are also plotted.

Background Sedimentation Rates (Pre-1850 AD)

The time-averaged SAR of 1 mm yr^{-1} for the inlet before catchment deforestation is based on: (1) the depth of sediment deposited in the inlet during the last 14,000 years (i.e., $13 \text{ m}/14,000 \text{ yr} = \sim 1 \text{ mm yr}^{-1}$, Healy, 1980); and (2) the average ^{14}C SAR for the last ~ 2000 years derived from dated shell samples taken from the BRN (0.7 mm yr^{-1}) and BAS4 (1.2 mm yr^{-1}) long cores. This “background” sedimentation rate for the Pauatahanui inlet is relatively high in comparison to pre-deforestation SAR of $\leq 0.5 \text{ mm yr}^{-1}$ for other North Island estuaries in the Auckland and Coromandel regions (Hume and McGlone, 1986; Hume and Dahm, 1992; Vant et al. 1993; Goff, 1997; Swales et al. 1997; Swales et al. 2002a).

Sedimentation Rates: Post-1850 AD

The effect of large-scale deforestation on inlet sedimentation are shown by the increase in average SAR values during the last 150 years. This time period includes all the changes in landcover including and subsequent to deforestation. The ^{210}Pb and pollen data are in close agreement and indicate that SAR doubled to $\sim 2.4 - 2.0 \text{ mm yr}^{-1}$ from background values (Figure 4.1). There is negligible difference in average SAR for the basin and outlet core sites, which suggests widespread dispersal of catchment sediments.

Sedimentation Rates: Post-1950 AD

In the last ~ 50 years average SAR have increased by an additional $\sim 1 - 1.7 \text{ mm yr}^{-1}$ to $3.1 - 3.7 \text{ mm yr}^{-1}$ (Figure 4.1). SAR are more than three times higher than pre-deforestation values. The last 50 years include the time period immediately before urban development in the Browns Bay and Duck Creek sub-catchments from the late-1960's and the planting of 2000 ha of mainly pine forest since the mid-1970's. These data show more differentiation between the basin and sub-catchment outlet sites with average SAR at outlet sites being as much as 1 mm yr^{-1} higher than in the CMB. This indicates that the primary sediment source are eroded soils and that the supply rate now exceeds the ability of estuarine processes to redistribute sediments to the CMB at the same rate.

Sedimentation Rates: Post-1985 AD

The pine pollen profiles suggest further increases in inlet sedimentation rates during the last 20 years, with average SAR (all sites) of 4.6 mm yr^{-1} , which is almost five times higher than before catchment deforestation (Fig. 4.1). Average SAR at sub-

catchment outlets are ≤ 0.7 mm yr⁻¹ higher than in the CMB. Increased sedimentation has occurred at three outlet (PAT, HRK and KAH) and three basin (BAS1, BAS3–4) sites whereas post-1985 SAR at BRN, DUK and BAS2 are reduced in comparison to post-1950 values and are similar to post-1850 levels. The average SAR (all sites) of 4.6 mm yr⁻¹ is substantially influenced by the 10 mm yr⁻¹ observed at HRK, which is double the post-1985 SAR of 4–5 mm yr⁻¹ measured at other core sites where increases in SAR are observed. These between-core differences in SAR suggest (1) variations in sub-catchment sediment loads and/or sediment resuspension rates and/or (2) the pollen dating is unreliable. There is clear evidence of rapid sediment mixing of sediments to 5-cm depth at DUK primarily by wave-resuspension.

The key question, however, is the reliability of the pine pollen data on which the post-1985 SAR are solely based. We believe the post-1985 SAR are reliable based on the following observations:

- (1) There is a substantial and rapid increase in pine pollen abundance at all sites in the upper sediment column that is not observed deeper in the cores. This cannot be explained other than by a large increase in pollen production several years after planting, which has been documented in Auckland and Coromandel estuaries. We take a conservative approach to estimating time-averaged SAR in that we assume that (a) the increase in pine pollen production occurs ~10 years after planting and (b) rapid mixing (days–months) of sediment and pollen occurs in the ⁷Be layer. The effect of (a) and (b) are to reduce time-averaged SAR estimated for the post-1985 period in comparison to SAR derived from the “raw” pollen profile.
- (2) The close agreement (in most cases) between ²¹⁰Pb, ¹³⁷Cs and pollen dating for the earlier time periods suggests that decadal-scale SAR based on pollen dating is reliable.
- (3) Some 40% of the 2000 ha of exotic forest planting since the mid-1970’s have occurred in the Horokiri sub-catchment. The effect of this large-scale change in sub-catchment landcover is preserved in core HRK. The onset of increasing pine pollen production occurs at 25-cm depth. This coincides with a reduction in sediment particle size and increase in mud content above 25-cm depth.

These results suggest that sediment loads from the Horokiri sub-catchment have increased since large-scale exotic forest planting began in the mid-1970’s and that increasingly fine-sediments are being deposited in the inlet near the sub-catchment outlet.

4.2 Spatial patterns

Sedimentation

Figure 4.2 maps the spatial variations in time-averaged ^{210}Pb SAR during the last ~150 years in the Pauatahanui inlet. The size of the circle is proportional to the annual sedimentation rate. Sedimentation rates vary substantially over hundreds of metres. For example at BAS3, the sedimentation rate (1 mm yr^{-1}) remains at pre-deforestation levels whereas at the nearby KAH site the SAR is 2.5 mm yr^{-1} . Likewise, at DUK and BAS, ^{210}Pb SAR of 1.7 mm yr^{-1} are $\leq 60\%$ of values at the nearby BAS2 (3.4 mm yr^{-1}) and PAT (2.8 mm yr^{-1}) core sites.

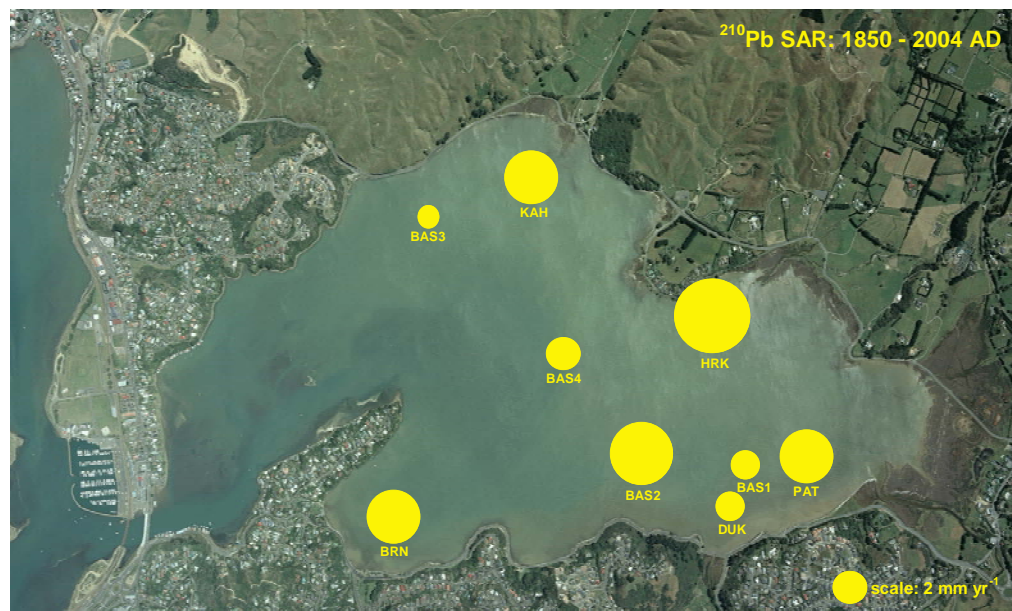


Figure 4.2: Spatial variations in time-averaged ^{210}Pb SAR (mm yr^{-1}) during the last ~150 years (post-1850) for each core site. The size of the circle is proportional to the annual sedimentation rate (scale at bottom right).

The sedimentation rate at BAS4 (1.9 mm yr^{-1}) in the centre of the central mud basin is ~50% of that at HRK, where the maximum ^{210}Pb SAR of 3.7 mm yr^{-1} is observed. At Browns Bay, the ^{210}Pb SAR of 2.9 mm yr^{-1} is relatively high given the small sub-catchment area and suggests that the bay is a long-term sink for sediments derived from elsewhere in the inlet.

Average sedimentation rates have increased at most core sites during the last 50 years (Figure 4.3). Between-site differences in ^{137}Cs SAR display similar patterns to the ^{210}Pb data with minimum SAR measured at the BAS3 and DUK sites on the shallow

subtidal flats in the north-west and south-east fringes of the inlet. The maximum ^{137}Cs SAR of 6 mm yr^{-1} occurs at Browns Bay, which is consistent with the pollen data. This integrates the effects sub-catchment urbanisation during the mid-1960's to mid-1970's, which resulted in the deposition of thousands of tonnes of eroded sub-soils in the bay (section 1.1). Sedimentation rates in the central mud basin also increased but not as rapidly as site close to sub-catchment outlets.

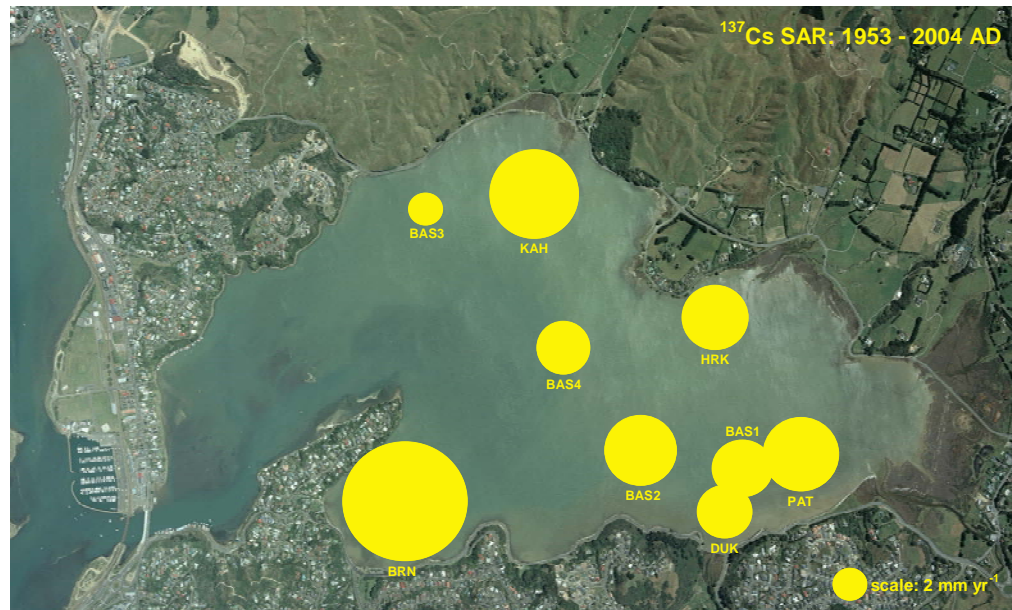


Figure 4.3: Spatial variations in time-averaged ^{137}Cs SAR (mm yr^{-1}) during the last ~50 years (post-1950) for each core site. The size of the circle is proportional to the annual sedimentation rate (scale at bottom right).

The pine pollen profiles indicate that sedimentation rates have substantially increased near the outlets of the largest sub-catchments and to a lesser extent in the central mud basin during the last 20 years (Figure 4.4). Between-site differences in pollen SAR are most marked in the south-east of the inlet. In the Duck Creek Bay, the post-1985 SAR of 1.6 mm yr^{-1} is similar to the ^{210}Pb value, while at BAS1 (only 250-m away) sedimentation rates have averaged 5 mm yr^{-1} . At Browns Bay, sedimentation rates have substantially reduced in the last 20 years in comparison with the last 50 years. This suggests that sub-catchment sediment loads have declined markedly as the urban area has matured since the late-1970's. Figure 4.4 also highlights the dramatic rise in sedimentation rates at the Horokiri outlet in the last 20 years. The fact that the ^{210}Pb SAR for the last 150 years is higher at HRK than the other core sites suggests that: (1) the Horokiri sub-catchment is prone to soil erosion; and/or (2) the Horokiri subtidal flat is a long-term sink for sediment from other sources.

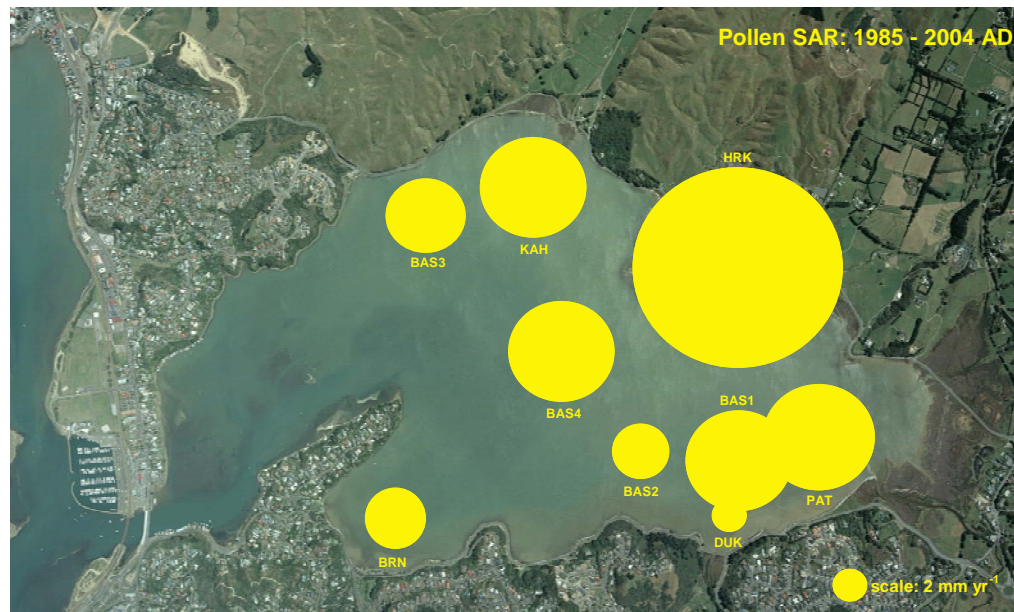


Figure 4.4: Spatial variations in time-averaged pollen SAR (mm yr^{-1}) during the last ~ 20 years (post-1985) for each core site. The size of the circle is proportional to the annual sedimentation rate (scale at bottom right).

Heavy Metals

The heavy metal profiles show systematic spatial and temporal differences at sub-catchment outlets and within the central mud basin (Fig. 4.5). Browns Bay is the most contaminated sub-catchment outlet site, albeit well below ANZECC ISQG-low values. Cu, Pb and Zn concentrations reduce (at all depths) with distance alongshore from Browns Bay (BRN) towards the Pauatahanui stream site (PAT). The estimated depth of the ^{137}Cs 1953 layer (corrected for the ^{210}Pb sediment mixing depth, L) is also shown in Fig. 4.5 to enable the heavy-metal profiles to be evaluated in light of spatial differences in sedimentation rates. It can be seen that the initial increase in heavy-metal concentrations at DUK and PAT pre-dates the 1953 layer. In the central mud basin (CMB), similar spatial variations in heavy metal concentrations are observed, with the BAS2 profiles being very similar to Browns Bay.

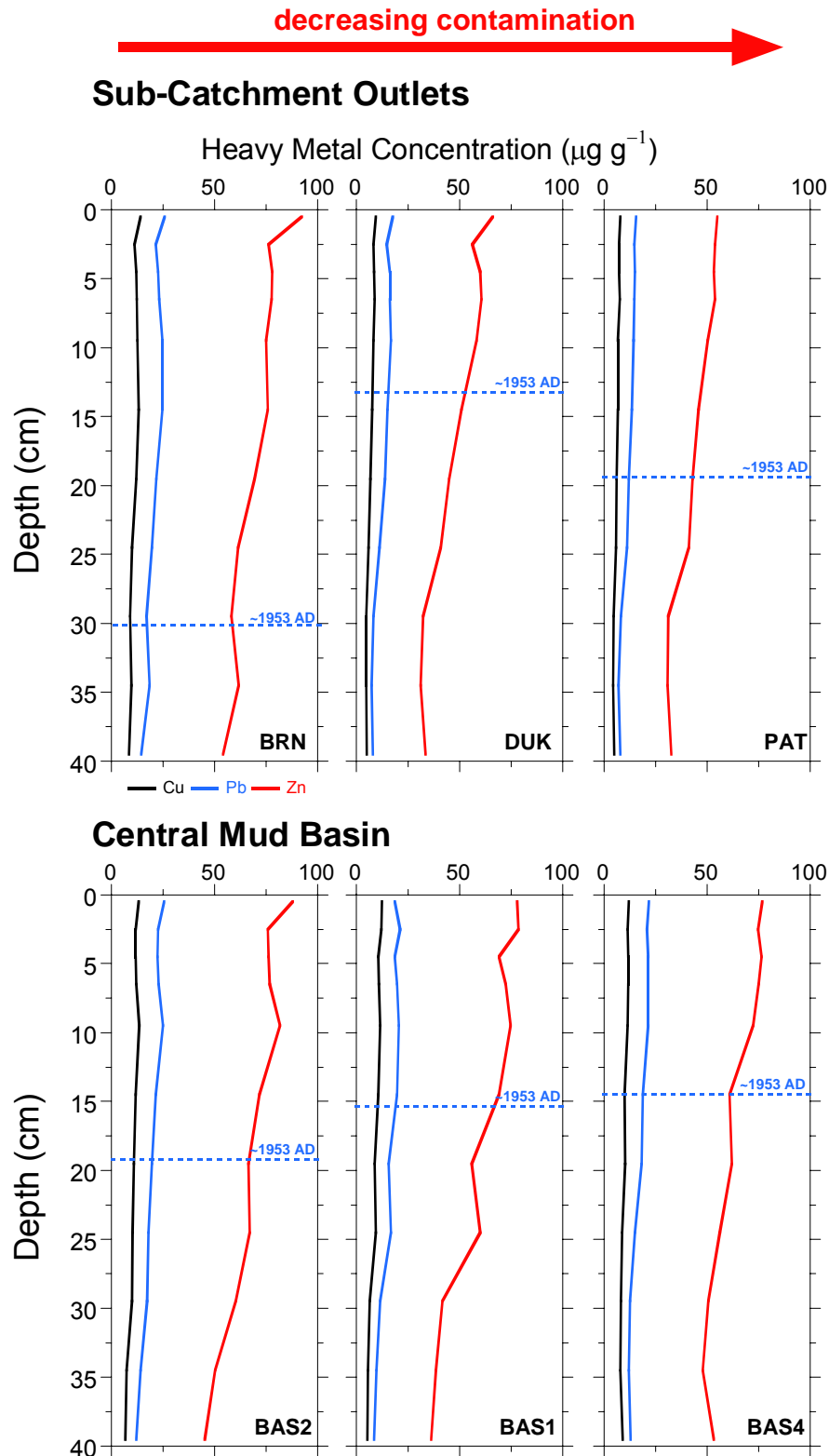


Figure 4.5: Between-core variations in heavy metal concentrations at sub-catchment outlet and central mud basin sites. Note: 1953 AD corrected for depth of surface-mixed layer.

Interpretation of the central mud basin profiles is more straight-forward because: (1) sedimentation rates have been more uniform, as shown by the maximum depths of the ^{137}Cs layer; and (2) there is less variability in the type of sediment deposited in the CMB, where uniformly fine sediments accumulate.

4.3 Catchment sedimentation loads

Historical changes in average catchment sediment loads can be reconstructed from the sediment core data and are more correctly termed sedimentation loads. This technique has previously been applied to the Mahurangi estuary (section 1.4). Sedimentation loads are based on the average SAR (all cores) for each historical landcover phase. We assume that sedimentation occurs mainly in the 3.7 km² subtidal compartment, which represents ~80% of the inlet's surface area. The product of the average SAR and the subtidal compartment area gives the sediment volume deposited in a given time period (V_S). The depth range of dry bulk sediment density (ρ_d) values to apply to each historical landcover phase are identified using time-averaged SAR. The average sediment mass deposited annually is given by $\rho_d \cdot V_{ST}$. This technique provides conservative estimates of the average annual catchment sediment load because; (1) sedimentation is also likely to occur on the intertidal flats; and (2) the sediment trapping efficiency (S_{trap}) of the inlet is less than 100%, so that a proportion of the annual catchment sediment load is flushed from the inlet. Furthermore, S_{trap} will have declined as the inlet has infilled with sediment because of changes in tidal flows and (in general) the increasing effectiveness of sediment resuspension by waves. This relates to the fact that short-period (1–3 s) waves (typical of NZ estuaries) are substantially attenuated in the upper several metres of the water column so that wave-orbital motions may not penetrate to the bed. Potential changes in sediment remobilisation by waves due to estuary infilling were modelled for the Mahurangi estuary (Swales et al. 1997). This work showed that the potential for sediment remobilisation by waves was substantially less 3000 years ago when the water column was ~ 3 metre deeper than today.

A small proportion of the sedimentation load will be fine suspended sediment delivered to the inlet from other sources by the flood tide. We assume that external sediment sources are negligible (except before deforestation) in comparison with catchment inputs. Furthermore, annual sediment loads estimated from the core data will be more reliable than estimated from stream flow and sediment loads data if the inlet is adequately sampled. This is because the core data integrate the effects of inter-annual variability in sediment loads associated with climate and long-term changes in catchment landcover over years–centuries. By comparison, it is rare to have reliable

sediment load data of more than a few years. The annual sedimentation loads estimated for each historical time period are presented in Table 4.2.

Sediment core data indicate that annual average sediment loads of $90 \text{ t km}^{-2} \text{ yr}^{-1}$ during the last 150 years are almost double average sediment loads delivered to the inlet for most of its history before catchment deforestation. It is likely that sediment loads were higher during (and in the decades immediately after) catchment deforestation (1840–1900). This effect is averaged out to some extent over the last 150 years. During the last 50 years, sediment loads have increased by $\sim 30\%$ to $120 \text{ t km}^{-2} \text{ yr}^{-1}$, which coincides with urban development in the Browns Bay and Duck sub-catchments and planting of 2000 ha of exotic forest since the mid 1970's. The pine-pollen profiles suggest that sediment loads have further increased since the mid-1980's.

Table 4.2: Average annual sediment loads delivered to the Pauatahanui inlet for historical time periods before and after catchment deforestation. nb: (1) average dry bulk sediment density (*standard deviation, sample size*); (2) specific sediment load calculated as average value for total catchment area.

Time Period	SAR (mm yr ⁻¹)	Sed. Volume (m ³)	Dry Bulk ⁽¹⁾ Density (g cm ⁻³)	Sed. Load (tonnes)	Sed. Load ⁽²⁾ (t km ⁻² yr ⁻¹)
Pre-1850	1	3700	1.37 (0.14, 24)	~5,000	~50
Post-1850	2.4	8900	1.09 (0.28, 83)	~9,700	~90
Post-1950	3.4	12600	1.05 (0.28, 55)	~13,000	~120
Post-1985	4.6	17000	1.01 (0.30, 39)	~17,000	~160

Comparison with Other Studies

Curry (1981) estimated a long-term average sediment load of $\sim 30 \text{ t km}^{-2} \text{ yr}^{-1}$ based on (1) analysis of a seven-year (1970–1976) measured/synthetic flow and (2) compilation of a 30-year normal rainfall year from records for the Pauatahanui sub-catchment (1959–1976). Hicks (1999) re-analysed the Pauatahanui stream data (site 30802, 1975–1996) for a 39.5 km^2 catchment area and included 26 suspended sediment gauging during floods. The specific yield for this sub-catchment area was $77 \text{ t km}^{-2} \text{ yr}^{-1}$ and Hicks (1999) concluded that Curry's (1981) sediment load estimate was not reliable. Pickrill (1979) estimated a long-term average sediment load to the inlet of $\sim 9600 \text{ t yr}^{-1}$ or $90 \text{ t km}^{-2} \text{ yr}^{-1}$ based on radiocarbon dating of sediment cores (PEP study) and measurements of monthly changes in intertidal elevations over a 15-month period. The Pickrill (1979) and Hicks (1999) estimates are similar to our estimates based on ²¹⁰Pb and ¹³⁷Cs dating of sediment cores in the present study.

The suspended sediment load to the Pauatahanui inlet has also been estimated using an empirical model of catchment suspended sediment yields to the New Zealand coast (Hicks and Shankar, 2003). This model relates specific suspended sediment yield to mean annual rainfall and an erosion-terrain classification (slope, geology, soils and erosion processes) and was calibrated using data from 200 sites (Hicks et al. 2004). Based on this model, the suspended sediment load to the Pauatahanui inlet in recent decades is estimated at 23,000 t yr⁻¹ or 210 t km⁻² yr⁻¹ (Dr Murray Hick, NIWA, pers com. 5 April 2005). This model estimate is considered more appropriate than Hick's (1999) value because it includes the entire inlet catchment. The model estimate is also similar to the ~160 t km⁻² yr⁻¹ estimated for the last 20 years from the sediment cores.

Our sediment cores and the results of other studies indicate that: (1) sediment loads delivered to the Pauatahanui inlet are several times higher than before catchment deforestation; and (2) the rate of sediment input is increasing.

5. Sedimentary processes: implications for resource management

5.1 Sedimentary processes – summary

The Pauatahanui inlet cores show strong evidence of rapid (days–months) mixing of surficial sediments (≤ 5 cm depth) by physical and biological processes and deeper (≤ 14 cm depth) and more gradual sediment mixing by infauna (i.e., bioturbation) over years–decades. The process can be visualised with the SML acting as a filter which smoothes input signals, such as seasonal and annual variations in the pollen rain or heavy metal loads associated with stormwater runoff. These core mixing characteristics as well as the unsupported ^{210}Pb inventory, $A(o)$, mean annual supply rate (P) and model parameters used to fit the observed unsupported ^{210}Pb profiles are summarised in table 3.1. Sediment mixing that occurs in the surface mixed layer (SML) reduces the temporal resolution of the cores as new sediments are mixed with older deposits.

The maximum depth of ^7Be occurrence is a useful indicator of short-term (days–months) sediment mixing because of its relatively short half-life (53.3 days). Thus physical processes such as sediment resuspension by waves and the feeding and burrowing activities of benthic infauna (section 1.4) rapidly homogenise the upper 2–5 cm of the sediment column. We can estimate the mass of subtidal sediment in the ^7Be layer by averaging the mass of sediment in the ^7Be layer ($^7\text{Be}_{\text{mass}}$) for each core site (kg m^{-2}) and scaling it by the subtidal surface area ($\sim 3.7 \text{ km}^2$). The calculations are also weighted because $^7\text{Be}_{\text{mass}}$ is higher and more variable in the DUK and PAT cores ($^7\text{Be}_{\text{mass}} = 52 \text{ kg m}^{-2}$, standard deviation = 16 kg m^{-2}) than for the central mud basin and remaining sub-catchment outlet cores ($^7\text{Be}_{\text{mass}} = 25 \text{ kg m}^{-2}$, standard deviation = 5 kg m^{-2}). We assume that the DUK–PAT subtidal flat accounts for 10% of the total area. These calculations indicate that $\sim 100,000$ tonnes of surficial sediments are mixed over days–months in the subtidal compartment. This is equal to 8–10 years of average sedimentation based on ^{137}Cs and ^{210}Pb SAR. Thus, on average, the shortest time scale that we can resolve in the Pauatahanui cores is of the order of decades rather than years.

The ^{210}Pb inventories, $A(o)$ and mean annual supply rates (P) for the Pauatahanui cores show that the direct atmospheric flux of unsupported ^{210}Pb to the inlet ($\sim 0.006 \text{ Bq cm}^{-2} \text{ yr}^{-1}$) is substantially augmented by indirect sources. Table 3.1 shows that the mean annual supply rates derived from the cores are 1.5–2.5 times higher than the atmospheric flux. Thus, unsupported ^{210}Pb is also supplied to the inlet from: (1) eroded catchment topsoil and (2) oceanic water delivered by tidal flows, which typically have higher ^{210}Pb concentrations than freshwater.

Unsupported ^{210}Pb is largely associated with the clay and fine silt fraction of sediments. The fact that the ^{210}Pb inventories ($0.25\text{--}0.47\text{ Bq cm}^{-2}$) vary between core sites is indicative of winnowing and concentration of these fine sediments due to resuspension and subsequent redeposition in quiescent settling zones, such as the central mud basin. For example, $A(o)$ values for the BAS3, DUK and PAT sites ($0.25\text{--}0.30\text{ Bq cm}^{-2}$) are $\sim 70\%$ of inventories in the central mud basin (BAS1, BAS2, BAS4). This spatial pattern is consistent with the prevailing north-west – south-east winds which generate waves in the inlet. Thus, sedimentary processes in the Pauatahanui inlet are extremely dynamic and variable. The upper decimetre of the sediment column is mixed by physical and biological processes and redistribution of fine sediments by resuspension and subsequent redeposition in sediment sinks, such as the central mud basin.

5.2 Implications for future landcover changes

Population projections predict that growth over the next ~ 15 years will be largely concentrated in the Duck Creek sub-catchment (section 1.1). A projected increase of 21% (~ 800 people) by 2021 is \sim double the total population growth in all other sub-catchments draining to the Pauatahanui inlet. These projections indicate that: (1) substantial urbanisation of the Duck Creek sub-catchment over the next ~ 15 years; (2) the Pauatahanui, Ration Point, Horokiri and Kakaho sub-catchment will remain predominantly rural in the foreseeable future. No data are available on future pasture conversion to pine plantations, while the bulk of the ~ 2000 ha of pine forest planted since the mid-1970's (Page et al. 2004) is likely to be harvested in the next 5–10 years. The first of these stands to be harvested, is the Silverwood forest in the Duck sub-catchment, where harvesting began in early 2003 (Mr Tim Porteous, GWRC Biodiversity Co-ordinator, pers. com.). Many of these forest plantations occupy steeplands, which are likely to be prone to soil erosion.

5.2.1 Urbanisation of Duck Creek sub-catchment

Planning the future urban development of the Duck Creek sub-catchment will require special care if adverse effects on the inlet are to be avoided or mitigated. The: (1) steep terrain; (2) erodability of the clay–silt loess soil and (3) estuarine processes all favour soil erosion and the dispersal of fine-sediments and contaminants in the inlet. The adverse effects of urban development in the adjacent Browns Bay sub-catchment are already documented (section 1.4) and highlight the potential for soil erosion and rapid sedimentation in the inlet. Our core data show that Browns Bay is a long-term sink for catchment sediments and much of the soil eroded from the urban earthworks

was deposited in Brown Bay itself. The potential environmental effects of fine-sediment eroded from the urbanising Duck Creek sub-catchment will be different.

The time-averaged ^{210}Pb SAR of 1.7 mm yr^{-1} for the DUK and nearby BAS1 core near the sub-catchment outlet are substantially lower than the inlet average (2.4 mm yr^{-1}) during the last 150 years. The ^7Be layer at DUK extends to 5-cm depth which is the maximum value measured in the Pauatahanui inlet. Elsewhere, the ^7Be layer is ≤ 3 -cm thick. The x-radiograph evidence indicates that the ^7Be layer is due largely to physical mixing of the sediment column (section 3.3). This interpretation is supported by the fact that at BAS4, where the ^7Be layer is absent, there are numerous mm-scale burrows in the upper few cm of the core (section 3.10). These trace fossils do not occur in cores where a ^7Be layer is present. The BAS4 data indicate that bioturbation is not rapid or efficient enough to homogenise near-surface sediments over days–months.

The Paraparaumu wind record (1971–2004) shows that the prevailing wind is from the north. The north-west – north-east quadrant (292 – 067°) accounts for 53% of the record whereas winds from the south-west – south-east (158 – 247°) occur only 22% of the time. Calm conditions occur 12% of the time. Thus, the southern shore of the inlet is exposed to the prevailing winds. These winds generate waves which propagate and grow as they travel down wind. Theoretical calculations (Healy, 1980 and section 1.4) indicated that waves are capable of resuspending sediment throughout the inlet. In the present study, data collected by the DOBIE wave gauges at the BAS2 and DUK sites (29 April – 8 June 2004) show that sediment resuspension occurs in the central mud basin and on the subtidal flats and that this process is driven by waves.

The DOBIE deployment period sampled neap- (0.5 m range) and spring-tide (1.5 m range) cycles. Strong winds associated with the storm of 4–5 May 2004 generated waves that resuspended large quantities of estuarine sediments. The storm coincided with spring tides. Wind speed and direction measured at Paraparaumu (site 4991) show that average wind speeds during the storm reached 54 km hr^{-1} , with gusts to 104 km hr^{-1} . Wind direction was consistently from the north-west (320° True). Sediment resuspension recorded by the wave-gauges closely coincide with the wind data.

The optical backscatter sensor (OBS) measured suspended sediment concentrations (SSC) ~ 0.3 -m above the bed. Background SSC during the ~ 4 days before the storm averaged 16 mg l^{-1} ($s = 13 \text{ mg l}^{-1}$) and 24 mg l^{-1} ($s = 19 \text{ mg l}^{-1}$) at the BAS2 and DUK sites respectively. Waves initially resuspended sediment at the shallower DUK site ($+0.25 \text{ m}$ elevation) and then one hour later at BAS2. At the height of the storm, suspended sediment concentrations at BAS2 ($\sim 800 \text{ mg l}^{-1}$) were substantially higher

than at DUK ($\sim 500 \text{ mg l}^{-1}$). SSC declined rapidly within several hours after the storm but did not return to “background” values until after three tidal cycles.

Sediment resuspension occurs in the wave-boundary layer, which over a flat bed is typically a few centimetres thick. Ripples and burrow mounds alter the flow by creating turbulence (Nielsen, 1992). The most intense suspension occurs in the boundary layer and on a mud bed, fluidisation can occur due to wave loading. In this situation the surface layer of the bed (depending on wave and bed characteristics) can be mobilised and transported by waves (Whitehouse et al. 1999). Suspended sediment concentrations in the \sim cm-thick wave-boundary immediately above the mobile mud layer can be several thousand grams per litre. Mud is mixed higher into the water column by turbulent diffusion (Dyer, 1986) where SSC will typically be several hundred milligrams per litre.

The OBS, ^7Be and x-radiograph data show that: (1) sediment resuspension in the inlet is driven by waves. Tidal currents are by themselves too weak to resuspend these fine sediments; (2) the bed is mobilised and rapidly mixed to 5-cm depth by waves; (3) fine-sediment resuspension is episodic and SSC return to background levels within hours; (4) waves resuspend fine sediments in the central mud basin as the subtidal flats; and (5) the Duck Creek subtidal flat has a high potential for fine-sediment resuspension and transport.

Based on this analysis, we can develop a conceptual model to predict the fate of fine sediments and associated contaminants discharged from Duck Creek. The subtidal flat at the catchment outlet is a transitional sedimentary environment. During flood events, fine-sediment is delivered to the inlet in stormwater. In large events, some of this sediment will be dispersed in the surface freshwater plume until it is mixed with seawater and flocculation occurs. A proportion of the mud and the bulk of the sand load will be deposited on the subtidal flat near the catchment outlet. The ^7Be and ^{210}Pb data demonstrate that these sediments are frequently and intensely mixed primarily due to bed mobilisation by waves. During these episodic wave events, the fine sand fraction is not widely dispersed because of its high fall speed ($w_s \sim 10^{-2} \text{ m s}^{-1}$). By comparison, once suspended by waves, the (non-cohesive) fine-silt fraction can potentially be transported 100–1000's metres by a weak current (i.e., $\sim 0.1 \text{ m s}^{-1}$) during a single tidal cycle because w_s is orders of magnitude lower ($\sim 10^{-4} \text{ m s}^{-1}$) than for fine sand. Some of this sediment will be deposited elsewhere on the subtidal flats, as occurred in 1974. Eroded subsoils from urban earthworks in the lower Duck sub-catchment (Whitby) were dispersed alongshore and a 5-cm deep layer deposited in Browns Bay. Fine sediment and its associated contaminants are being deposited in the central mud basin where ^{210}Pb SAR have averaged 1.9–3.4 mm yr^{-1} .

To conclude, sedimentary processes in Pauatahanui inlet are extremely dynamic and variable. The Duck Creek subtidal flat is a transitional sedimentary environment where sedimentation occurs but a large proportion of the fine-sediment fraction is resuspended and widely dispersed. The relatively low ^{210}Pb SAR values for the DUK core show that these processes has occurred for at least the last 150 years. Future urban development of the Duck sub-catchment will require careful planning to mitigate the potential adverse environmental effects of fine-sediment runoff on the inlet.

Evaluation of the *ecological risk* associated with fine-sediment and contaminant runoff is not part of the present study brief. Such an evaluation would require location-specific information on predicted inputs of fine sediments and contaminants and the history of past inputs of fine sediments and contaminants at a scale relevant to the ecological communities inhabiting particular areas. Information on the ecological communities and their sensitivities to fine sediments and the specific contaminants would also be needed.

Prediction of contaminant accumulation to support urban planning

To mitigate the adverse effects of urban stormwater contaminants in the Pauatahanui inlet and to make informed planning decisions about future development, we need to: (1) predict rates and locations of contaminant accumulation; and (2) do so at a relevant time-scale. For urban planning purposes, predictions are required at decadal time-scales. Using numerical models it is possible to predict the dispersal of freshwater/sediments/contaminants discharged from streams and stormwater overflows during rainstorms. But, such models cannot be used in any direct way to make predictions on the planning timescale.

The USC-2 (Urban Stormwater Contaminant) model has been developed by NIWA to make long-term predictions of contaminant accumulation in estuaries (Green et al. 2004). Accumulation is treated as the result of many injections and dispersals at the scale of the individual rainstorm, combined with other processes such as bioturbation and physical mixing by waves and currents that occur between rainstorms. At the heart of the model is a set of mass-balance equations that describe generation and fate of contaminants and sediments in the system at hand. Sediments need to be addressed in the model because these carry much of the contaminant load, and because they also ultimately dilute contaminants in the estuary bed sediments. The set of mass-balance equations is established through analysis with three “core” models: (1) GLEAMS (catchment sediment erosion/transport model); (2) NIWA STORMQUAL (contaminant generation based on housing, commercial activities and traffic); and (3)

MIKE 3 (estuary hydrodynamics and sediment-transport model). The USC-2 model is driven by a future rainstorm series that is either constructed randomly (e.g., by a Monte Carlo process) or that can be biased to represent worst-case or best-case outcomes.

The USC-2 model has recently been applied to identify the level of development and controls necessary to secure the long-term protection of the Upper Waitemata Harbour (UWH). Build-up of zinc, copper and PAHs in the bed sediments of 11 sub-estuaries of the harbour under a number of scenarios has been predicted over a 50 year time-frame. An existing landcover scenario provides baseline information against which future trends can be compared to various future development scenarios, which include certain levels of stormwater treatment.

In the UWH, the contaminant build-up modeling was applied in iterative way, with discussion of results after each loop, until an acceptable development strategy was found. As part of this iteration in the Upper Waitemata study, it has been found that stormwater treatment alone may not deliver acceptable environmental outcomes in some critical parts of the harbour, which has turned attention to benefits that could be derived by new methods of source control, such as regulating galvanised building materials. By linking “planning cause” to “environmental effect”, the USC-2 model is providing the information needed to develop and defend regional planning policies aimed at protecting estuarine receiving waters in developing catchments.

5.2.2 Exotic forest harvesting

Horokiri sub-catchment

The Horokiri (HRK) core tells us that sedimentation rates near the sub-catchment outlet have been relatively high for at least the last 150 years. The ^{210}Pb SAR of 3.7 mm yr^{-1} is 50% higher than the inlet average ^{210}Pb SAR. This relatively rapid sedimentation on the subtidal flat is consistent with the fact that the 1852 land survey (Lands and Survey D.P. 1505) indicates that the Horokiri stream formerly had a long and narrow tidal creek (Eiby, 1990). The tidal creek has subsequently infilled and a delta built at the stream mouth where it enters the inlet. A similar process has occurred in the Pauatahanui stream, as shown by the presence of estuarine shell layers in sediment deposits several hundred metres upstream of the present-day stream mouth (section 5.3.1). The presence of the delta on the intertidal flat in an aerial photograph taken in 1947 (Fig. 40, Healy, 1980) suggests that these environmental changes resulted from increased soil erosion in the Horokiri sub-catchment as the native forest was removed.

More recently, the pine-pollen profile in core HRK indicates that sedimentation rates (post-1985 $\sim 10 \text{ mm yr}^{-1}$) have more than doubled in the last 20 years. This period coincides with the planting of ~ 800 ha of pine forest, representing $\sim 25\%$ of the sub-catchment area, since the mid-1970's. The onset of increasing pine pollen abundance at 25-cm depth also coincides with an increase in the mud content of these recent deposits. These data suggest that: (1) sediment loads have remained relatively high following sub-catchment deforestation; and (2) activities associated with exotic-forest planting in the last 20 years or so have accelerated soil erosion in the Horokiri sub-catchment.

Pine plantations established in the mid-1970's – early-1980' are nearing maturity. Although there is some uncertainty in the recent sedimentation rates based on pine pollen (because we have no complimentary dating) we are certain that sedimentation has been relatively rapid since original catchment deforestation. Careful planning will be required to minimise the potential for further increases in sediment loads delivered to the inlet when these exotic forest are harvested in the next 5–10 years.

Kakaho sub-catchment

The BAS3 core data indicate that the secondary mud basin near the Kakaho sub-catchment outlet is also a transitional sedimentary environment where fine sediment appears to occur. The BAS3 time-averaged ^{210}Pb SAR of 1 mm yr^{-1} is 40% of the inlet average value (2.4 mm yr^{-1}) and is similar to the background sedimentation rate. The ^{137}Cs SAR for BAS3 (1.8 mm yr^{-1}) is also the lowest measured in the inlet. ^7Be occurs to 2-cm depth and the average mud content of the core is $\sim 30\%$ as opposed to 75–90% for the central mud basin (BAS1–2, BAS4). The wind record (1971–2004) also shows that winds from the southerly quarter occur 22% of the time, which is second only the prevailing northerly winds. Thus, the secondary mud basin has similar characteristics to the DUK site in that fine-sediments deposited here during floods are likely to be resuspended by waves and dispersed widely. The 11.3 km^2 Kakaho sub-catchment (Fig. 1.2) is considerably steeper than the Horokiri (Table 1.1) and some 15% of its landcover is composed of exotic forest planted since the mid-1970's (Page et al. 2004). This forest will reach maturity in the next 5–10 years. Careful planning will also be required here to minimise the potential for further increases in sediment loads delivered to the inlet when these exotic forest is eventually harvested.

5.3 What does the future hold?

GWRC and PCC recognise that the Pauatahanui inlet is sensitive to the effects of human activities in its catchment. An assessment of potential future sedimentation in the inlet is required to provide an objective basis for making resource management decisions relating to the future catchment development. This assessment is based on existing landcover and land management practices. Predictions are based on historical changes in catchment landcover and observed trends in time-averaged sedimentation rates. The close agreement between (1) SAR estimated from independent and complimentary dating techniques; and (2) sediment loads estimated from the cores and other techniques provides confidence in our results. The cores also demonstrate that physical and biological processes rapidly mix (days–months) the upper ≤ 5 -cm of the sediment column. Thus, the shortest time-scales we can resolve in the Pauatahanui cores is of the order of decades rather than years. We assume a management time-scale of 50 years and acknowledge that uncertainty increases with the prediction time-scale.

5.3.1 Inlet evolution – controls and changes

Estuaries follow similar evolutionary paths as they infill with sediment. Subtidal areas and water depths decrease over time. As a result, the hydrodynamic, sedimentological and biological communities change (Roy et al. 2001). The relative influence of the fluvial system increases as the tidal volume shrinks. Sedimentation rates may increase even if catchment sediment loads remain constant because the available depositional areas reduce in size. Thus, the longevity of an inlet depends on its original area and the capacity of the central mud basin, sediment supply rate, trapping efficiency and rate of sea level rise. In the case of the Pauatahanui inlet, the original basin was ≤ 13 -m deep and today is ≤ 3 -m deep.

The fact that the inlet remains largely subtidal today is significant given that the inlet represents only $\sim 4\%$ of the catchment area. North Island estuaries with similar catchment-to-inlet size ratios have infilled to the extent that they are now intertidal (e.g., Wharekawa – Coromandel, Wairoa, Puhoi and Okura – Auckland). Our results indicate that infilling of the Pauatahanui inlet is moderated by the processes of wave resuspension and winnowing of fine sediments. Pickrill (1979) estimated that $\sim 70\%$ of the suspended sediment load delivered during a 15-month period (1976–1977) was flushed from the inlet. Tidal gaugings of flows and suspended sediments also made at the inlet mouth during two storms (June–July 1976) showed that of the 3300 tonnes delivered to the inlet during these floods $\sim 20\%$ was flushed from the inlet (Healy, 1980). Anecdotal evidence, such as the presence of silt laden water in the Mana Marina, at the inlet mouth during the 15–16 February 2004 storm (Marina manager,

pers. comm., April 2004), also suggests that, fine suspended sediments can be discharged from the inlet during floods. However, at least as important as the process of stormwater discharge to the sea, is the resuspension of sediments already deposited in the inlet. It is also likely that the sediment trapping efficiency is lower in today's inlet than in prehistory when it was deeper because of changes in hydrodynamics and, crucially, the increased effectiveness of sediment resuspension by waves.

Evolution of the Pauatahanui inlet has also been affected by sea-level rise associated with climate warming. At Wellington, the rate of sea level rise (SLR) since 1891 has averaged 1.78 mm yr^{-1} , with no change in the rate of SLR detected (Hannah, 2004). At Pauatahanui, tectonic uplift or subsidence of the land would modify the rate of historical sea level rise observed in Wellington harbour. The Ohariu fault crosses the Pauatahanui inlet between its mouth and the Kakaho stream outlet. The highest Holocene beach ridge east and west of the fault shows no significant height difference, which indicates no relative vertical fault movement (In: Gibb, 1986). An average rate of tectonic uplift for the Pauatahanui inlet over the last ~6500 years B.P. of 0.3 metres per thousand years (0.3 mm yr^{-1}) has been estimated by Gibb (1986). However, more recent ages from estuarine shell sampled by Dr Kelvin Berryman (IGNS) from Karehana Bay (Plimmerton), the northern shore of the inlet near Kakaho Stream and from the Pauatahanui Stream about 200 metres south of the Pauatahanui Hall, all suggest that the 0.3 mm yr^{-1} uplift rate reported by Gibb (1986) should be regarded as a maximum value (Table 5.1).

Table 5.1: Average rates of uplift/subsidence in the vicinity of Pauatahanui inlet estimated from ^{14}C ages of estuarine shell in the vicinity of Pauatahanui Inlet (source: Dr Kelvin Berryman, IGNS).

NZ Number	Calibrated ^{14}C Age	Sample	Grid Ref.	Elevation (m MSL)	Elev. Change (mm yr^{-1}) ²
7379	2950 (± 70)	Cockle	R26/661132	0.2–0.4	≤ 0.14
7381	6650 (± 95)	Cockle	R27/711091	-0.15	-0.02
7383	6720 (± 95)	Cockle	R27/711091	0.66	-0.1
7387	5079 (± 90) ¹	Estuarine Shell	R26/690118	0–0.3	≤ 0.06
7393	3258 (± 78) ¹	Estuarine Shell	R26/690118	0.6	0.18
7421	3487 (± 88) ¹	Estuarine Shell	R26/690118	0.6	0.17

Note: (1) Recalculated calibrated ^{14}C age; (2) For ^{14}C ages younger than 6500 years before present (1950 AD) we assume that eustatic sea level has been relatively constant.

These data suggest that: (1) rates of tectonic uplift at Pauatahanui over the last several thousand years are small and (2) have not been influenced by the Ohariu fault. Based on Table 5.1 and the data of Gibb (1986), we assign a historical average rate of sea level rise at Pauatahanui of $1.8 - 0.3 \text{ mm yr}^{-1} = 1.5 \text{ mm yr}^{-1}$.

Large-scale Physical Changes

Sedimentation rates in the inlet have averaged 2.4 mm yr^{-1} (range: $1\text{--}3.7 \text{ mm yr}^{-1}$) over the last 150 years. Thus, the net average SAR corrected for the local rate of sea level rise at Pauatahanui is $2.4 - 1.5 \text{ mm yr}^{-1} = 0.9 \text{ mm yr}^{-1}$ or an increase of 0.135 m over the last 150 years. Changes in the large-scale inlet morphology following catchment deforestation have included an increase in the intertidal flat area (Eiby, 1990). We can estimate the increase in intertidal area over the last 150 years using the net increase in bed elevation adjusted for sea-level rise (0.135 m) and the average slope(s) of the intertidal flats. Average slopes for intertidal-flat areas between Browns Bay and Camborne were estimated from surveyed transects (Pickrill, 1979) and inlet bathymetry (Healy, 1980, Fig. 38). The increase in the horizontal offshore extent or excursion distance of the intertidal flat is given by the product of the intertidal slope and net SAR. The increase in intertidal area is estimated from the product of

excursion distance and shoreline length. Table 5.2 summarises the estimated increases in intertidal area that have occurred in the Pauatahanui inlet during the last 150 years.

Table 5.2: Increase in intertidal area during the last 150 years estimated from net SAR corrected for local rate of sea level rise (0.9 mm yr^{-1}) and average intertidal flat slopes.

Compartment	Ave. Slope	Hz Distance (m)	Intertidal Area (ha)
Browns Bay to Duck Creek	1:50	+7	+1.2 (10%) ¹
Duck Creek to Ration Pt	1:200	+26	+3.5 (30%)
Ration Pt to Camborne	1:280	+45	+7.1 (60%)

(1) Percentage of the estimated total increase in intertidal area during last 150 years.

The estimated increase in intertidal area of about 12 ha during the last 150 years represents a 15% increase. Intertidal flats now account for ~20% of the 4.6 km² area of Pauatahanui inlet. Table 5.2 indicates that 90% of this increase in intertidal area has occurred along the northern and eastern shores of the inlet. This spatial pattern results from the low gradients of these intertidal flats relative to the more steeply-sloping southern shore. The southern shore of the inlet is exposed to the prevailing north-east winds so that waves winnow silt from the intertidal flat leaving the coarser sand fraction behind. Well-sorted sands form steeper-sloping beaches (Komar, 1976) in comparison to poorly sorted intertidal sediments composed of silt and sand. The steep narrow beaches which fringe the southern shore of the inlet are an example of this process (Pickrill, 1979).

Net infilling of the estuary at 0.9 mm yr^{-1} , allowing for sea-level rise, during the last 150 years has also reduced the tidal volume of the estuary by some 600,000 m³. This reduction in tidal volume represents as much as 4% of the average spring–neap tidal volume. These changes in intertidal area and tidal volume are likely to have resulted in changes in inlet hydrodynamics and sediment transport processes. Potential changes include a reduction in tidal-current velocities and an increase in the effectiveness of silt resuspension by waves. Accelerated infilling of the inlet during the last 150 years has also likely resulted in ecological changes. For example, the increase in intertidal area potentially provides more habitat for intertidal fauna, such as cockle. However, the total estimated population of cockle in the inlet has reduced by more than 50% since 1976, although the population appears to have stabilised in the last decade (Grange and Tovey, 2002). Thus, other environmental changes, such as increased water turbidity associated with soil erosion and/or wave resuspension of silt, are also likely to be influential factors controlling estuary ecology in addition to large-scale habitat change.

Finally, the ~40% increase in SAR since 1950 has reduced the effectiveness of sea-level rise as a moderating factor on the infilling process. The fact that SAR have increased in recent decades suggests that the increasing rate of sediment input to the inlet has exceeded its capacity to flush catchment-derived sediment.

5.3.2 Future sedimentation – existing landcover

The ^{210}Pb dating provides the most reliable estimates of sedimentation in the inlet since ~1850. This is because: (1) the SAR values are based on analysis of depth profiles that integrate the effects of sedimentation over many decades; (2) ^{210}Pb inventories, $A(o)$, and supply rates (P) enable the ^{210}Pb chronology to be validated; and (3) in this study ^{210}Pb dating is supported by analytical modelling, which quantifies the effects of sediment mixing on the profiles. Unlike ^{210}Pb , ^{137}Cs and pine pollen have been introduced as pulses only in the last 50–20 years. Uncertainty in the ^{137}Cs and pollen dating relates to sediment mixing and the depth increment between sediment samples. For ^{137}Cs , we have reduced this uncertainty from ± 25 mm to ± 12.5 mm (i.e., ± 4 years of inlet-average SAR) by sampling at intermediate depths to better resolve the maximum ^{137}Cs depth. Because of this uncertainty, we have taken a conservative approach to estimating ^{137}Cs and pollen SAR by subtracting the depth of the surface mixed layer (≤ 14 cm) before calculating time-averaged SAR. Figure 4.1 shows that there is good agreement between ^{210}Pb , ^{137}Cs and pollen SAR for the last ~150 and ~50 years.

The inlet average post-1985 SAR of 4.6 mm yr^{-1} is solely based on the rise of pine pollen abundance and cannot be verified by an independent dating method. Consequently, these results are less certain than the ^{210}Pb and ^{137}Cs dating. Despite this, the good agreement between ^{210}Pb , ^{137}Cs and pollen dating in most cores for the early time periods supports the pollen method itself. The average post-1985 SAR is skewed by the exceptional SAR measured at HRK (10 mm yr^{-1}), which is double that measured elsewhere (range: $1.6\text{--}5.3 \text{ mm yr}^{-1}$) in the inlet. It is unclear how representative the HRK sedimentation rate is of the subtidal flat near the Horokiri outlet. Removing the HRK result reduces the average post-1985 SAR to 4 mm yr^{-1} and this value is adopted for predictions.

Estimates of future inlet sedimentation are matched to each dating technique by limiting the prediction time frame to $\leq 50\%$ of the historical-record span. For example, we use the ^{210}Pb data (last 150 years) to estimate inlet-average sedimentation rates for the next 50 years and pine pollen data (last 20 years) to estimate SAR in the next 10 years. We also make *qualitative* assessments of the likelihood of future inlet average sedimentation rates based on the core data and our expert opinion.

Based on these considerations, we predict *inlet-average* sedimentation rates based on *existing landcover* over the next 50 years:

- SAR ≥ 2.4 mm yr⁻¹ (very high likelihood – certain).
- SAR ≥ 3.4 mm yr⁻¹ (high likelihood).
- SAR ≥ 4.0 mm yr⁻¹ (likely).

Future landcover changes and earthworks associated with urbanisation of the Duck sub-catchment and/or harvesting of exotic forest have the potential to further increase sediment loads to the inlet.

6. Acknowledgements

We thank Tim Porteous (GWRC Biodiversity Co-ordinator), Matt Trlin (PCC – Manager Environmental Policy), Paul Denton (GWRC Policy Advisor – Environment), Geoff Skene (GWRC) and Laura Watts (GWRC – Hydrologist) for assistance in the preparation of this report. We are grateful to Mr John Wells (Chairperson – Guardians of Pauatahanui inlet) for keeping a watchful eye on the DOBIE wave gauges. Drs Noel Trustrum (Institute of Geological and Nuclear Sciences) and Mike Page (Landcare Research Ltd) provided historical DSIR aerial photographs (images held by Landcare Research). Dr Judi Hewitt (NIWA Hamilton) provided advice on inlet infauna behaviour and life-history. We thank Dr Murray Hicks (NIWA Christchurch) for the updated estimates for the total catchment sediment loads. Drs Chris Hollis, Kelvin Berryman, Gaye Downes and Ursula Cochran (Institute of Geological and Nuclear Sciences) advised on the potential effects of the 1855 earthquake as well as the tectonic setting of the Pauatahanui inlet. Andrew Swales thanks Drs Catherine Chagué-Goff and Terry Hume for carefully reviewing the report. We thank the Auckland Regional Council for permission to reproduce the Te Matuku Bay (Waiheke Island) ^{210}Pb profiles and model results in Appendix I. Field work, additional analysis of two core sites and DOBIE wave-gauge deployment was funded by NIWA-NSOF (Non Specific Output Funding) Project NNTF042.

7. References

- Abraham, G. & Parker, R. (2002). Heavy-metal contaminants in Tamaki estuary: impacts of city development and growth, Auckland, New Zealand. *Environmental Geology* 42: 883–890.
- Adkin, G.L. (1921). Porirua Harbour: a study of its shoreline and physiographic features. *Transactions of the New Zealand Institute* 53: 144–156.
- Alexander, C.R.; Smith, R.G.; Calder, F.D.; Schropp, S.J.; Windom, H.L. (1993). The historical record of metal enrichment in two Florida estuaries. *Estuaries* 16(3B): 627–637.
- Aller, R.C. (1982). The effects of macrobenthos on chemical properties of marine sediment and overlying water, p 53–101. In: McCall, P.L.; Tevesz, M.J.S. (1982). Animal–sediment relations: the biogenic alteration of sediments, Volume 2: Topics in Geobiology. Plenum Press, New York, 336 p.
- ANZECC (2000). Australian and New Zealand guidelines for fresh and marine water quality. National Water Quality Management Strategy, Australian and New Zealand Environment and Conservation Council. Agriculture and Resource Management Councils of Australia and New Zealand. Canberra, Australia.
- Auckland Regional Council (1995). The environmental effects of stormwater runoff. ARC Environment and Planning Division Technical Publication No 53. Auckland Regional Council, Auckland, New Zealand.
- Benoit, G.; Rozan, T.F.; Patton, P.C.; Arnold, C.L. (1999). Trace metals and radionuclides reveal sediment sources and accumulation rates in Jordan Cove, Connecticut. *Estuaries* 22(1): 65–80.
- Blais, J.M.; Kalff, J.; Cornett, R.J.; Evans, R.D. (1995). Evaluation of ^{210}Pb dating in lake sediments using stable Pb, Ambrosia pollen and ^{137}Cs . *Journal of Paleolimnology* 13: 169–178. Goldberg, E.D. (1963). Geochronology with ^{210}Pb . In: *Radioactive Dating*, 121–131. International Atomic Energy Agency, Vienna.
- Bromley, R.G. (1996). Trace fossils: biology, taphonomy and applications, second edition. Chapman and Hall, London, 361 p.

- Bunt, J.A.C.; Larcombe, C.P.; Jago, C.F. (1999). Quantifying the response of optical backscatter devices and transmissometers to variations in suspended particle matter. *Continental Shelf Research* 13: 181–191.
- Chagué-Goff, C.; Nichol, S.L.; Jenkinson, A.V.; Heijnis, H. (2000). Signatures of natural catastrophic events and anthropogenic impact in an estuarine environment, New Zealand. *Marine Geology* 167: 285–301.
- Curry, R.J. (1981). Hydrology of the catchments draining to the Pauatahanui inlet. Water and Soil Technical Publication No. 23. National Water and Soil Conservation Organisation, Wellington, 27 p.
- Dyer, K.R. (1986). Coastal and Estuarine Sediment Dynamics. John Wiley and Sons, Chichester, 342 p.
- Eiby, G. (1990). Changes to Porirua harbour in about 1855: historical tradition and geological evidence. *Journal of the Royal Society of New Zealand* 20(2): 233–248.
- Fahey, B.D.; Coker, R.J. (1992). Sediment production from forest roads in Queen Charlotte Forest and potential impact on marine water quality, Marlborough Sounds, New Zealand. *New Zealand Journal of Marine and Freshwater Research* 26: 187–195.
- Gibb, J.G. (1986). A New Zealand regional Holocene eustatic sea-level curve and its application to determination of vertical tectonic movements. A contribution to IGCP-Project 200. *Royal Society of New Zealand Bulletin* 24: 377–395.
- Glasby, G.P.; Moss, R.L.; Stoffers, P. (1990). Heavy-metal pollution in Porirua Harbour, New Zealand. *New Zealand Journal of Marine and Freshwater Research* 24: 233–237.
- Goff, J. (1997). A chronology of natural and anthropogenic influences on coastal sedimentation, New Zealand. *Marine Geology* 138: 105–117.
- Goldberg, E.D. (1963). Geochronology with ²¹⁰Pb. In: *Radioactive Dating*, 121–131. International Atomic Energy Agency, Vienna.
- Goldberg, E.D. & Kiode M. (1962). Geochronological studies of deep sea sediments by the ionium/thorium method. *Geochimica et Cosmochimica Acta* 26: 417–450.

- Graham Spargo Partnerships Limited (2005). Review of population projections for Porirua City. Graham Spargo Partnerships Limited, Wellington, 21 p.
- Grange K. & Tovey, A. (2002). Cockle in Pauatahanui inlet: results of the 2001 sampling programme. NIWA Client Report NEL02401/2.
- Grapes, R.; Downes, G. (1997). The 1855 Wairarapa, New Zealand, earthquake – analysis of historical data. *Bulletin of the New Zealand National Society for Earthquake Engineering* 30(4): 271–373.
- Green, M.O.; Timperly, M.H.; Collins, R.W.; Senior, A.K.; Swales, A.; Williamson, R.B.; Mills, G. (2004). Prediction of contaminant accumulation in the Upper Waitemata Harbour – Methods. NIWA Client Report HAM2003-087/1, 97 p.
- Guinasso, N.L. Jr. & Schink, D.R. (1975). Quantitative estimates of biological mixing rates in abyssal sediments. *Journal of Geophysical Research* 80: 3032–3043.
- Hannah, J. (2004). An updated analysis of long-term sea level change in New Zealand. *Geophysical Research Letters* 31(L03307), 4 p.
- Healy, W.B. (1980). Pauatahanui inlet – an environmental study. New Zealand Department of Scientific and Industrial Research, DSIR Information Series No. 141, Wellington, 198 p.
- Heath, R.A. (1977). Heat Balance in a small coastal inlet, Pauatahanui inlet, North Island, New Zealand. *Estuarine Coastal Marine Science* 5: 783–792. Hewitt, J.E.; Hatton, S.; Safi, K.; Craggs, R. (2001). Effects of suspended sediment levels on suspension-feeding shellfish in the Whitford embayment. NIWA Client Report ARC01267.
- Hicks, D.M. (1999). Written advice (6 January 1999) to Mr R. Forlong, Wellington Regional Council. Moonshine Stream: advice on sedimentation impacts of a proposed bank reinstatement on Moonshine Stream, Pauatahanui Catchment.
- Hicks, D.M.; Shankar, U. (2003). Sediment from New Zealand Rivers. NIWA Miscellaneous Chart 236, Wellington.

- Hicks, D.M.; Quinn, J.; Trustrum, N. (2004). Stream sediment load and organic matter, p 12.1–12.16. In: Harding, J.; Mosley, P.; Pearson, C.; Sorrell, B. (2004). *Freshwaters of New Zealand*, NZ Hydrological Society and NZ Limnological Society. The Caxton Press, Christchurch.
- Hume, T.M. & McGlone, M.S. (1986). Sedimentation patterns and catchment use changes recorded in the sediments of a shallow tidal creek, Lucas Creek, Upper Waitemata Harbour, New Zealand. *New Zealand Journal of Marine and Freshwater Research* 20: 677–687.
- Hume, T.M.; Fox, M.E.; Wilcock, R.J. (1989). Use of organochlorine contaminants to measure sedimentation rates in estuaries: a case study from the Manukau Harbour. *Journal of the Royal Society of New Zealand* 19: 305–317.
- Hume, T.M.; Dahm, J. (1992). An investigation of the effects of Polynesian and European land use on sedimentation in Coromandel estuaries. DSIR Marine and Freshwater Consultancy Report No. 6104. Department of Scientific and Industrial Research, Water Quality Centre, Hamilton, 56 p + appendices.
- Hume, T.; Bryan, K.; Berkenbusch, K.; Swales, A. (2002). Evidence for the effects of catchment sediment runoff preserved in estuarine sediments. NIWA Client Report ARC01272, 57 p.
- Irwin, J. (1976). Morphological stability of Pauatahanui Inlet, Porirua Harbour. *New Zealand Journal of Marine and Freshwater Research* 10(4): 641–650.
- Kennedy, P. (1980). Pauatahanui inlet – a closer look. *Soil and Water* 16(5): 7–10.
- Komar, P.D. (1976). Beach processes and sedimentation. Prentice-Hall Inc., Englewood Cliffs, New Jersey, 429 p.
- Lohrer, A.M.; Thrush, S.F.; Hewitt, J.E.; Berkenbusch, K.; Ahrens, M.; Cummings, V.J. (2004). Terrestrially derived sediment: response of marine macrobenthic communities to thin terrigenous deposits. *Marine Ecology Progress Series* 273: 121–138.
- Matthews, K.M. (1989). Radioactive fallout in the south pacific: a history. Part 1: Deposition in New Zealand. Report NRL1989/2, National Radiation Laboratory, Christchurch New Zealand.

- Maurer, D.; Keck, R.T.; Tinsman, J.C.; Leathem, W.A.; Wethe, C.; Lord, C.; Church, T.M. (1986). Vertical migration and mortality of marine benthos in dredged material: a synthesis. *International Revue Gesheimschaft Hydrobiologie* 71: 49–630.
- McDowell, D.M. & B.A. O'Connor. (1977). Hydraulic behaviour of estuaries. The Macmillan Press Ltd, London, 292 p.
- McKnight, D.G. (1969). A recent, possible catastrophic burial in a marine molluscan community. *N.Z. Journal of Marine and Freshwater Research* 3: 17–179.
- Mildenhall, D.C. (1979). Holocene pollen diagrams from Pauatahanui inlet, Porirua, New Zealand. *New Zealand Journal of Geology and Geophysics* 5: 585–591.
- Moore, P.G. (1977). Inorganic particulate suspensions in the sea and their effects on marine animals. *Oceanography and marine Biology: An Annual Review* 15: 225–363.
- Moore, P.D. & J.A. Webb. (1978). An illustrated guide to pollen analysis. Hodder and Stroughton.
- Morrisey, D.J.; Roper, D.S.; Williamson, R.B. (1997). Biological effects of the build-up of contaminants in sediments in urban estuaries. In: L.A. Roesner (ed.), *Effects of Watershed Development and Management on Aquatic Ecosystems, Proceedings of an Engineering Foundation Conference*. American Society of Civil Engineers, New York.
- Morrisey, D.J.; Williamson, R.B.; Van Dam, L.; Lee, D.J. (2000). Stormwater contamination of urban estuaries. 2. Testing a predictive model of the build-up of heavy metals in sediments. *Estuaries* 23(1): 67–79.
- Morton, J.; Miller, M. (1973). The New Zealand Sea Shore, Second Edition. William Collins and Sons, Glasgow, 653 p.
- Nielsen, P. (1992). Coastal bottom boundary layers and sediment transport. Advanced Series on Ocean Engineering – Volume 4, World Scientific, Singapore, 324 p.

- Norkko, A.; Talman, S.; Ellis, J.; Nicholls, P.; Thrush, S. (2001). Macrofaunal sensitivity to fine sediments in the Whitford embayment. NIWA Client Report ARC01266/2.
- Norkko, A.; Thrush, S.F.; Hewitt, J.E.; Cummings, V.J.; Norkko, J.; Ellis, J.I.; Funnell, G.A.; Schultz, D.; MacDonald, I. (2002). Smothering of estuarine sandflats by terrigenous clay: the role of wind-wave disturbance and bioturbation in site-dependent macrofaunal recovery. *Marine Ecology Progress Series 234*: 23–41.
- Oldfield, F.; Appleby, P.G. (1984). Empirical testing of ^{210}Pb -dating models for lake sediments. In: Lake sediments and environmental history, Haworth and Lund (eds): 93–124.
- Olsen, C.R.; Simpson, H.J.; Peng, T.-H.; Bopp, R.F.; Trier, R.M. (1981). Sediment mixing and accumulation rate effects on radionuclide depth profiles in Hudson Estuary sediments. *Journal of Geophysical Research 86 (C11)*: 11020–11028.
- Page, M.; Heron, D.; Trustrum, N. (2004). Pauatahanui Inlet – Analysis of historical catchment land use and land use change. Institute of Geological and Nuclear Sciences Client Report 2004/169, 20 p.
- Pickrill, R.A. (1979). A micro-morphological study of intertidal estuarine surfaces in Pauatahanui Inlet, Porirua Harbour. *New Zealand Journal of Marine and Freshwater Research 13(1)*: 59–69.
- Richards, K. (1982). Rivers: form and process in alluvial channels. Methuen, London, 361 p.
- Richardson, J.R.; Aldridge, A.E.; Main, W. de L. (1979). Distribution of the New Zealand cockle, *Chione stutchburyi*, at Pauatahanui inlet. New Zealand Oceanographic Institute Oceanographic Field Report No. 14, Wellington, 11 p.
- Ritchie, J.C. & McHenry, J.R. (1989). Application of radioactive fallout cesium-137 for measuring soil erosion and sediment accumulation rates and patterns: A review with bibliography. Hydrology Laboratory, Agriculture Research Service, U.S. Department of Agriculture, Maryland.

- Roberts, E. (1855). Memorandum on the earthquake in the islands of New Zealand, January 23, 1855. In: Taylor, R. (1855) *Te Ika a Maui or New Zealand and its Inhabitants*. Wertheim and MacIntosh, London.
- Robbins, J.A. & Edgington, D.N. (1975). Determination of recent sedimentation rates in Lake Michigan using ^{210}Pb and ^{137}Cs . *Geochimica et Cosmochimica Acta* 39: 285–304.
- Robbins, J.A. (1978). Geochemical and geophysical applications of radioactive lead. In *Biogeochemistry of Lead in the Environment*, Nriagu, J.O. (ed.): 285–393.
- Roy, P.S.; Williams, R.J.; Jones, A.R.; Yassini, I.; Gibbs, P.J.; Coates, B.; West, R.J.; Scanes, P.R.; Hudson, J.P.; Nichol, S. (2001). Structure and function of south-east Australian estuaries. *Estuarine, Coastal and Shelf Science* 53: 351–384.
- Sharma, K.; Gardner, L.R.; Moore, W.S.; Bollinger, M.S. (1987). Sedimentation and bioturbation in a salt marsh as revealed by ^{210}Pb , ^{137}Cs and ^7Be studies. *Limnology and Oceanography* 32(2): 313–326.
- Stroud, M.J.; Cooper, A.B. (1997). Modelling sediment loads to the Mahurangi. NIWA Client Report ARC60211.
- Swales, A.; Hume, T.M.; Oldman, J.W.; Green, M.O. (1997). Sedimentation history and recent human impacts. NIWA Client Report ARC60201, 90 p.
- Swales, A.; Williamson, R.B.; Van Dam, L.; Stroud, M.J.; McGlone, M.S. (2002a). Reconstruction of urban stormwater contamination of an estuary using catchment history and sediment profile dating. *Estuaries* 25(1): 43–56.
- Swales, A.; Hume, T.M.; McGlone, M.S.; Pilvio, R.; Oviden, R.; Zviguina, N.; Hatton, S.; Budd, R.; Hewitt, J. E.; Pickmere, S.; Costley, K. (2002b). Evidence for the physical effects of catchment sediment runoff preserved in estuarine sediments: Phase II (field study). Auckland Regional Council Technical Publication 221, 177 p.
- Watts, L.; Gordon, M. (2004). The 15–16 February 2004 storm in the Wellington region: hydrology and meteorology. Greater Wellington Resource Investigations Department Technical Report, Greater Wellington Regional Council, 28 p.

- Thrush, S.F.; Hewitt, J.E.; Cummings, V.J.; Ellis, J.I.; Hatton, C.; Lohrer, A.; Norkko, A. (2004). An over looked pollutant muddies the waters: elevating sediment input to coastal and estuarine habitats. *Frontiers in Ecology and Environment* 2: 299–306.
- Tinker, R.A.; Pilvio, R. (2000). Environmental radioactivity in New Zealand and Rarotonga – annual report. National Radiation Laboratory Report NRL-F/80, 24 p.
- Valette-Silver, N.J. (1993). The use of sediment cores to reconstruct historical trends in contamination of estuarine and coastal sediments. *Estuaries* 16(3B): 577-588.
- Vant, W.N.; Williamson, R.B.; Hume, T.M.; Dolphin, T.J. (1993). Effects of future urbanisation in the catchment of Upper Waitemata Harbour. NIWA Consultancy Report No. ARC220.
- Whitehead, N.E.; Ditchburn, R.G.; McCabe, W.J.; Mason, W.J. (1998). Application of natural and artificial fallout radionuclides to determining sedimentation rates in New Zealand lakes. *New Zealand Journal of Marine and Freshwater Research* 32: 489–503.
- Whitehouse, R.J.S.; Soulsby, R.L.; Roberts, W.; Mitchener, H.J. (1999). Dynamics of Estuarine Muds: a manual for practical applications. HR Wallingford Report SR527. Wallingford, 81 p.
- Williamson, R.B.; Morrissey, D.J. (2000). Stormwater contamination of urban estuaries. 1. Predicting the build-up of heavy metals in sediments. *Estuaries* 23(1): 56–66.
- Williamson, R.B.; Olsen, G.; Green, M. (2004). Greater Wellington Regional Council long-term baseline monitoring of marine sediments in Porirua Harbour. NIWA Client Report HAM2004-128, 61 p.
- Wilmshurst, J.; Eden, D.N.; Frogatt, P.C. (1999). Late Holocene forest disturbance in Gisborne, New Zealand. *New Zealand Journal of Botany* 37: 523–540.
- Wise, S. (1977). The use of radionuclides ^{210}Pb and ^{137}Cs in estimating denudation rates and in soil erosion measurement. Occasional Paper No. 7 University of London, King's College, Department of Geography, London.

8. Appendix I: ^{210}Pb dating models

Oldfield and Appleby (1984) provide guidelines to select the most appropriate ^{210}Pb dating model. Both the CIC and CRS dating models may be applicable, depending on the depositional environment. For example, at sites close to catchment sediment sources the primary unsupported ^{210}Pb source is likely to be due to catchment soil inputs. Also, small estuaries and tidal creeks are largely intertidal and therefore the residence time of the estuarine water body is short (i.e., one tidal cycle) in comparison to most lakes (10–100's yr). Direct atmospheric ^{210}Pb deposition is likely to be important in sub-tidal basins and/or in sheltered coastal waters because of their large surface areas, distance from catchment sediment sources and relatively long residence times compared to intertidal flats. In these environments the CRS model would likely be more applicable.

Constant Initial Concentration (CIC) Model

The main assumption of the constant initial concentration (CIC) model is that sediments have a constant initial unsupported ^{210}Pb concentration (at the sediment-water interface), despite temporal variations in the net dry-mass sedimentation rate (Robbins, 1978). Since sediments have the same initial unsupported ^{210}Pb concentration (C_0), the value of C (Bq kg^{-2} , $\text{Bq} = \text{Becquerel} = \text{one disintegration per second}$) will decline exponentially with age (t):

$$C_t = C_0 e^{-kt} \quad \text{Eq. A1}$$

where k is the radioactive decay constant for ^{210}Pb (0.03114 yr^{-1}), C_0 is the unsupported ^{210}Pb concentration (Bq kg^{-2}) at time zero, which in the absence of surface mixing will coincide with the sediment-water interface. The CIC model is feasible when the main source of unsupported ^{210}Pb is from eroded catchment soils. Furthermore, in environments where the water residence time is low, changes in the sediment flux would affect ^{210}Pb retention in sediments (Blais et al. 1995).

Using the CIC model, the age of sediments at depth x is given by:

$$t = \frac{1}{k} \ln \frac{C_0}{C} \quad \text{Eq. A2}$$

Constant Rate of Supply (CRS) Model

The CRS model assumes that there is a constant rate of supply of unsupported ^{210}Pb from the atmosphere to the lake or estuary waters and hence a constant rate of ^{210}Pb supply to the sediments despite variations in the dry-mass sedimentation rate (Goldberg, 1963). Furthermore, the assumptions of the CRS model are satisfied where the total cumulative unsupported ^{210}Pb in sediment cores collected at different sites, in the same sedimentary environment (e.g., a sub-tidal flat), are similar. In lake systems, the CRS model has generally been favoured over the CIC model because the main source of unsupported ^{210}Pb is believed to be direct atmospheric deposition and the water residence time is long compared to the particle settling time (e.g., Blais et al. 1995).

Using the CRS model, the age of sediments at depth x is given by:

$$t = \frac{1}{k} \ln \frac{A(o)}{A} \quad \text{Eq. A3}$$

where $A(o)$ is the total unsupported ^{210}Pb in the sediment column (Bq cm^{-2}) and A is the cumulative unsupported ^{210}Pb below sediments of depth x . The parameters A and $A(o)$ are estimated by integration of the unsupported ^{210}Pb profile and expressed as Bq cm^{-2} to correct for depth variations in sediment dry bulk density.

A more reliable sedimentation history can be established by constraining the CRS depth-age curve to pass through a sediment layer of age t_0 that has been independently dated. Furthermore, because the unsupported ^{210}Pb concentration decays exponentially with depth, an objective method is required to determine the depth of sediment over which to integrate the unsupported ^{210}Pb profile and thereby estimate $A(o)$ and A . The maximum depth of ^{137}Cs ($^{137}\text{Cs}_{\text{max}}$) in a sediment core can be used to constrain the CRS model by calculating the residual unsupported ^{210}Pb in the sediment column below this sediment layer (A_{res}):

$$A_{\text{res}} = \frac{\Delta A}{e^{kt_0} - 1} \quad \text{Eq. A4}$$

where ΔA is the integrated unsupported ^{210}Pb in the sediment column above the dated sediment layer, e is 2.7182818..., k is the decay constant for ^{210}Pb and t_0 is the age of the $^{137}\text{Cs}_{\text{max}}$ sediment layer (i.e., 50 years). The total unsupported ^{210}Pb in the sediment column, $A(o)$ used in Eq. 3 is then given by:

$$A(o) = \Delta A + A_{res} \quad \text{Eq. A5}$$

Time-series of historical changes in annual sedimentation rates can be reconstructed for cores using the constrained CRS ^{210}Pb dating model where evidence of surface mixing is absent, with good linear-regression models fits to the natural-log transform ^{210}Pb profiles, good agreement with pollen and ^{137}Cs dating and sediment mixing is shallow or absent. In these cases, dry-mass annual sedimentation rates (S_{mass}):

$$S_{\text{mass}} = \frac{kA}{C} \quad \text{Eq. A6}$$

where S_{mass} is measured as the dry mass accumulation rate per unit area per year ($\text{g cm}^{-2} \text{yr}^{-1}$), which can be converted to an annual SAR (mm yr^{-1}) using the dry bulk sediment density ($\rho_d = \text{g cm}^{-3}$):

$$\text{SAR} = \left(\frac{S}{\rho_d} \right) 10 \quad \text{Eq. A7}$$

Figure A1 shows an example of the constrained ^{210}Pb CRS modelling applied to a sediment core collected from Te Matuku Bay (TM-I3), Auckland. This technique is not appropriate for the Pauatahanui cores because of relatively deep and rapid mixing of the sediment column by physical and biological mixing processes.

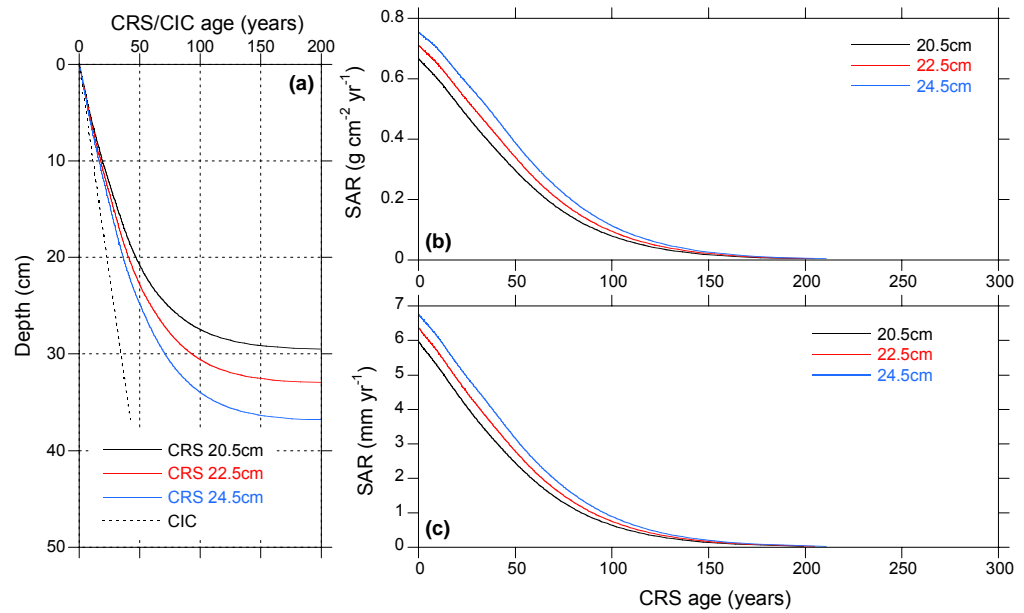


Figure A1: Core TM-I3 sedimentation chronology: (a) depth-age curves for CRS and CIC ²¹⁰Pb models; (b) age-mass (g cm⁻² yr⁻¹) sediment accumulation; and (c) age-SAR (mm yr⁻¹) ~annual time-series based on a constrained CRS model. The coloured curves represent the uncertainty associated with the maximum depth of ¹³⁷Cs due to the sampling increment.

9. Appendix II: Solution to general equations for sedimentation and mixing

Solutions to general equations for Aller (1982) one-dimensional analytical model for steady-state sedimentation, sediment mixing and radioactive decay:

$$A_1(z) = \beta_1 \exp(\alpha_1 z) + \beta_2 \exp(\alpha_2 z) \quad (\text{above } L) \quad \text{Eq. A6}$$

$$A_2(z) = \beta_3 \exp(-kz/\omega) \quad (\text{below } L) \quad \text{Eq. A7}$$

$$\beta_1 = \frac{P\alpha_2 \exp(\alpha_2 L)}{\alpha_1(D\alpha_2 - \omega) \exp(\alpha_1 L) - \alpha_2(D\alpha_1 - \omega) \exp(\alpha_2 L)} \quad \text{Eq. A8}$$

$$\beta_2 = \frac{-P\alpha_1 \exp(\alpha_1 L)}{\alpha_1(D\alpha_2 - \omega) \exp(\alpha_1 L) - \alpha_2(D\alpha_1 - \omega) \exp(\alpha_1 L)} \quad \text{Eq. A9}$$

$$\beta_3 = \beta_1 \exp(\alpha_1 L) + \beta_2 \exp(\alpha_2 L) \exp\left(\frac{kL}{\omega}\right) \quad \text{Eq. A10}$$

$$\alpha_1 = \frac{\omega + \sqrt{\omega^2 + 4Dk}}{2D} \quad \text{Eq. A11}$$

$$\alpha_2 = \frac{\omega - \sqrt{\omega^2 + 4Dk}}{2D} \quad \text{Eq. A12}$$

where A is unsupported ^{210}Pb concentration per unit volume of sediment (Bq cm^{-3}), z is depth in the seabed (cm), D is the bio-diffusion coefficient ($\text{cm}^2 \text{ yr}^{-1}$), k is the radioactive decay constant for ^{210}Pb (0.03114 yr^{-1}), ω is the sediment accumulation rate (cm yr^{-1}) and P is the excess ^{210}Pb flux to the sediment water interface ($\text{Bq cm}^2 \text{ yr}^{-1}$).

10. Appendix III: Radiocarbon dating

Secular variations in the production of atmospheric ^{14}C , which relate to solar and geomagnetic influences and the apparent differences (offset) in atmosphere-ocean carbon reservoirs and activity requires ^{14}C dated samples to be calibrated for these effects. Calibration converts a radiocarbon age to a solar (calendar) date. In dating estuarine and marine samples the lag between atmospheric ^{14}C entering the oceans (the global marine offset or reservoir effect) and the mixing of deep 'old' seawater with 'young' surface waters must be taken into account. In the New Zealand coastal marine environment, a reservoir correction of -336 years is required. Consequently, a shellfish that died today would have a radiocarbon age of ~300 years.

The absence of an absolute dating method for the ocean (e.g., c.f. dendrochronology from tree rings on land) requires the modelling of atmospheric-ocean carbon exchange, based on actual variations in the former. Because of the uncertainties inherent in this approach a local correction factor, which in New Zealand is +30 years, is included in the reservoir correction. This is the difference between the radiocarbon age for the modelled surface layers of the world ocean (1950 A.D.) and that derived locally by an independent source, and is applied prior to calibration. The historical fluctuations in atmospheric carbon demonstrated by dendrochronological studies produces characteristic 'wiggles' in the radiocarbon-calendar age curves. Consequently for any given radiocarbon date there may be several calibrated ages (multiple curve intercepts), any of which could be the true date. Given this and other errors inherent in the analysis the 'wobble effect' can result in substantial total errors and a wide calibrated age range. Consequently, radiocarbon ages less than ~500 years have calibrated (calendar) age ranges (95% confidence intervals) with upper values reported as modern (i.e., present day). Also, burning of fossil fuels has altered the atmospheric $^{14}\text{C}/^{12}\text{C}$ ratio, so that it is problematic to use radioactive carbon to date samples less than ~500 years old. Nonetheless, ^{14}C dating provides a useful tool to estimate long-term average SAR for estuaries based on dating of suitable samples buried at depth in the sediment column.

11. Appendix IV: Sediment core locations

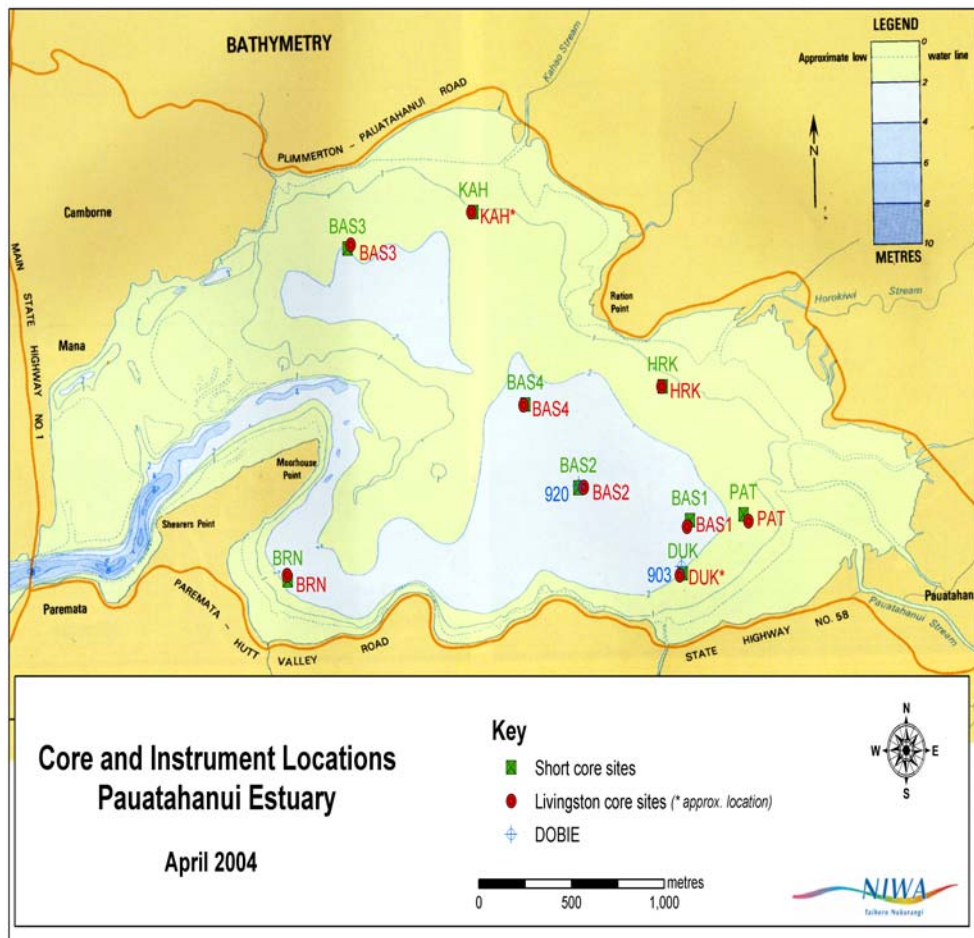


Figure A2: Locations of short and long (Livingston) core sites in the Pauatahanui inlet. Also shown are the locations of the DOBIE wave gauges deployed at BAS2 and DUK for 7 weeks from 29th April 2004.

Table A1: Pauatahanui inlet short-core site locations.

Core Site	Latitude	Longitude	Water depth (m)
BAS1	41° 6.097'S	174° 54.118'E	2
BAS2	41° 6.031'S	174° 53.792'E	2.5
BAS3	41° 5.539'S	174° 53.119'E	1.9
BAS4	41° 5.860'S	174° 53.638'E	2.5
BRN	41° 6.221'S	174° 52.945'E	2
DUK	41° 6.206'S	174° 54.097'E	1.8
PAT	41° 6.085'S	174° 54.274'E	1.8
HRK	41° 5.823'S	174° 54.038'E	1.5
KAH	41° 5.464'S	174° 53.486'E	1.5

12. Appendix V: Livingston piston core summary

Table A2: Pauatahanui inlet Livingston piston core site locations and core length details.

Core Site	Latitude	Longitude	Water Depth (m.)	Core Driven (m)	Core Retained (m)	
					A	B
BAS1	41° 6.110'S	174° 54.109'E	1.9	2.5	1.74	2.04
BAS2	41° 6.030'S	174° 53.808'E	1.9	2.5	2.03-	
BAS3	41° 5.531'S	174° 53.128'E	1.5	2.5	1.83	1.87
BAS4	41° 5.861'S	174° 53.632'E	1.8	2.5	2.15	
BRN	41° 6.210'S	174° 52.943'E		2.5	1.79	2.02
DUK	41° 6.105'S	174° 54.062'E	1.9	2.5	2.39-	
PAT	41° 6.099'S	174° 54.288'E	1.5	2.5	2.04	2.04
HRK	41° 5.823'S	174° 54.034'E	1.2	2.5	1.95	1.6
KAH	41° 5.830'S	174° 53.660'E	2.38	2.2-		0.8

13. Appendix VI: Long-core particle diameter and mud content profiles

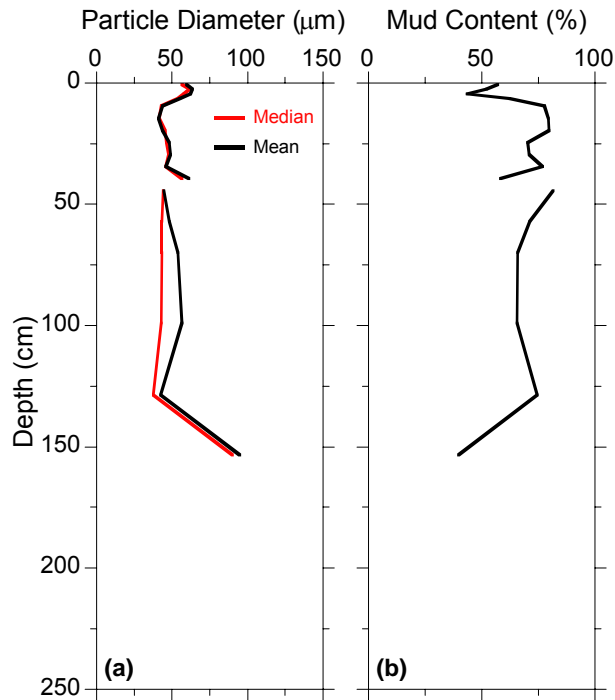


Figure A3: Browns Bay combined short- and long-core sediment profiles of: (a) median and mean particle diameter (μm): and (b) mud content (%). Long core depths are compression compensated (assuming linear compression). BRN long-core compression = 19%.

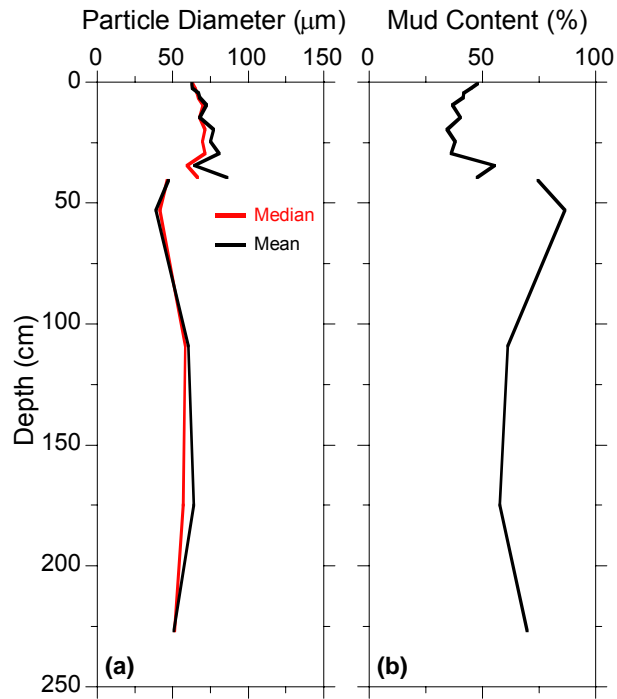


Figure A4: Duck Creek combined short- and long-core sediment profiles of: (a) median and mean particle diameter (μm): and (b) mud content (%). Long core depths are compression compensated (assuming linear compression). DUK long-core compression = 4%.

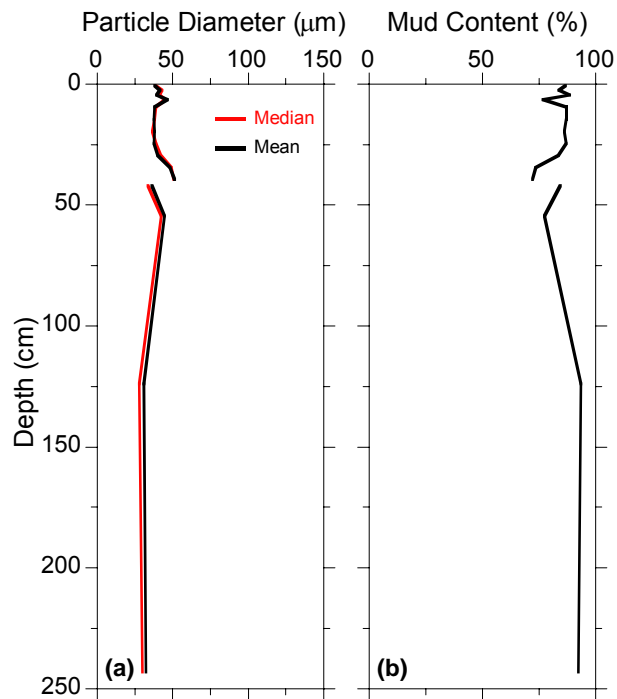


Figure A5: Basin Site 2 combined short- and long-core sediment profiles of: (a) median and mean particle diameter (μm): and (b) mud content (%). Long core depths are compression compensated (assuming linear compression). BAS2 long-core compression = 11%.

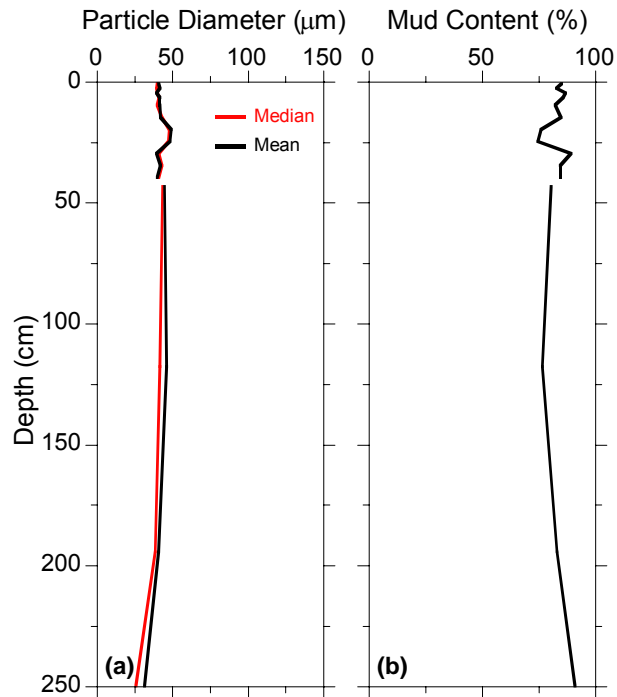


Figure A6: Basin Site 4 combined short- and long-core sediment profiles of: (a) median and mean particle diameter (μm): and (b) mud content (%). Long core depths are compression compensated (assuming linear compression). BAS4 long-core compression = 14%.

14. Appendix VII: Pauatahanui inlet short-core x-radiographs.

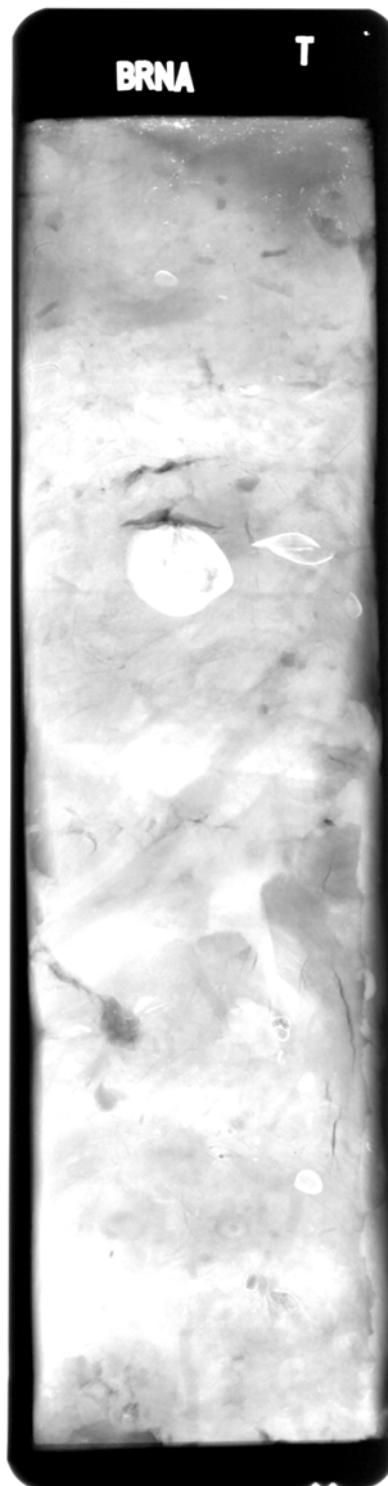


Figure A7: Browns Bay (BRN) short-core x-radiograph of 2-cm thick slab. Exposure: 50 kV, 25 mA, 2 minutes. Scale: core width is 10 cm, length is 40 cm.

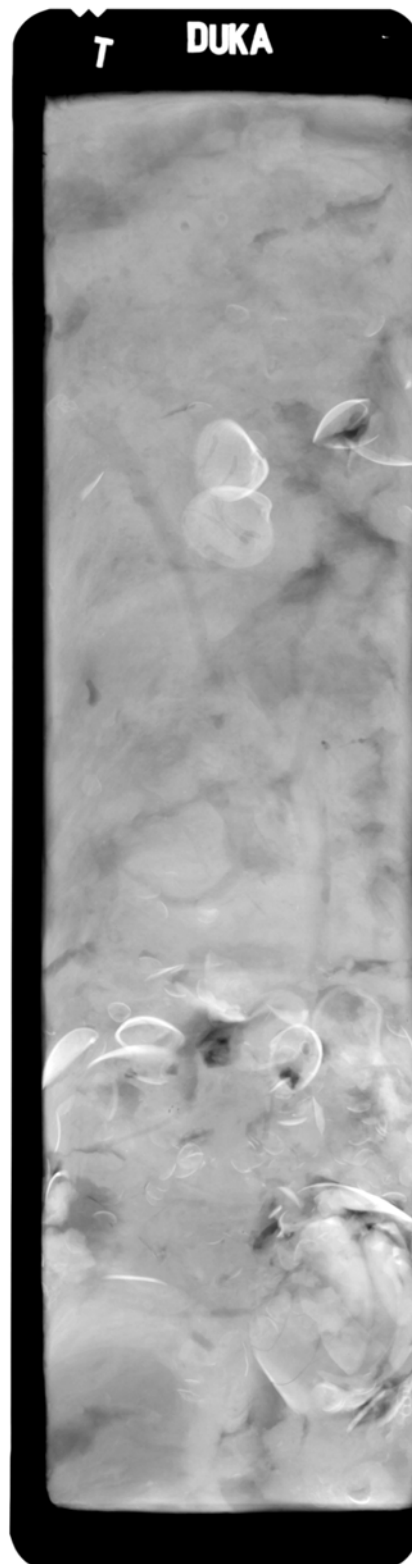


Figure A8: Duck Creek (DUK) short-core x-radiograph of 2-cm thick slab. Exposure: 50 kV, 25 mA, 2 minutes. Scale: core width is 10 cm, length is 40 cm.

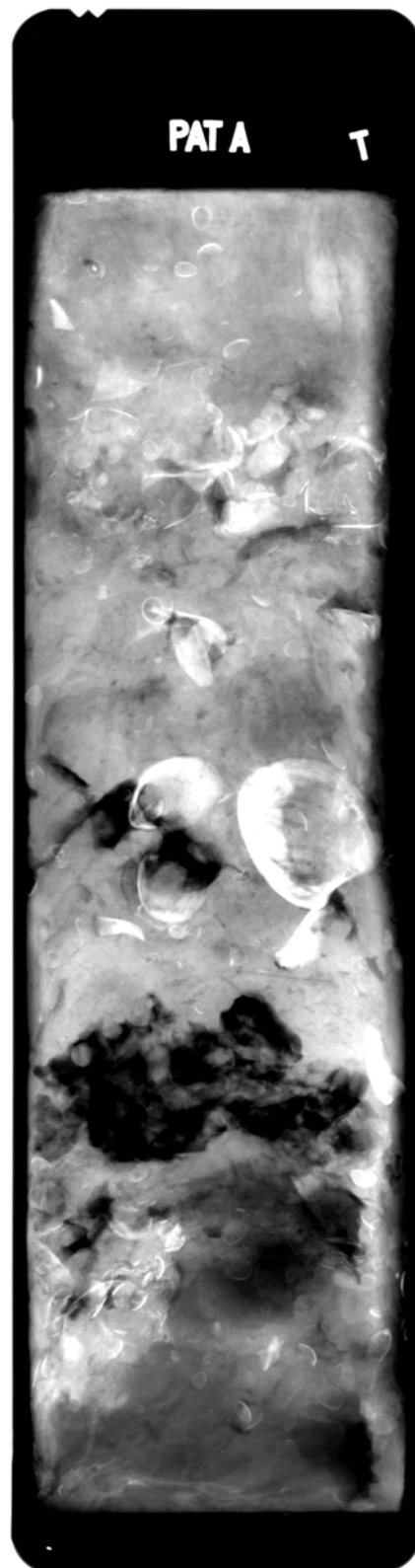


Figure A9: Pauatahanui Stream (PAT) short-core x-radiograph of 2-cm thick slab. Exposure: 50 kV, 25 mA, 2 minutes. Scale: core width is 10 cm, length is 40 cm.

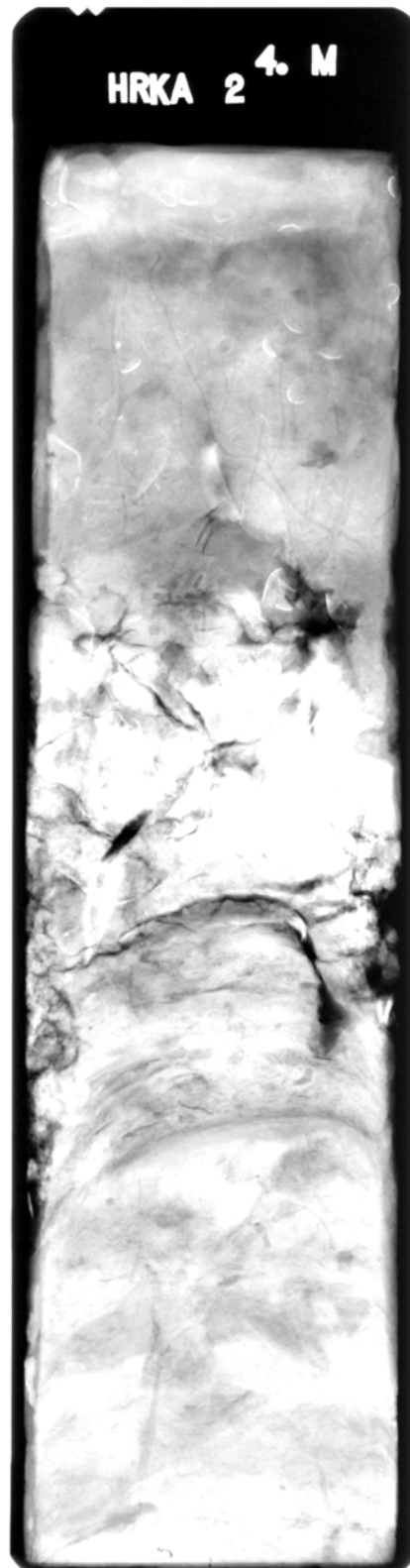


Figure A10: Horokiri (HRK) short-core x-radiograph of 2-cm thick slab. Exposure: 50 kV, 25 mA, 4 minutes. Scale: core width is 10 cm, length is 40 cm.

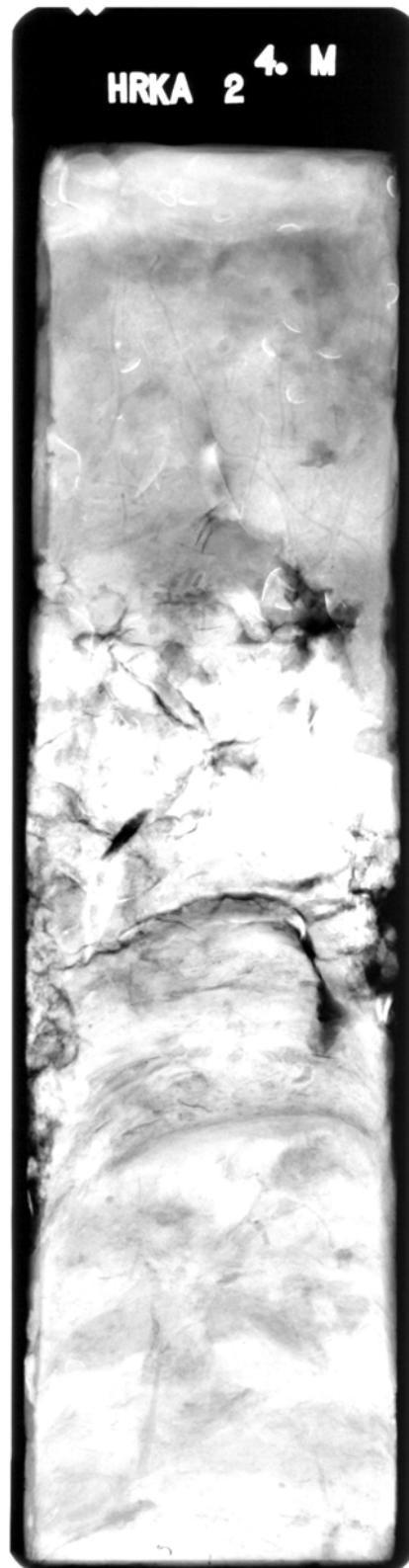


Figure A11: Horokiri (HRK) short-core x-radiograph of 2-cm thick slab. Exposure: 50 kV, 25 mA, 4 minutes. Scale: core width is 10 cm, length is 40 cm.

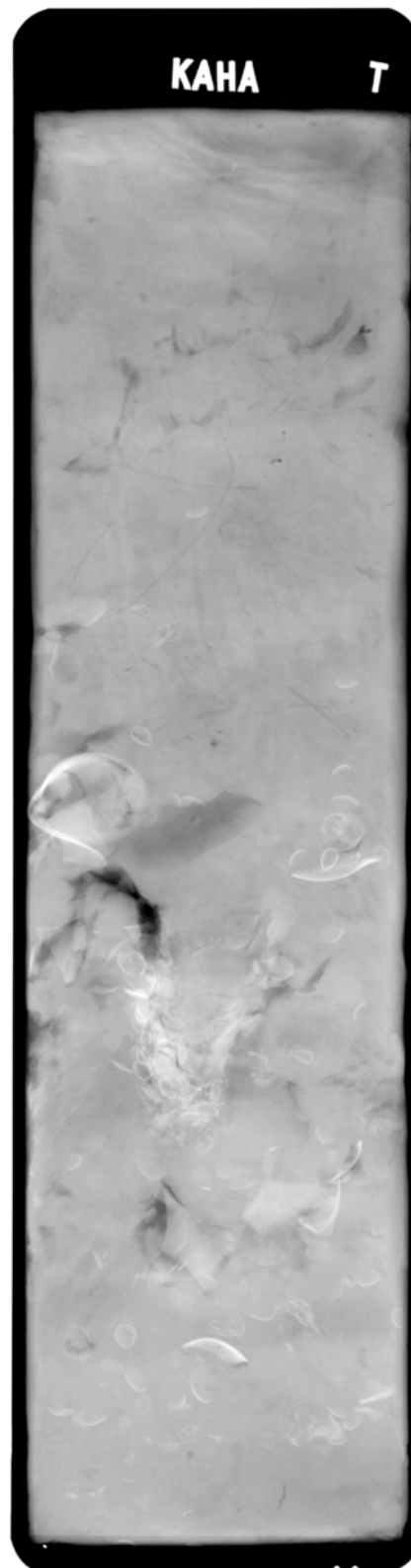


Figure A12: Kakaho (KAH) short-core x-radiograph of 2-cm thick slab. Exposure: 50 kV, 25 mA, 2 minutes. Scale: core width is 10 cm, length is 40 cm.

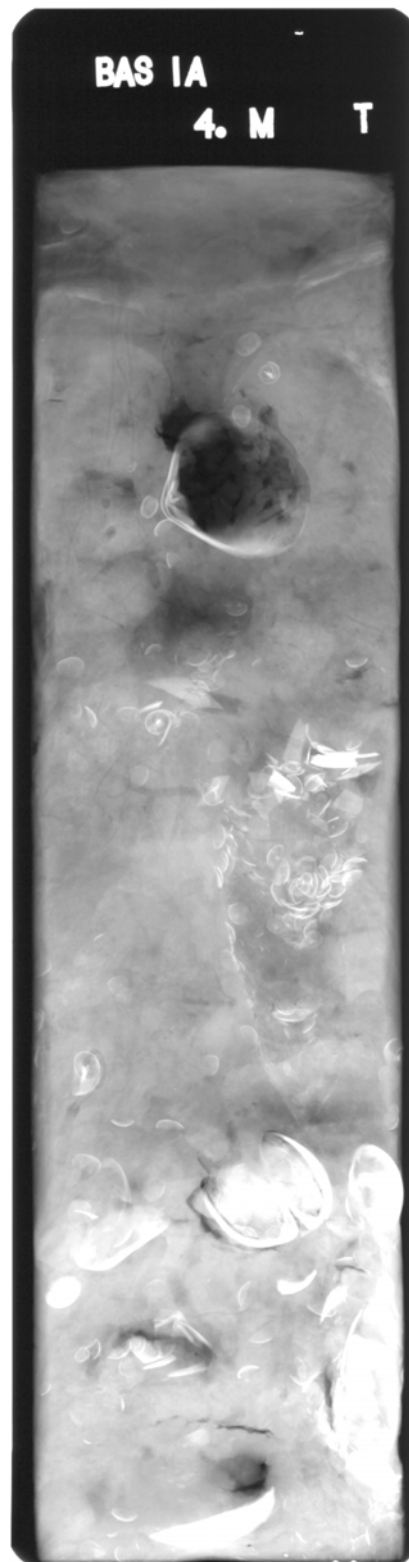


Figure A13: Basin Site One (BAS1) short-core x-radiograph of 2-cm thick slab. Exposure: 50 kV, 25 mA, 4 minutes. Scale: core width is 10 cm, length is 40 cm.

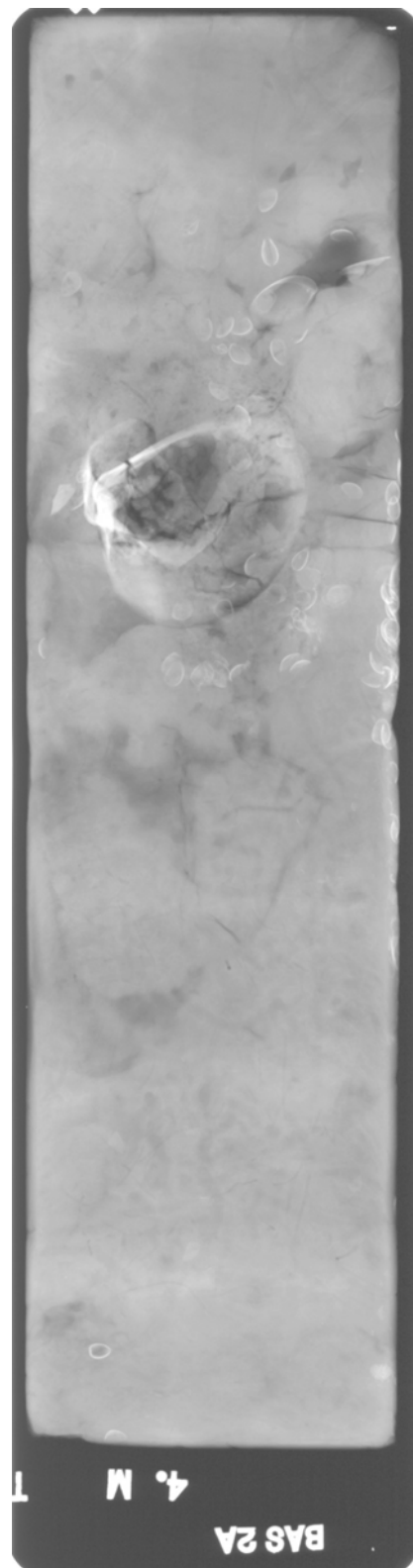


Figure A14: Basin Site Two (BAS2) short-core x-radiograph of 2-cm thick slab. Exposure: 50 kV, 25 mA, 4 minutes. Scale: core width is 10 cm, length is 40 cm.

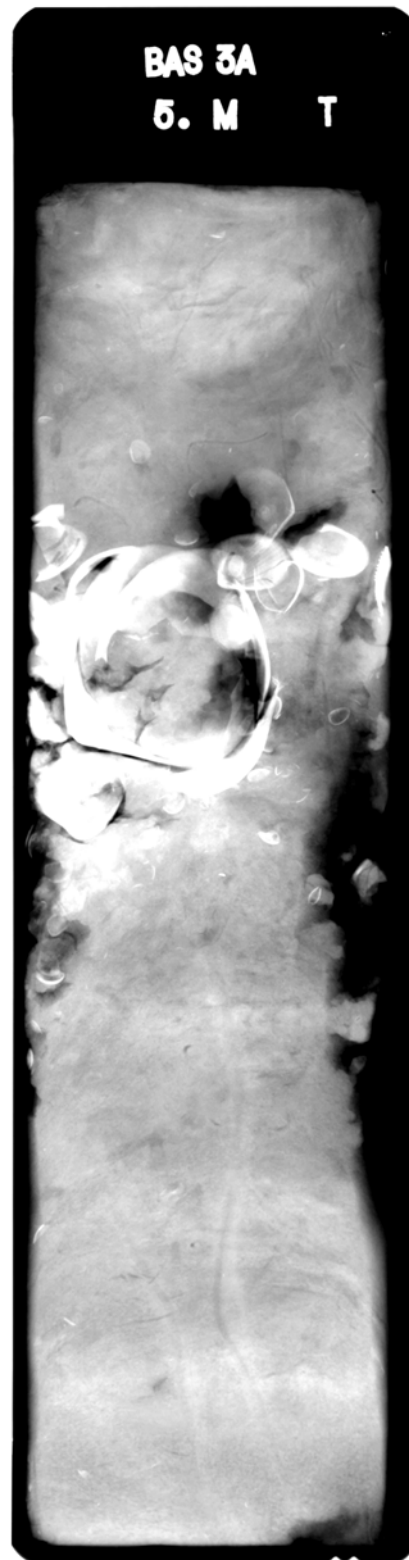


Figure A15: Basin Site Three (BAS3) short-core x-radiograph of 2-cm thick slab. Exposure: 50 kV, 25 mA, 5 minutes. Scale: core width is 10 cm, length is 40 cm.